Karlsruher Institut für Technologie

Development of Analysing Tools and Automatisation of Run Control for KATRIN

Diplomarbeit
von

Norman Haußmann

An der Fakultät für Physik
Institut für Experimentelle Kernphysik (IEKP)

Erstgutachter:	Prof. Dr. Guido Drexlin
Zweitgutachter:	Prof. Dr. Wim de Boer
Betreuender Mitarbeiter:	Dr. Klaus Schlösser
Zweiter betreuender Mitarbeiter:	Dr. Joachim Wolf

Bearbeitungszeit: 15. März 2012 – 14. März 2013

Erklärung

Hiermit versichere ich, die vorliegende Arbeit selbständig verfasst und alle dem Wortlaut oder Sinn nach entnommenen Inhalte anderer Werke an den entsprechenden Stellen, unter Angabe der Quelle, kenntlich gemacht und keine weiteren Hilfsmittel verwendet zu haben.

.....
Norman Haußmann
Karlsruhe, 14. März 2013

Zusammenfassung

Im Jahre 1930 hatte Wolfgang Pauli die Idee ein Teilchen einzuführen, welches die beim β-Zerfall beobachtete scheinbare Verletzung der Erhaltungssätze für Energie, Impuls und Drehimpuls erklären kann. Paulis' Ansatz eines Dreikörperzerfalls, durch Postulierung eines neutralen Partikels, er nannte es "Neutron", führt auf ein kontinuierliches Elektronenspektrum, so wie es beobachtet wird, ohne das Erhaltungssätze verletzt werden. Allerdings hat Pauli angenommen, dass sich dieses Teilchen im Kern befindet, es relativ schwer und bereits entdeckt sein müßte. Pauli war nicht völlig überzeugt von seiner Idee.
Im Jahre 1934 hat Enrico Fermi diese Idee aufgegriffen und den β-Zerfall durch einen Dreikörperzerfall mit einem freien Teilchen, dem "Neutrino", beschrieben. Im Jahre 1956 folgte die experimentelle Bestätigung des freien Neutrinos. Insgesamt gibt es drei Generation von Neutrinos, das Elektron -,Myon - sowie das Tau - Neutrino. Im Standardmodell der Teilchenphysik werden Neutrinos als masselos angenommen, allerdings haben Neutrinooszillationsexperimente gezeigt, dass Neutrinos von einer Generation in eine andere übergehen können. Dies ist einhergehend mit der Annahme, dass Neutrinos nicht masselos sein können. Demzufolge musste das Standardmodell erweitert werden. Durch die Neutrinoflavouroszillationen ist auch die Leptonenzahl innerhalb einer Teilchenfamilie verletzt und das Standardmodell musste dementsprechend angepasst werden.

Da es nicht möglich ist aus Oszillationsexperimenten auf die absolute Masse der Neutrinos zu schließen, sind weitere Experimente notwendig. Man unterscheidet zwischen modellabhängigen - (Neutrinoloser Doppelbetazerfall) und weniger modellabhängigen - Experimenten. Das KATRIN-Experiment (**KA**rlsruhe **TRI**tium **N**eutrino) wird aus dem Tritiumbetazerfall auf die Neutrinomasse rückschließen und setzt damit lediglich Fermis wohletabliertes Modell der schwachen Wechselwirkung voraus. Hierzu wird das Elektronenspektrum des Tritiumbetazerfalls am Endpunkt untersucht. Die Sensitivität wird 0.2eV(90% C.L.) betragen, also eine Größenordnung besser als die direkten Vorgängerexperimente in Mainz und Troitsk. Dazu besteht der 70m lange experimentelle Aufbau aus einer fensterlosen, gasförmigen Tritiumquelle, die durch den β-Zerfall freiwerdenden Elektronen werden durch die Transportstrecke geleitet und vom Tritium getrennt. Der Elektronenfluss wird im Vorspektrometer um einen Faktor 10^6 verringert und die verbliebenen Elektronen werden im Hauptspektrometer weiter gefiltert. Somit können nur Elektronen mit einer Energie von 18.6keV den Filter passieren. Diese Elektronen werden am Fokalebenendetektor registriert.

Um diese hohe Sensitivität zu erreichen ist eine sehr genaue Filterspannungsmessung

am Hauptspektromer nötig. Hierzu gibt es zwei Hochspannungsteiler, die ein direktes Auslesen der Spannung über kommerziell erhältliche Voltmeter ermöglichen. Desweiteren wurde das Monitorspektrometer installiert, welches eine Hochspannungsüberwachung basierend auf einem nuklearen Standard ermöglicht. Im Rahmen dieser Arbeit wurde die Messsteuerung am Monitorspektrometer komplett auf ORCA, dem Datenaufnahme und Kontrollsystem, umgestellt sowie ein neues Programm zur Rohdatenanalyse geschrieben. Desweiteren wurde die Linienstabilität unter verschiedenen Laufzeiten und äußeren Einflüssen untersucht.

- **Messbetriebssteuerung:**
  In Zukunft soll es möglich sein den kompletten KATRIN-Messbetrieb automatisch zu steuern. Hierzu wurde am Monitorspektrometer die Prozesssteuerung von einem externen LabVIEW Programm in ORCA integriert. Die Steuerung funktioniert über ORCA Scripts. Die Setzwerte werden über das Interface ADEI-control auf ZEUS (ZEntrale datenerfassung Und Steuerung) geschrieben und erreichen von dort aus den compact Field Point, welcher direkt mit den Endgeräten, zum Beispiel Netzgeräten, kommunizieren kann. Die Istwerte werden auch von diesen compact Field Point ausgelesen und von ZEUS in ADEI geschrieben, von wo aus sie vom Endnutzer abgerufen werden können.
  Ein Run wird mit Hilfe der Run List, welche in der Lage ist, vorher in das ".csv" Format exportierte Messteuerungsdateien einzulesen, gestartet. Die Run List ist mit einem ORCA Script verbunden, welches dafür sorgt, dass die entsprechenden Setzwerte gesetzt werden. Nachdem dieses Script beendet ist, wird Run Control gestartet, welches mit der Auslesehardware des Detektors kommunizieren kann. Der abgeschlossene Run wird auf der lokalen Festplatte gespeichert und über ein Skript auf einen Server am IPE (Institut für Prozessdatenverarbeitung und Elektronik) transferiert und ist dort als ROOT file oder als original ORCA Ausgabedatei für den Endnutzer zugänglich.
  Im Rahmen dieser Diplomarbeit wurde der Messbetrieb auf Sub Runs umgestellt. Diese ermöglichen es den kompletten Scan einer Linie in einer Ausgabedatei zu speichern. Zuvor war für jeden Setzwert ein separater Run notwendig. Allerdings haben Sub Runs den Nachteil, dass sie mehr Platz benötigen, da alle Histogramme eines Runs gespeichert werden müssen und ein zuvor benutztes Filterskript nicht mehr verwendet werden kann.
  Momentan gibt es noch Probleme mit der Prozesssteuerung, da Setzwerte Endgeräte nicht erreichen und die Zeit zwischen Absenden des Setzwertes bis zum entsprechenden Istwert sehr lang sein kann.

- **Rohdatenanalyse:**
  Im Zuge der Umstellung auf Sub Runs wurde ein neues Analyseprogramm notwendig. Es ist in der Lage sowohl alte als auch neue Runs auszulesen, die Quellenposition, die benutzte Quelle sowie die angelegte Quellspannung zu bestimmen, desweiteren kann es Histogramme automatisch analysieren und die ungefähre Linienposition bestimmen. Alle Daten werden in einer ROOT Datei gespeichert. Dieses kann vom Fit Programm eingelesen werden um die Linienposition zu bestimmen.
  Das Analyseprogramm bezieht die Run Daten(ROOT) von einem IPE Server, summiert über alle Histogramme für einen (Sub)Run und sucht darin nach Peaks. Wenn es die korrekten gefunden hat, werden die passenden Integrationsgrenzen bestimmt und es wird über diesen Peak integriert. Das so bestimmte Integral enthält die Anzahl der detektierten Elektronen und aus der Laufzeit des (Sub)Runs läßt sicht die Detektionsrate bestimmen. Aufgetragen über die entsprechende Spannung pro Messpunkt, ergibt sich das Filterspektrum. Die Spannungen werden vom Analyseprogramm auch von einem IPE Server heruntergeladen.

- **Stabilität der Linienposition:**
  Um die Linienposition im KATRIN Messbetrieb zu bestimmen, ist es notwendig die K-32 Konversionselektronen der ^{83}Kr/^{83m}Rb Quelle zu beschleunigen, damit sie mit ca. 17.8keV in der Lage sind, die am Haupt - und Monitorspektrometer anliegende Retardierungsspannung von 18.6kV zu überwinden. Es wurde bereits in vorherigen Diplomarbeiten gezeigt, dass das Monitorspektrometer in der Lage ist eine hohe Stabilität der K-32 Linienposition zu gewährleisten, allerdings wurden die Elektronen vorher nicht beschleunigt und die Retardierunsspannung war unabhängig vom Hauptspektrometer und lag bei ca. 17.8kV für K-32 Konversionselektronen.
  Im Rahmen dieser Diplomarbeiten wurden unterschiedliche Retardierungsspannungen verwendet und die Beschleunigungsspannung dementsprechend eingestellt. Die Differenz zwischen beiden Messmethoden liegt unter 20mV, allerdings gibt es noch keine Langzeitmessungen und das verwendete Voltmeter für die Beschleunigungsspannung wird gegen ein präziseres ausgetauscht.
  Desweiteren ist es wichtig die Messzeit für einen Messpunkt zu optimieren und so gering wie möglich zu halten. Sub Runs ermöglichen es einen Einblick in jedes einzelne Histogramm zu nehmen und so ein Verhältnis von Messdauer und Fehler auf die Linienposition zu bestimmen. Mit Hilfe der Aktivität der verwendeten Quelle läßt sich somit eine Aussage über die Messdauer pro Quellaktivität treffen. Für einen Fehler auf die Linienposition unter 20mV, darf die Messdauer $\cdot$ Aktivität nicht unter 16100kBqs liegen. Die experimentell bestimmte Transmission des Monitorspektrometers ist nur ca. 53% der erwarteten.
  Äußere Einflüsse, wie zum Beispiel Temperaturschwankungen, können die Spannungsstabilität der Hochspannungsnetzgeräte beeinflussen. Dieser Einfluß wurde untersucht und für geringe Messzeiten pro Messpunkt gibt es keine gravierenden Einflüsse auf die Linienposition.

Contents

Erklärung iii

Zusammenfassung v

1. Introduction 1

2. Neutrinos 3
2.1. Standard Model . . . 4
2.2. Neutrino Sources . . . 5
2.2.1. Primordial Neutrinos . . . 5
2.2.2. Atmospherical Neutrinos . . . 6
2.2.3. Supernovae Neutrinos . . . 7
2.2.4. Solar Neutrinos . . . 8
2.2.5. Reactor Neutrinos . . . 9
2.2.6. Accelerator Neutrinos . . . 9
2.3. Neutrino Oscillations . . . 9
2.4. The Neutrino Mass . . . 12
2.4.1. Double β-Decay . . . 14
2.4.2. β-Decay . . . 15
Tritium . . . 16
Rhenium . . . 16

3. The KATRIN-Experiment 17
3.1. Main Components . . . 17
3.1.1. The Tritium Source . . . 18
3.1.2. Transport Section . . . 18
3.1.3. Pre-Spectrometer . . . 19
3.1.4. Main Spectrometer . . . 19
3.1.5. Detector . . . 20
3.2. MAC-E-Filter . . . 21
3.3. High Voltage Monitoring . . . 23
3.4. Monitor Spectrometer . . . 24
3.4.1. Sources . . . 25
3.4.2. Spectrometer . . . 25
3.4.3. Solenoids . . . 26
3.4.4. Low Field Correction System . . . 26
3.4.5. Earth Magnetic Field Compensation System . . . 26
3.4.6. Detector . . . 27

4. Slow Control of KATRIN 29
4.1. Introduction to ORCA . . . 29
4.2. Overview of the Server System . . . 32

4.3. Run Control of the Monitor Spectrometer . . . 32
4.4. ORCA Scripting . . . 35
4.5. Problems and Solutions . . . 36
4.5.1. Sub Runs . . . 36
4.5.2. Timestamps . . . 38
4.5.3. Slow Control . . . 38

5. Data Analyis Software **41**
5.1. Introduction to the Server Structure . . . 41
5.2. The Monitor Spectrometer Analysis Software . . . 42
5.2.1. Raw Data Analysis . . . 43
The Parameter File . . . 43
Deriving peak counts from the Energy Histogram . . . 43
The Run Time . . . 45
The Slow Control Data . . . 45
Visualisation of Data . . . 46
Storing of Data . . . 46
5.2.2. The Fit-Program . . . 46
5.2.3. Outlook . . . 47

6. Line Position Stability during KATRIN-Measurements **49**
6.1. Measurements with varying Source Potential . . . 49
6.2. Least Required Measurement Time . . . 51
6.3. Temperature Dependencies . . . 54
6.3.1. Influence on the High Voltage System . . . 54
6.3.2. General influence on the Monitor Spectrometer . . . 55
6.4. Problems and Solutions . . . 57
6.4.1. Accuracy and Precision of Set Values . . . 57
6.4.2. Time Discrepancy . . . 58

7. Conclusion **59**

Glossary **61**

Bibliography **63**

Appendix **69**
A. Orca . . . 69
A.1. Additional Orca graphics . . . 69
A.2. Orca Script library package functions at the Monitor Spectromter . . . 75
A.3. Orca Slow Control Script at the Monitor Spectrometer . . . 77
A.4. Parameter file of createfilterspec . . . 78

Danksagung **79**

1. Introduction

Almost eighty years ago Enrico Fermi developed the theory of the β decay as a three body process [Fer34]. That idea originated from Wolfgang Pauli in 1930 originally. At that time the continuous β spectrum could not be explained, Pauli was thinking of an undiscovered third particle in the nucleus, which he called "neutron" [1]. This could explain the β spectrum. Between the first idea of a neutral particle by Pauli and the theory of Fermi, four years passed by, meanwhile a neutral particle within the nucleus was found by James Chadwick [Cha32]. It was called "neutron", nevertheless it could not explain the β decay. Fermi's theory introduced a third and this time free particle, he called the little neutron ("neutrino"). The first experimental confirmation of free neutrinos was in 1956 [CRH$^+$56].

The neutrino only interacts weakly and gravitational, and gravitational if the neutrino is not massless. Within the standard model, the neutrino is assumed to be massless. In the 1960s experiments to measure the neutrino flux from the sun were started. A deficit of solar neutrinos was found. In the mid 90s it turned out, that neutrinos can change their flavour by so-called flavour oscillations. Hence, the neutrinos cannot be massless and there is physics beyond the standard model.

Since the discovery of neutrinos, there is the ambition to measure the neutrino mass. As neutrino oscillation experiments cannot measure the absolute mass, different experiments are required. It can be differentiated between model-dependent and model-independent experiments. A model independent experiment is the **KA**rlsruhe **TRI**tium **N**eutrino Experiment (KATRIN), that can measure the neutrino mass to a sensitivity of 0.2eV/c^2 (90% C.L.) from the β decay of tritium. This is a factor of ten better than previous experiments at Mainz and Troitsk. To realise such a high sensitivity a spectrometer based on the MAC-E-Filter principle is used. It is very important to guarantee a stable filtering voltage on this spectrometer, therefore high voltage divider with the worlds best precision are used as well as the monitor spectrometer, that enables voltage monitoring on a nuclear basis.

This thesis will introduce the neutrinos (chapter 2) to the reader and explain the KATRIN experiment in more detail (chapter 3). Afterwards the Run Control of the monitor spectrometer is explained, which is the pre-test of measurement control for the whole KATRIN experiment (chapter 4). The recorded data needs to be analysed, in the course of this thesis a raw data analysis program has been rewritten, what will be explained in

[1] An excerpt of his letter, stating out a third involved particle called "neutron", can be found on page 3.

chapter 5. Afterwards, a look at the line position stability under different prerequisites is done in chapter 6.

2. Neutrinos

"Liebe Radioaktive Damen und Herren!
Wie der Überbringer dieser Zeilen, den ich huldvollst anzuhören bitte, Ihnen des näheren auseinandersetzen wird, bin ich angesichts der "falschen" Statistik der N- und Li 6-Kerne, sowie des kontinuierlichen β-Spektrums auf einen verzweifelten Ausweg verfallen, um den "Wechselsatz" der Statistik und den Energiesatz zu retten. Nämlich die Möglichkeit, es könnten elektrisch neutrale Teilchen, die ich Neutronen nennen will, in den Kernen existieren, welche den Spin 1/2 haben und das Ausschließungsprinzip befolgen und sich von Lichtquanten außerdem noch dadurch unterscheiden, daß sie nicht mit Lichtgeschwindigkeit laufen. Die Masse der Neutronen müßte von derselben Größenordnung wie die Elektronenmasse sein und jedenfalls nicht größer als 0.01 Protonenmasse. Das kontinuierliche β-Spektrum wäre dann verständlich unter der Annahme, daß beim β-Zerfall mit dem Elektron jeweils noch ein Neutron emittiert wird, derart, daß die Summe der Energie von Neutron und Elektron konstant ist."
Wolfgang Pauli, Offener Brief an die Gruppe der Radioaktiven bei der Gauvereins-Tagung zu Tübingen, Dezember 1930[1]

"Dear Radioactive[2] Ladies and Gentlemen!
The bearer[3] of this letter, I beg you to listen to graciously, will explain to you in detail, that I came, in face of the "wrong" statistics of N- and Li 6-nuclei as well as the continuous β-spectrum, to a desperate solution to save the "exchange theorem" of statistics and the energy theorem. There is the opportunity, that electrical neutral particles, I would like to call neutrons, are existing within the nucleus, these have a spin 1/2 and obey the exclusion principle[4], that differ to light quanta by not traveling with the speed of light. The magnitude of the mass of neutrons has to be same as the ones of electrons, at least not higher than 0.01 the proton mass. The continuous β-spectrum becomes perspicuous under the presumption, that the β-decay emits an electron and a neutron in a way, that the sum of energy of the neutron and electron is constant."
Wolfgang Pauli, December 1930, loose translation

[1] Wolfgang Pauli, wissenschaftlicher Briefwechsel mit Bohr, Einstein, Heisenberg u.a., scientific correspondence with Bohr, Einstein, Heisenberg a.o. Band II: 1930 - 1939
[2] Radioactive is the name of a group of people
[3] unknow person
[4] Pauli principle

Within this letter Pauli is stating out two problems. On the one hand the "wrong" statistics of N- / Li 6-nuclei and on the other hand the continuous β spectrum. For a two body decay energy and momentum conservation would be violated. At that time there were also ideas, that the energy conservation for the β decay is wrong . By introducing a new particle, Pauli called neutron, the β spectrum can be explained and the energy and momentum conservation is working again.
It was known, that the electron does have a spin of 1/2 and the given example of $^{14}N_7$ was supposed to have 14 protons and 7 electrons. Hence, the nitrogen nucleus is a bound state of these particles with half integer spin. But it was found out, that the nitrogen follows the Bose-Einstein statistics. Thus by implementing a neutron into the nucleus with a spin of 1/2 this problem is solved also. (This section is partly taken from [Bil12].)
Pauli himself was very uncertain with his own theory. He assumed, that the neutron has to have a mass as part of the nuclei and it may not be above 0.01 of the proton mass. In the complete letter he states, that he does not want to publish his idea, because he is sure, that this particle must have been found already. Ironically the "neutron" as we know it today was found in 1932 by James Chadwick [Cha32]. It has the mass of about the proton, has no charge and spin 1/2. But it is not the particle Pauli was talking of. One problem, that Pauli described in his letter was solved by the theory, that the nucleus consists of a bound state of neutrons and protons. But the problem of the β spectrum still remained. Enrico Fermi picked up the problem and developed a theory with a small spin 1/2 "neutron" - the neutrino in 1934 [Fer34]. The β^- decay, that Pauli describes can be explained with the following formula:

$$ {}^{A}_{Z}X \rightarrow {}^{A}_{Z+1}Y + e^- + \overline{\nu}_e \tag{2.1} $$

It took additional 22 years until an experimental verification of neutrinos at the Savannah river nuclear power plant in the USA in 1956. This work verified the Hanford experiment, that might have proven the free neutrino in 1953 already. It was using the inverse β decay:

$$ p + \overline{\nu}_e \rightarrow n + e^+ \tag{2.2} $$

The neutrino flux was gained by a reactor and the target were protons. Afterwards the emanating neutron and the positron were detected. The Hanford experiment had the problem of a huge background, thus a succession experiment was required to prove the free neutrino. It was using the inverse β decay also [CRH$^+$56].
In 1962 a second generation of neutrinos - the muon neutrino was discovered [DGG$^+$62] and in 2001 the tau neutrino [KUA$^+$01].
In this chapter a detailed introduction to neutrinos and their origin as well as their properties is given.

2.1. Standard Model

The standard model of particle physics includes the weak -, the strong - and the electromagnetic - interactions. An overview of these interactions and their gauge boson is given in table 2.1. The gravitation could not be included into the standard model yet. But the coupling constant of gravitation is much smaller than the others and can be neglected. This section is based on the book [PRSZ09].

As photons have no mass, their electromagnetical interaction has an infinite range. The gluon is massless also, but the range is limited by interactions of the gluons with one another. In a distance over 1fm the energy of the field is very high and new quark anti-quark particles emerge. The weak interaction is limited to a distance of 10^{-3}fm due to the high mass of its gauge bosons. The electromagnetic and the weak interaction can be combined to one interaction - the electroweak interaction.

Interaction	Couples With	Gauge Boson	Mass(GeV/c^2)
weak	weak charge	$W^{\pm}$,Z^0	$\approx 10^2$
strong	color	8 gluons(g)	0
electromagnetic	electrical charge	photon(γ)	0

Table 2.1.: Overview on interactions in the standard model. The table is taken from [PRSZ09].

Besides the gauge bosons the standard model contains fermions with spin 1/2. An overview is given in table 2.2. All fermions have their own anti particles with identical mass, but opposite charge and color. In the standard model are just three generations of fermions and from the Z^0 resonance it can be derived, that there may not be a fourth generation, except one with a massless neutrino. The standard model predicts a negative helicity for neutrinos. In 1958 Goldhaber,Grodzins and Sunyar [GGS58] measured the helicity of neutrinos and found out, that it is indeed -1. That means, that there are only left-handed neutrinos and right-handed anti neutrinos coupling to the gauge bosons of weak interaction, just as the standard model predicts.

Fermions	Generation			Charge	Color	Interaction
	I	II	III			
Leptons	ν_e	ν_μ	ν_τ	0	-	weak
	e	μ	τ	-1		electromagnetic,weak
Quarks	u	c	t	+2/3	r,b,g	electromagn.,weak, strong
	d	s	b	-1/3		

Table 2.2.: This table shows the fermions in the standard model. These are split into three generations. The table is taken from [PRSZ09].

2.2. Neutrino Sources

On the earth is a neutrino flux of $6.6 \cdot 10^{10}/\mathrm{cm}^2\mathrm{s}$ [Dre10] of neutrinos from the sun. Neutrinos can only interact with particles through gravity, if they have a mass, what is discussed later and through weak interaction. Due to a low coupling constant and a short range of the weak interactions - humans cannot recognise the high flux of neutrinos. But there are not just neutrinos from the sun. Some sources for neutrinos are described within this chapter and their flux is depicted in figure 2.1.

2.2.1. Primordial Neutrinos

Shortly after the big bang the neutrons and protons were in a thermal and chemical equilibrium ($T \gg 1\mathrm{MeV}$, $t \ll 1\mathrm{s}$). At a temperature of 10MeV and $t = 10\mathrm{s}$ protons and neutrons were still in a thermal equilibrium through the weak interaction. This equilibrium can be described by the following equations:

$$p + e^- \leftrightarrow n + \nu_e \tag{2.3}$$

$$p + \overline{\nu}_e \leftrightarrow n + e^+ \tag{2.4}$$

$$p + e^- + \overline{\nu}_e \leftrightarrow n \tag{2.5}$$

The rate of $n \to p$ and $p \to n$ sinks rapidly with decreasing temperatures. After about 0.02s the reaction rate is smaller than the expansion rate and the weak interaction freezes

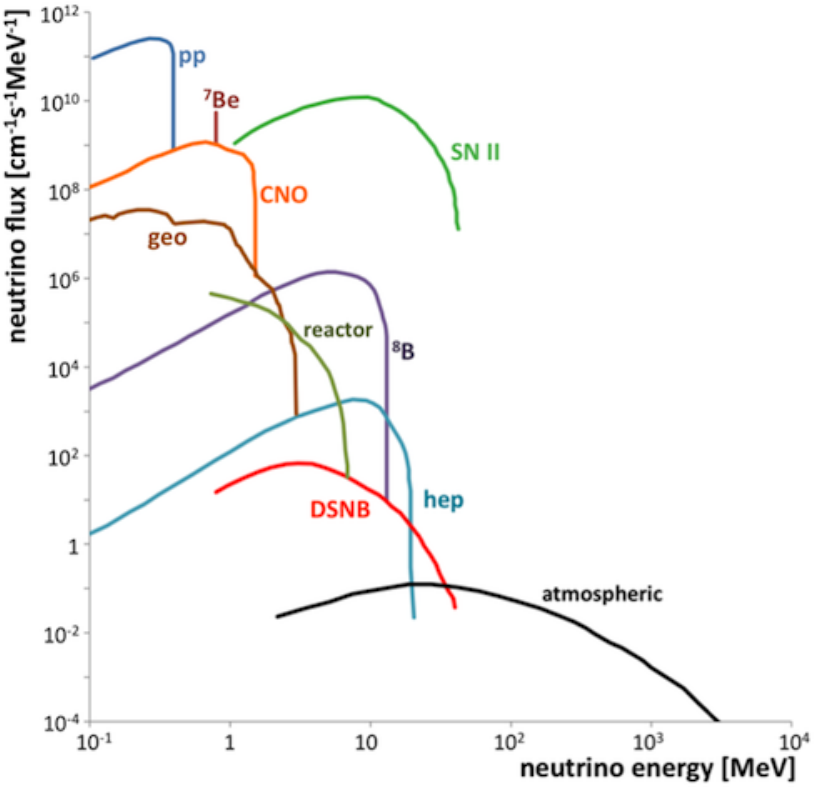

Figure 2.1.: **Overview neutrino sources and their energies.** The neutrinos with a high flux are derived from the sun and the neutrinos with high energies are atmospheric. Except "geo" neutrinos, which originate from radioactive isotopes on the earth, the different neutrinos fluxes are explained in the following sections. This figure is taken from [For13].

out(decouples). The decoupled neutrons decay. And the decoupled neutrinos are the primordial neutrinos with a temperature of about 1.95K at present. The primordial neutrino density is about $336/\text{cm}^3$.(see [KKZ97] pages 148-149)

2.2.2. Atmospherical Neutrinos

When protons from the cosmic radiation hit particles in the upper layers of the atmosphere of the earth, for instance a nitrogen nucleus:

$$p + N \rightarrow \pi^{\pm}, K^{\pm} \tag{2.6}$$

pions and kaons can originate from it. These can result in a cascade of particles and if they dot not have sufficient energy, possibly lost through interactions, they decay:

$$\pi^{\pm}, K^{\pm} \rightarrow \mu^{\pm} + \nu_{\mu}/\overline{\nu}_{\mu} \tag{2.7}$$

These muons are not stable also and decay:

$$\mu^{\pm} \rightarrow e^{\pm} + \nu_e/\overline{\nu}_e + \overline{\nu}_{\mu}/\nu_{\mu} \tag{2.8}$$

This results into a ratio of:

$$\frac{\nu_{\mu} + \overline{\nu}_{\mu}}{\nu_e + \overline{\nu}_e} = 2 \tag{2.9}$$

if all muons disintegrate. In case they have a high energy, the ratio shifts towards the electron neutrinos. A particle shower can be seen in figure 2.2.(see [KKZ97] pages 235-238,246)

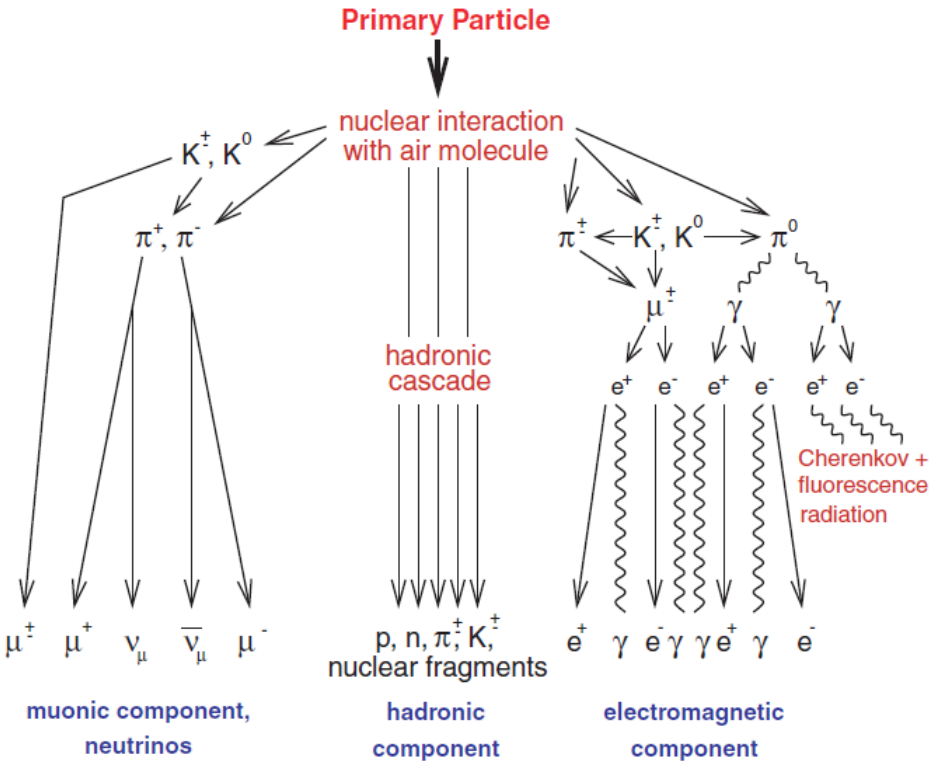

Figure 2.2.: **Air shower caused by cosmic radiation.** On the left side the described neutrinos can be seen. This figure is taken from [HRR03].

2.2.3. Supernovae Neutrinos

There are two types of supernovae, type I and II. Supernovae with hydrogen lines in their spectrum are called type II, with none type I. These supernovae types can be subdivided even further. In this section only a look at type II is taken as plenty of neutrinos do arise from that type.
After a star burned all the internal hydrogen, the pressure of radiation is not sufficient to counteract the gravitation and the star contracts. Caused by this contraction the internal temperature does rise again and the star can burn helium, what removes the star from the main sequence as it becomes a red giant. After a short time this helium is burned and the produced elements like nitrogen, oxygen and carbon are burnt after further contraction also. When the star begins to burn carbon the energy losses through neutrinos become dominant. If the mass of such a star is at least eight times the mass of the sun, it is able to generate enough pressure and high temperatures to burn everything to iron. After everything is burned to iron, the star does not have any fuel left. Finally, if the mass of the iron core is higher than the Chandrasekhar-mass[5], the star becomes instable and collapses to a neutron star.
The collaps is caused by photodesintegration and electron capture:

$$p + e^- \rightarrow n + \nu_e \tag{2.10}$$

Depending on its mass, afterwards a neutron star or a black hole remains. A neutron star is very hot and not transparent to photons. Thus the energy is released by pair production.

$$e^+ + e^- \rightarrow \nu_l + \overline{\nu}_l \tag{2.11}$$

[5] $M_{Ch} \approx 1.5 M_{sun}$

and l can be any of the three neutrino generations (e, μ, τ). Usually 10^{57} neutrinos arise from such a supernovae. So far only the neutrinos of one supernova (1987A in the Large Maglanic Cloud) have been observed.(see [KKZ97] pages 391-405)

2.2.4. Solar Neutrinos

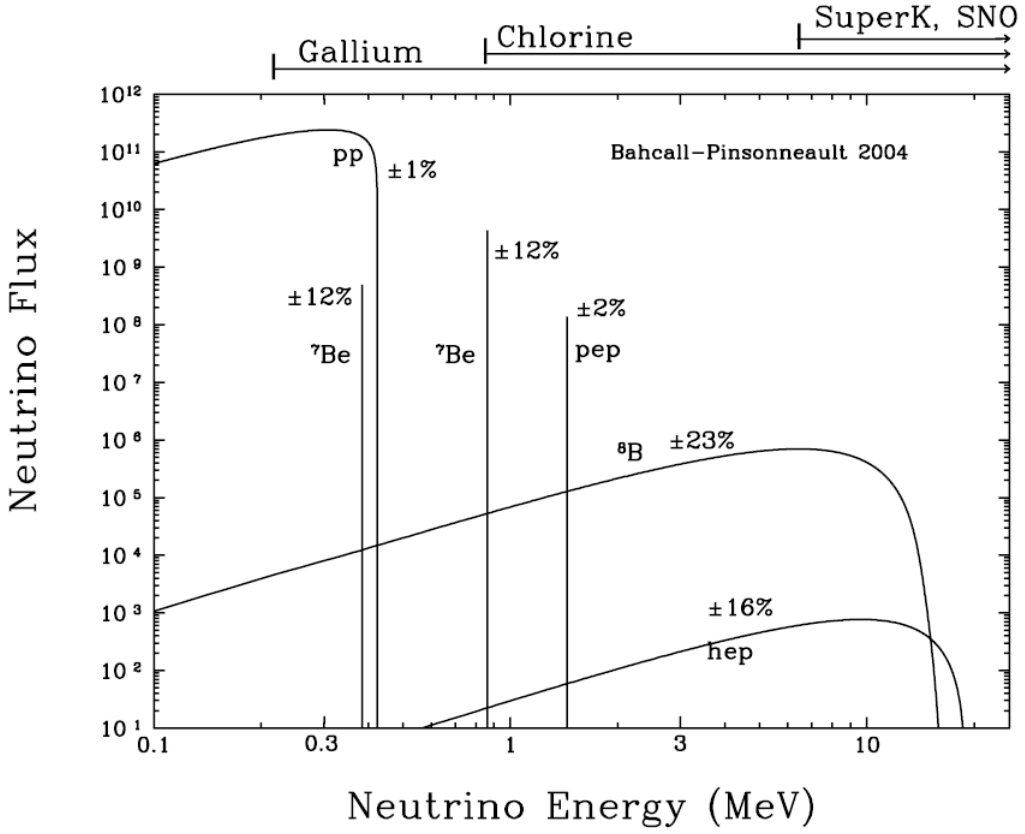

Figure 2.3.: **The solar neutrino spectrum.** On the y-axis the neutrino flux can be seen and on the x-axis the neutrino energy. The ^7Be is the ppII process and ^8B the ppIII process. It shows the originated neutrinos from the pp- and CNO cycle with the corresponding energy and flux. This figure is taken from [BPG04].

Stars derive their energy from nuclear fusion. The equation is:

$$4p \rightarrow {}^4He + 2e^+ + 2\nu_e + 26.73MeV \tag{2.12}$$

This can be reached by the pp-cycle and the CNO-cycle. For stars with lower temperatures (about the temperature of the sun) the pp-cycle is dominant and for higher temperatures the CNO-cycle.
Within the pp-cycle, neutrinos are produced by the following reactions:

$$p + p \rightarrow {}^2H + e^+ + \nu_e \qquad (E_\nu \leq 0.42MeV) \qquad (pp) \tag{2.13}$$

$$p + e^- + p \rightarrow {}^2H + \nu_e \qquad (E_\nu = 1.44MeV) \qquad (pep) \tag{2.14}$$

$$^3He + p \rightarrow {}^4He + \nu_e + e^+ \qquad (E_\nu \leq 18.77MeV) \qquad (hep) \tag{2.15}$$

$$^7Be + e^- \rightarrow {}^7Li + \nu_e \qquad (E_\nu = 0.862MeV, 0.384MeV) \qquad (ppII) \tag{2.16}$$

$$^8B \rightarrow {}^8Be + e^+ + \nu_e \qquad (E_\nu \leq 14.06MeV) \qquad (ppIII) \tag{2.17}$$

The processes without neutrino production are omitted. These reactions result into monoenergetic neutrinos (pep, ppII) and neutrinos with continuous energy distribution (pep,

hep and ppIII). Within the sun the pp-process is dominant.

Neutrinos from the CNO-cycle result from the following reactions:

$$^{13}N \rightarrow {}^{13}C + e^+ + \nu_e \qquad (E_\nu < 1.2MeV) \tag{2.18}$$

$$^{15}O \rightarrow {}^{15}N + e^+ + \nu_e \qquad (E_\nu < 1.73MeV) \tag{2.19}$$

These neutrinos are not monoenergetic and for the sun these processes can be neglected as the CNO-cycle is responsible for just 1.6% of the overall energy production. An overview of the solar neutrinos and their fluxes can be seen in figure 2.3. (see [KKZ97] pages 348-355)

2.2.5. Reactor Neutrinos

Reactor neutrinos originate from the decay of neutron rich nuclei. In the β^- decay, they emit anti neutrinos. The neutron rich nuclei are the result of the fission of ^{235}U and ^{239}P for instance. The average emitted number of anti neutrinos for ^{235}U are 6.1 neutrinos and 5.6 neutrinos for ^{239}P. Hence, a reactor of 1MW causes approximately $2 \cdot 10^{17}$ anti neutrinos. These neutrinos are perfect for neutrino oscillation measurements. Experiments, considering neutrino oscillations, will be discussed in the next chapter.(see [FY03] page 143)

2.2.6. Accelerator Neutrinos

Protons can be accelerated and shot on a target material like beryllium. The targets are usually several interactions lengths long, but should be as short as possible, so the secondary particles cannot interact with the target material. The resulting particles are pions and kaons. During their flight they decay into neutrinos, see equation 2.7.
The neutrino spectrum is split into two lines. On the one hand the low energy neutrinos from the pion decay and the high energy neutrinos from the kaon decay on the other hand. The neutrinos are muon neutrinos mostly, but they are contaminated with electron neutrinos, especially from the decay of kaons, what makes oscillation experiments more difficult.(see [FY03] page 145)

2.3. Neutrino Oscillations

In 1998 first evidences for neutrino oscillations were discovered at Homestake. Homestake is placed in a gold mine at Lead, South Dakota in a depth of 4400m. This depth is necessary to suppress the argon production by neutrons and protons. The experiment is based on the inverse beta decay:

$$\nu_e + {}^{37}Cl \rightarrow {}^{37}Ar + e^- \tag{2.20}$$

Hence, the solar neutrinos induce argon into the chlorine detector. The discovered rate was $0.478 \pm 0.030(\text{stat.}) \pm 0.029(\text{syst.})$ per day. This causes a rate per target atom of $(2.56 \pm 0.16(\text{stat.}) \pm 0.16(\text{syst.})) \cdot 10^{-36} \frac{1}{s}$, but the expected rate is $(9.3 \pm 1.3) \cdot 10^{-36} \frac{1}{s}$. Thus, the measured neutrino flux is too low for the expected electron neutrino flux [CDD+98]. This experiment was the first evidence for neutrino oscillations.
In 1968 a paper from the Homestake experiment was publicized pointing out a low neutrino flux, but it was not clear whether it is a problem caused by the standard model of the sun or the experiment and background suppression[DHH68].
Experiments for different energies of the neutrinos were done at SAGE and GALLEX. SAGE was using the inverse beta decay also and was sensitive to low energy neutrinos from pp fusion[Ell01]. The GALLEX [CHH+99] experiment derived the same results.

Hence, there is a deficit of solar neutrinos.

In 2001 the Sudbury Neutrino Observatory (SNO) was able to measure all neutrinos from the ppIII process (^8B) as it was sensitive to all neutrino flavours by measuring the neutral current (NC), the gauge boson is the neutral Z boson, in the following way:

$$\nu_x + d \to p + n + \nu_x \tag{2.21}$$

this is sensitive to all neutrino flavours with an equal sensitivity. SNO did also measure the charged current (CC), the gauge bosons are $W^{\pm}$, as follows:

$$\nu_e + d \to p + p + e^- \tag{2.22}$$

The CC is only sensitive to electron neutrinos. Additionally SNO measured the rate of elastic scattering (ES).

$$\nu_x + e^- \to \nu_x + e^- \tag{2.23}$$

This ES is sensitive to all neutrinos, but the cross section for electron neutrinos is about six times larger than for the other neutrino flavours. With these methods it became possible to calculate the total flux, which is equal to the expected flux and proves neutrino oscillations.(see [AAA$^+$11])

Hand in hand with the discovery of neutrino oscillations comes the insightful, that the lepton count of one family cannot be conserved and it is necessary, that the neutrino flavours do have different masses and at least one flavour has to have a non vanishing mass. This is in contrast to the standard model, which is not valid in this case and has to be extended.

The oscillations can be described phenomenologically. The flavours $|\nu_\alpha\rangle$ with $\alpha = e, \mu, \tau$ and $\langle\nu_\beta|\nu_\alpha\rangle = \delta_{\alpha\beta}$ can be described through their mass eigenstates:

$$|\nu_\alpha\rangle = \sum_i U_{\alpha i} |\nu_i\rangle \qquad |\nu_i\rangle = \sum_\alpha (U^\dagger)_{i\alpha} |\nu_\alpha\rangle = \sum_\alpha U^*_{\alpha i} |\nu_\alpha\rangle \tag{2.24}$$

with a unitary mixing matrix U. The time dependence of the eigenstates can be described in the following way:

$$|\nu_i(x,t)\rangle = e^{-\imath E_i t} |\nu_i(x,0)\rangle \tag{2.25}$$

The transition probability of one flavour to another can be calculated:

$$P(\alpha \to \beta)(t) = |\langle\nu_\alpha(t)|\nu_\beta(t)\rangle|^2 \tag{2.26}$$

$$= \sum_i \sum_j U_{\alpha i} U^*_{\alpha j} U^*_{\beta i} U_{\beta j} e^{\imath(E_i - E_j)t} \tag{2.27}$$

$$= \sum_i \left|U_{\alpha i} U^*_{\beta i}\right|^2 + 2\Re \sum_{j>i} U_{\alpha i} U^*_{\alpha j} U^*_{\beta i} U_{\beta j} e^{\imath(E_i - E_j)t} \tag{2.28}$$

$$= \sum_i \left|U_{\alpha i} U^*_{\beta i}\right|^2 + 2\Re \sum_{j>i} U_{\alpha i} U^*_{\alpha j} U^*_{\beta i} U_{\beta j} e^{-\imath \frac{\Delta m^2}{2}} \frac{L}{E} \tag{2.29}$$

using CP invariance the formula simplifies to:

$$= \sum_i U^2_{\alpha i} U^2_{\beta i} + 2 \sum_{j>i} U_{\alpha i} U_{\alpha j} U_{\beta i} U_{\beta j} \cos\left(\frac{\Delta m^2_{ij}}{2} \frac{L}{E}\right) \tag{2.30}$$

$$= \delta_{\alpha\beta} - 4 \sum_{j>i} U_{\alpha i} U_{\alpha j} U_{\beta i} U_{\beta j} \sin^2\left(\frac{\Delta m^2_{ij}}{4} \frac{L}{E}\right) \tag{2.31}$$

with $\Delta m_{ij}^2 = m_i^2 - m_j^2$ and $L = ct$.

By taking a look at just two neutrino flavours, the transformations can be described by the Cabbibo matrix:

$$\begin{pmatrix} \nu_e \\ \nu_\mu \end{pmatrix} = \begin{pmatrix} \cos\theta & \sin\theta \\ -\sin\theta & \cos\theta \end{pmatrix} \begin{pmatrix} \nu_1 \\ \nu_2 \end{pmatrix} \tag{2.32}$$

with the mixing angle θ. The transition probability can be calculated from formula 2.31 and the Cabbibo matrix:

$$P(\nu_e \to \nu_\mu) = \sin^2 2\theta \cdot \sin^2 \left(\frac{\Delta m^2}{4} \frac{L}{E} \right) \tag{2.33}$$

From this equation it can be derived, that the mixing angle θ and the mass difference Δm^2 cannot vanish if there are neutrino oscillations. Hence, for oscillations to occur a distance to the source

$$\frac{L}{E} \geq \frac{4}{\Delta m^2} \tag{2.34}$$

is necessary. This is essential for neutrino oscillation measurements at reactors. For accelerator neutrinos it is possible to influence the energy of the neutrinos, but usually high energies are preferred as these have higher cross sections.
Of course, this is just an approximation for two flavours. It becomes a little bit more difficult using all three of them. This matrix is called the Maki-Nakagava-Sakata (MNS) matrix, which is a 3×3 matrix.

$$U_{MNS} = \begin{pmatrix} c_{12}c_{13} & s_{12}c_{13} & s_{13}e^{-\imath\delta} \\ -s_{12}c_{23} - c_{12}s_{23}s_{13}e^{\imath\delta} & c_{12}c_{23} - s_{12}s_{23}s_{13}e^{\imath\delta} & s_{23}c_{13} \\ s_{12}s_{23} - c_{12}s_{23}s_{13}e^{\imath\delta} & -c_{12}s_{23} - s_{12}c_{23}s_{13}e^{\imath\delta} & c_{23}c_{13} \end{pmatrix} \tag{2.35}$$

with $s_{ij} = \sin\theta_{ij}$, $c_{ij} = \cos\theta_{ij}$(see [Zub04] pages 190-196;124)

Neutrino oscillation experiments aim to measure the mixing angles and the mass square differences. They are not able to measure the absolute mass. Latest experiments are the Double Chooz, the Daya Bay and the RENO experiment. All of them are looking for the mixing angle θ_{13}.
The Double Chooze experiment is placed at the nuclear power station Chooz in France. Double Chooz has two detectors, one at a distance of 400m and one in a distance of 1050m. The anti electron neutrinos from the reactor do not have the chance to change their flavour. The distance to the first detector is too short for oscillations to occur (region a) in figure 2.4), the second one is placed at the very left of area b), with an increased likelihood of a different flavour. Hence, if there are differences in the neutrino count at the second detector compared to the first one, the flavour has changed. Duo to a small probability of interaction the measurement time of the current phase is five years [Dou13].

The Daya Bay experiment consists of three detectors. Two near detectors, one is close to the Daya Bay core and one that is close to the LingAo cores. The advantage of this experiment is, that the reactor complex is amongst the five most powerful of the world. Additionally mountains are nearby, what eases background suppression [Day07].

The RENO experiment is placed at the Yonggwang reactor in South Korea. The power plant consists of six cores. The experiment is done with two detectors, a close one and one in a greater distance on the opposite side of the reactor [GTC12].

The latest results for these experiments are:

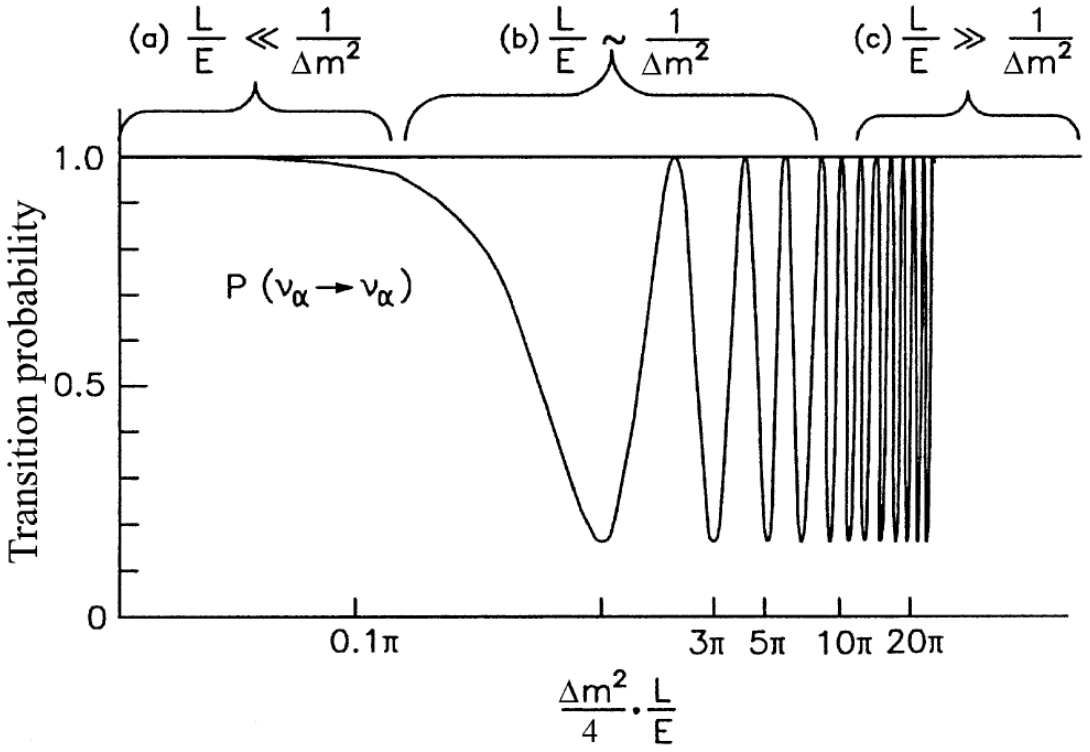

Figure 2.4.: **The neutrino oscillation in dependence of L/E.** In this figure $\sin^2\theta$ is chosen to be 0.83. The area a) shows L/E for no oscillation, b) oscillation and c) average oscillations. This figure is taken from [Zub04] page 198.

Double Chooz, January 2013 [AA+13]

$$\sin^2(2\theta_{13}) = 0.097 \pm 0.034(stat.) \pm 0.034(syst.) \tag{2.36}$$

Daya Bay, November 2012 [Web12]

$$\sin^2(2\theta_{13}) = 0.089 \pm 0.010(stat.) \pm 0.005(syst.) \tag{2.37}$$

RENO, May 2012 [ACC+12]

$$\sin^2(2\theta_{13}) = 0.113 \pm 0.013(stat.) \pm 0.019(syst.) \tag{2.38}$$

2.4. The Neutrino Mass

From the neutrino oscillations we know, that the neutrinos have mass. This has a huge impact on the standard model, as it assumes a zero mass for neutrinos. Overall the neutrino mass has an extensive influence on cosmological models as the structural development of the universe.

Although neutrinos interact weak and gravitational only, there are so many of them, that the mass has an influence of the structural development. This can be seen on the left side of figure 2.6.

There are two methods of neutrino mass measurements. On the one hand model-dependent and model-independent measurements on the other hand. In this section an introduction to both methods is given.

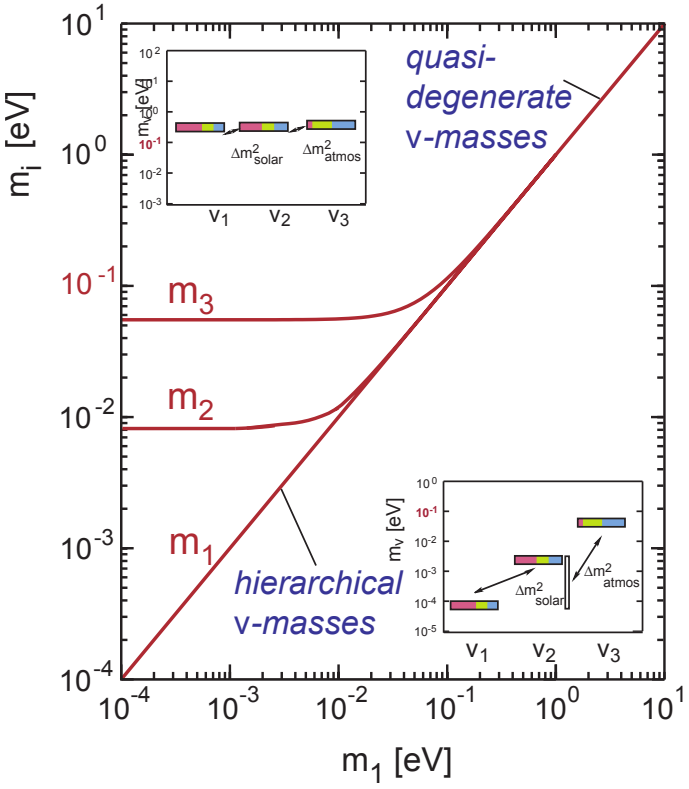

Figure 2.5.: **The neutrino mass eigenstates in dependence of m_1.** On the x-axis the mass m_1 in electron volts can be seen. Up to about 0.1eV the mass eigenstates are discrete and hierarchical with $m_3 > m_2 > m_1$. Afterwards the mass eigenstates are quasi degenerated mass eigenstates. This figure is taken from [Kat05] page 14.

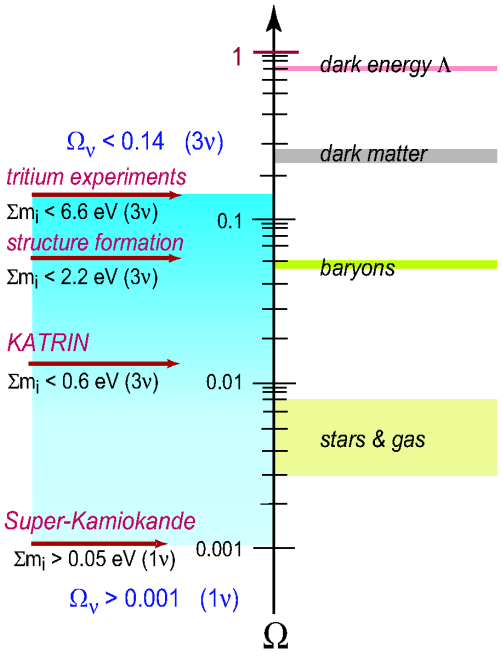

Figure 2.6.: **Energy Density within the universe.** On the left side the contribution of the neutrinos in dependence of their mass can be seen and on the right side the contribution of stars/gas, baryons, dark matter and the dark energy. This figure is taken from [Kat05] page 16.

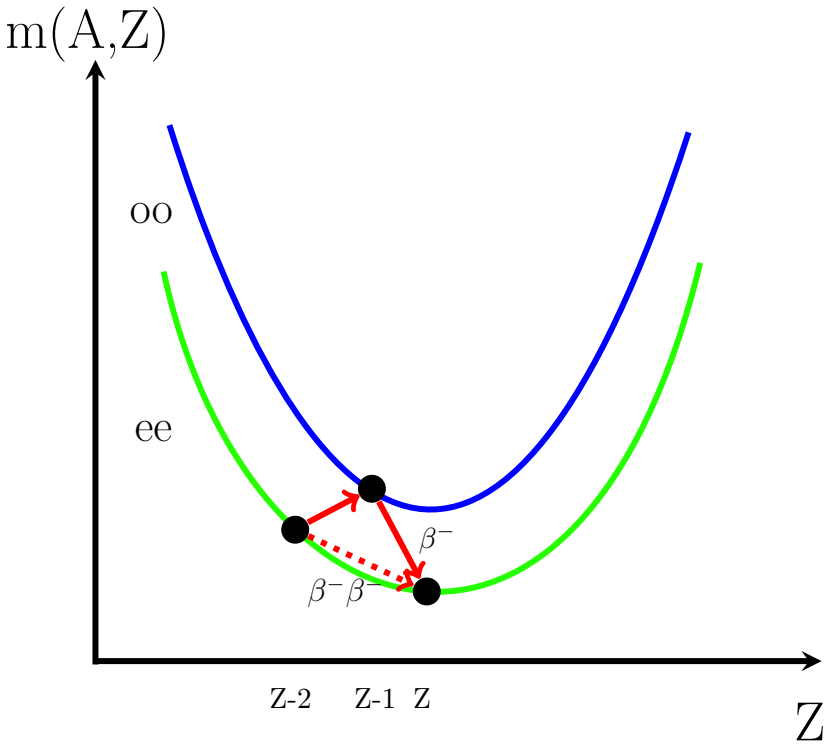

Figure 2.7.: **Mass parabola.** On the x-axis the proton count can be seen and on the y-axis the energy or mass. This figure describes the course of double beta decay.

2.4.1. Double β-Decay

The double beta decay describes the decay of two neutrons at the same time into an instable core. In comparison to the usual beta decay, the double beta decay is a rare process. Tow cases can be distinguished:

- **Normal Double β-Decay ($2\nu\beta\beta$)**

$$(A, Z) \rightarrow (A, Z + 2) + 2e^- + 2\overline{\nu}_e \tag{2.39}$$

- **Neutrinoless Double β-Decay ($0\nu\beta\beta$)**

$$(A, Z) \rightarrow (A, Z + 2) + 2e^- \tag{2.40}$$

For the first case the lepton count is correct and does not change ($\Delta L = 0$), the neutrinoless decay does not have a constant lepton count ($\Delta L = 2$). In an experiment it is easy to differentiate between them. The normal beta decay has a broad distribution $2m_e < E < E_{max}$. The double beta-decay does have a distinct peak at $E = E_{max}$ from which the neutrino mass can be derived. The normal double beta decay was observed in 1987 for the first time. There is no proof for the neutrinoless double beta decay yet.

The double beta decay is expected for an instable nucleus(A,Z), if (A,Z+1) has a higher mass than m(A,Z). This makes a normal beta decay from (A,Z)→(A,Z+1) impossible. Furthermore the mass of (A,Z+2) has to be lower than the mass of (A,Z). This can happen if the nucleus(A,Z) is an even-even core (ee-core), (A,Z+1) is an odd-odd core (oo-core) and the core(A,Z+2) is even-even again.

If the neutrinoless double beta decay does exist it means, that physics beyond the standard model does exist and the lepton count is not conserved. It means also, that neutrinos must be Majorana neutrinos ($\nu = \overline{\nu}$). Additionally the helicity between the vertices has to be adjusted. This can happen in two ways, first there is an additional right-handed current at the weak interaction, hence neutrinos with the "wrong" helicity can occur at the vertices. But this is not that interesting for mass measurements. The second possibility is, that neutrinos have mass, which is shown in the previous chapter, and these can change their helicity and these can be right-handed with a likelihood of:

$$W = \frac{1}{2}\left(1 - \frac{v}{c}\right) \approx \left(\frac{m_\nu}{2E_\nu}\right)^2 \tag{2.41}$$

If the double beta decay does exist, all energy is with the electrons and a distinct peak is observed. From the rate the half time can be obtained and hence the neutrino mass:

$$\Gamma_\nu \propto \langle m_\nu \rangle \tag{2.42}$$

The mass of the Majorana neutrino can be calculated:

$$\langle m_\nu \rangle = \sum_j m_j U_{ej}^2 \tag{2.43}$$

Unfortunately the matrix element U_{ej}^2 is necessary and two problems can occur:

- As U_{ej}^2 can also be negative, the m_j can cancel each other and if an upper boundary for $\langle m_\nu \rangle$ is found, it is not an upper boundary for the mass eigenstates.
- The neutrinoless double beta decay is only possible, if there is at least one Majorana neutrino with $m_j \neq 0$

The neutrinoless double beta decay is one example for model-dependent experiments as the required nuclear matrix element is model dependent.(see [Sch97] pages 300-306)

2.4.2. β-Decay

The normal beta decay was described by Fermi in the 1930s. The decay can be described as follows:

$$n \to p + e^- + \overline{\nu}_e \tag{2.44}$$

So by investigating the beta spectrum of electrons, statements about the absolute neutrino mass can be made. The energy spectrum for tritium beta decay electrons looks the following:

$$\frac{dN}{dE} = C \cdot F(Z,E) p (E + m_e c^2)(E_0 - E)\sqrt{(E - E_0) - m_\nu^2} \cdot \Theta(E_0 - E - m_\nu) \tag{2.45}$$

with:

m_ν = mass of the neutrino
m_e = mass of the electron
E = kinetic energy of the electron
p = momentum of the electron
E_0 = max. electron energy ($m_\nu = 0$)
$F(Z,E)$ = fermi function
Θ = step function for energy conservation
$C = \frac{G_F^2}{2\pi^3}\cos^2\theta_C\,|M|^2$
θ_C = Cabbibo angle
G_F = Fermi constant
M = nuclear matrix element

As $F(Z,E)$ and M are independent of the neutrino mass, the electron spectrum is only dependent of the neutrino mass within the square root term. Additionally there is just the square of the mass within that formula:

$$m_{\nu_e}^2 = \sum_i |U_{\alpha i}|^2 \, m_i^2 \tag{2.46}$$

For the equation 2.45 it does not matter, whether the neutrino is a Dirac or Majorana neutrino. While the neutrino mass has little influence on the spectrum in lower energy regions, the mass can be derived from the end point energy. The spectrum can be seen in figure 2.8. The figure shows spectra with a neutrino mass of 1eV and 0eV.

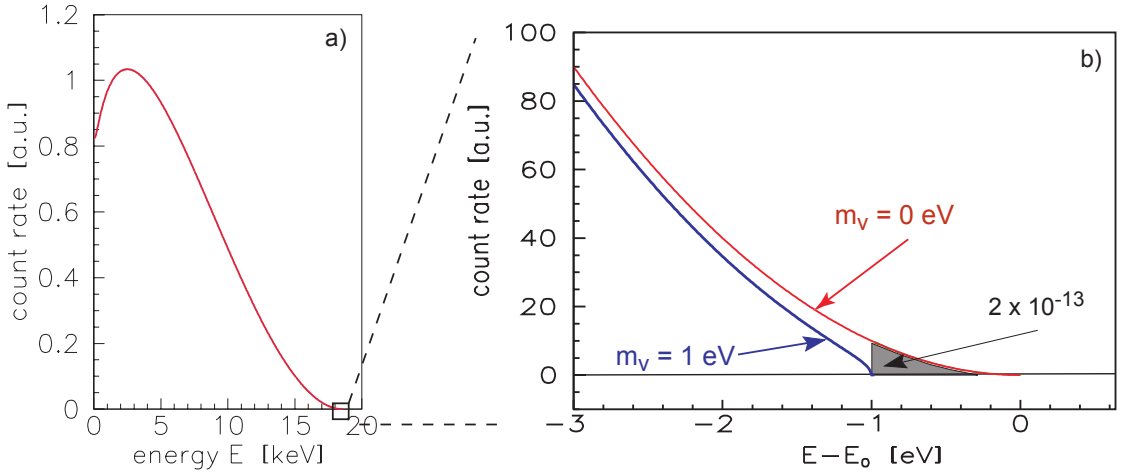

Figure 2.8.: **Tritium electron spectrum.** On the left side the complete spectrum can be seen with the energy on the x-axis and the count rate on the y-axis. The right picture shows the energy spectrum at the endpoint. The blue line shows the spectrum with a neutrino mass of 1eV and the red line with a massless neutrino. This figure is taken from [Kat05] page 29.

Tritium

To maximize the fraction of tritium beta decays close to the endpoint ($\propto (1/E_0)^3$), tritium turned out to be very useful as it has an endpoint energy of 18.6keV, which is the second lowest endpoint of all beta unstable isotopes. Additionally tritium has a short half life of 12.3 years. As tritium and the $^3He^+$ ion do have a simple electron shell configuration, atomic corrections can be calculated and through the low nuclear charge Z the inelastic scattering of electrons is small.
The decay of Tritium looks the following:

$$^3H \rightarrow {}^3He^+ + e^- + \overline{\nu}_e \tag{2.47}$$

Rhenium

The MARE experiment (Microcalorimeter Arrays for a Rhenium Experiment) uses the rhenium beta decay.

$$^{187}Re \rightarrow {}^{187}Os + e^- + \overline{\nu}_e \tag{2.48}$$

The advantage of Rhenium is a very small endpoint energy, which is 2.47keV and even smaller than the one of tritium. Unfortunately the half time is $43.2 \cdot 10^{10}$ years, which makes a lot of rhenium necessary for the source.[GGP+06].

3. The KATRIN-Experiment

The KATRIN-Experiment (Karlsruhe Tritium Neutrino Experiment) aims to measure the neutrino mass by measuring the tritium beta spectrum at the endpoint. The experiment does not involve nuclear models and will set the neutrino mass to an upper limit of $m_\nu = 0.2\text{eV/c}^2$ (90% C.L.), if no neutrino mass signal can be obtained above the limit. This is one order of improvement to previous neutrino mass experiments at Mainz and Troitsk.
In this chapter an introduction to the individual components of KATRIN is given as well as an explanation of the MAC-E-Filter as well as an introduction to the high voltage system and the monitor spectrometer. To be used as monitor spectrometer the setup from Mainz was installed in Karlsruhe, refurbished and modernised.
If not stated differently, this chapter is based on [Kat05].

3.1. Main Components

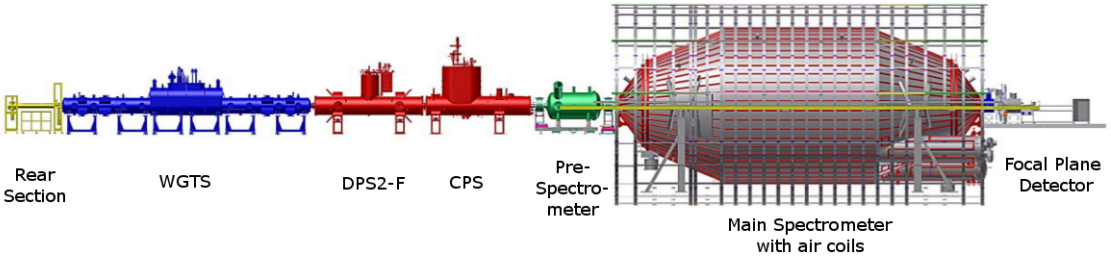

Figure 3.1.: **Overview of the KATRIN experiment.** The setup has a length of 70m and consists of the source(WGTS), the transport section(DPS and CPS), the pre-spectrometer, the main spectrometer, the detector as well as the rear section. This figure is a modified drawing from [Mel12].

An overview of the KATRIN experiment and its components is given in figure 3.1. It consists of a windowless gaseous tritium source (WGTS) emitting the β-electrons, that are detected at the focal plane detector (FPD). Before, the electrons have to pass the transport section, which is split into two parts, the differential pumping section (DPS2-F) and the cryogenic pumping section (CPS). These are necessary to reduce the tritium content. Afterwards the electrons have to pass the pre-spectrometer, it reduces the flux of the

electrons as only electrons with an energy above 18.3keV can pass. The flux reduction is about a factor of 10^{-6}. The pre-spectrometer as well as the main spectrometer are based on the MAC-E-Filter (Magnetic-Adiabatic Collimation combined with an Electrostatic Filter) principle.
The reduced electron flux enters the main spectrometer, where a precision measurement close to the tritium endpoint of β-electrons is performed. Finally the electrons that passed the filter are registered at the FPD.

In this section an introduction to the components and the MAC-E-Filter is given.

3.1.1. The Tritium Source

The electrons, that KATRIN wants to detect stem from the β-decay of Tritium. Therefore the KATRIN experiments can benefit from the Tritium Laboratory Karlsruhe (TLK), that is the only licensed scientific laboratory to handle the required amount of tritium. They have a license of 40g tritium, this equals $1.5 \cdot 10^{16}$Bq. The TLK has a closed tritium cycle also and their expertise may not be underrated.
Therefore the WGTS was developed (see figure 3.2), it offers highest luminosity and, compared to e.g. solid sources, small systematic uncertainties. The WGTS is a 10m long cylindrical tube with a diameter of 90mm. The tritium is injected through 250 capillaries with a diameter of 2mm in the middle of the tube. It has a temperature of 27K and is of high isotopic purity ($> 95\%$). The WGTS has a fixed column density reference value of $\rho d = 5 \cdot 10^{17} \frac{molecules}{cm^2}$. The injected tritium reaches the outer regions of the WGTS through diffusion. This leads to a non-linear decrease of tritium density towards the outer regions. The largest uncertainty of the WGTS is the column density, it has to be known to a precision of 0.1%. This can be adjusted by the gas injection pressure and the source tube temperature.

If tritium decays, the electrons are guided adiabatically to the tube ends. The applied magnetic field is 3.6T and the WGTS will deliver $9.5 \cdot 10^{10}$ β-decays per second. The tritium, that reached the outer regions is pumped in an inner loop by turbomolecular pumps(DPS1-R/F) and is re-injected. The injection rate per second is $1.7 \cdot 10^{11}$Bq which equals 40g of tritium per day.

The tritium that cannot be pumped out, reaches the transport section, either in the front or in the back. If it reaches the back, it enters the DPS2-R, that consists of two pumping ports to protect the Calibration and Monitoring System (CMS) from too high partial tritium pressure. The tritium pumped out enters the outer loop and is not re-injected immediately. The CMS will consist of electron detectors, to measure the electron flux, and of electron guns.

3.1.2. Transport Section

The tritium, that took the opposite direction and did not escape through DPS1-F, enters the transport section. It is desired, that the maximum tritium flow rate into the pre-spectrometer is of the order of 10^{-14}mbarl/s. This is necessary to reduce the electron background induced by tritium that decays in the spectrometer. It must be less than 10^{-3}counts/s. Hence, the flux of tritium from the WGTS outlet to the pre-spectrometer has to be suppressed by a factor of 10^{11}.
The transport section is split into two components, the DPS and CPS (see figure 3.3).

The flux of tritium is reduced by about 10^5 in the DPS2-F through four pumping ports with turbo molecular pumps. These have a pumping speed of 2000l/s. To achieve a sufficient reduction factor the beam line is tilted four times by twenty degrees, but the

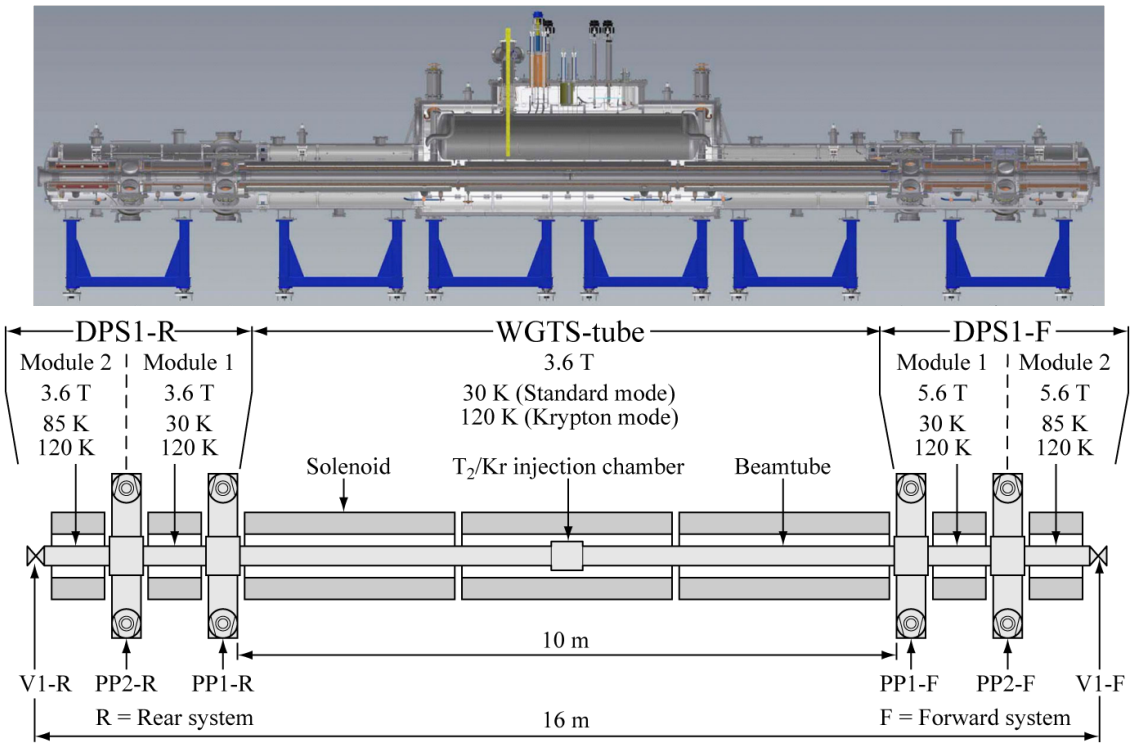

Figure 3.2.: **Scheme of the WGTS.** In the top the CAD view of the WGTS can be seen and in the bottom a scheme with its components. This figure is taken from [Höt12].

electrons do not hit the wall as they are guided by a magnetic field. In the CPS, the beam tube is cooled down to 4.5K. At this temperature the tritium molecules can be adsorbed on the inner tube surfaces. The surface is covered by a layer of argon frost and is cooled by liquid helium. The beam line in the CPS is tilted also.

3.1.3. Pre-Spectrometer

The pre-spectrometer has a length of 3.38m and an inner diameter of 1.68m(1.70m outer diameter) and has a cylindrical shape. It acts as an electron pre-filter. All electrons with an energy below 18.3keV are rejected. The electrons with an energy above that hurdle can enter the main spectrometer. The electron flux is reduced by a factor of 10^{-6}. This is necessary to reduce the likelihood of scattering electrons or residual gas molecules, which leads to an increased background. In the past the pre-spectromter served as a prototype for the main spectrometer.

3.1.4. Main Spectrometer

The main spectrometer is a vessel with an inner diameter of 9.8m and a length of 23.28m. This results into a volume of 1400m^3 and a mass of approximately 200tons. The electrons coming from the pre-spectrometer have a flux of $10^4/s$, these are guided adiabatically by a strong inhomogenous magnetic field (see MAC-E-Filter page 21), that is generated by two superconducting solenoids. The huge proportions are necessary as the flux tube expands to a diameter of 9m in the analysing plane in the center of the vessel. Additionally to the superconducting solenoids, air coils will be used to compensate the earth magnetic field and to allow fine tuning of the inner magnetic field. The KATRIN experiment is aligned with an inclination of 15° with respect the south-north axis.
The tank is made of stainless steel sheets. A potential of -18.4kV will be applied to it. The

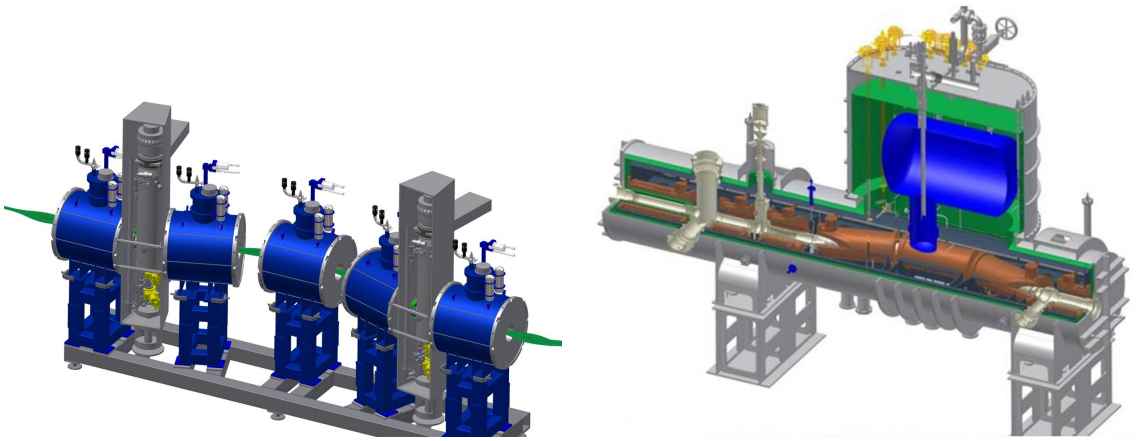

Figure 3.3.: **The transportsection with the DPS and CPS.** On the left side the DPS can be seen, figure taken from [Stu12], and on the right side the CPS, figure taken from [Gil12]

inner double layer wire electrodes will have a potential of -18.5kV respectively 18.6kV for the inner wire electrode. This creates the required retarding potential for the β electrons of the tritium decay and a background suppression of electrons, for instance from cosmic radiation. The inner wire electrode system consists of about 200 wire modules. Each has a weight of about 20-30kg and these were installed through the large flanges. The electrodes are mounted via insulators to the wall.

3.1.5. Detector

Electrons, that pass the analysing plane have to be detected at the FPD. Therefore the electrons are accelerated to their initial energy and magnetically guided by two magnets(pinch and detector magnet) to the detector. The FPD is a semiconductor detector and consists of 148 pixels made of one wafer. Each pixel has the same area with 44mm^2. The wafer is placed in the center of the detector magnet with a diameter of 125mm [A$^+$12].

The FPD has to be able to detect the 18.6keV electrons from the tritium beta decay, conversion electrons from ^{83}Kr (8 to 32keV) and electrons from an electron gun. Hence, the detection efficiency has to be very high in a huge range from low energies to high energies. Additionally it is possible to use the post acceleration electrode to accelerate the electrons further up to 30kV. The detector is very efficient in the 5keV to 50keV range and low energy electrons can be accelerated to that energy region with the post acceleration electrode.

As the expected count rate of electrons from the tritium beta decay close to the endpoint is very low, it is important to have an effective background suppression and sufficient energy resolution. Through the segmentation of the detector, it is possible to derive the x- and y-coordinates of an electron and thus calculated its origin, which enables background suppression of particles outside the flux tube. Additionally veto systems are installed to remove further background.
The high energy resolution is not necessary for measuring the actual energy of the electrons from the beta decay, this is done by the filter voltage on the main spectrometer, but to discriminate background even further. It is expected, that there will be a continuous background in the desired range of the detector (5-50keV) induced by betas and gammas. This could harm the sensitivity of KATRIN and therefore an energy resolution of

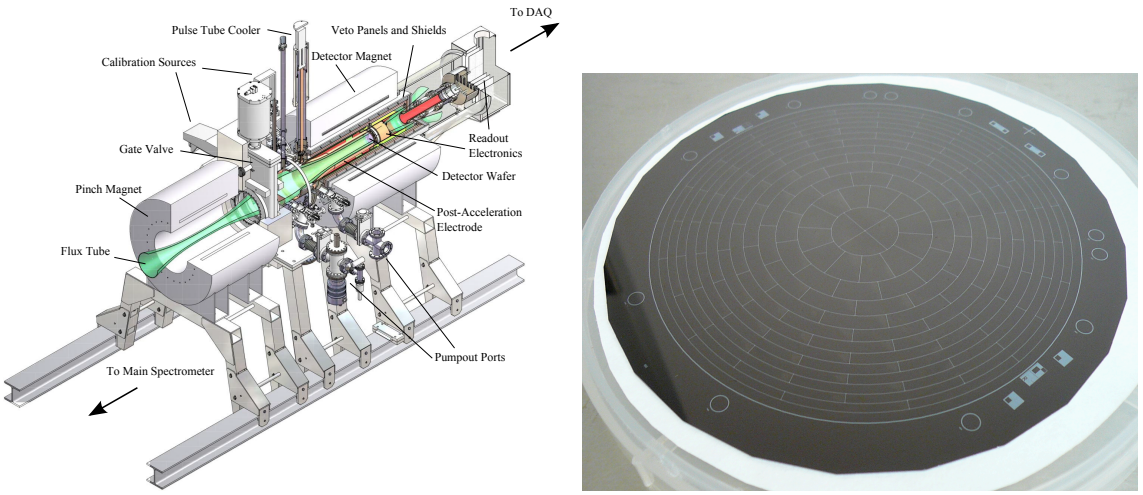

Figure 3.4.: **The Focal Plane Detector and the Detector Wafer.** On the left the FPD with its components can be seen and on the right side the wafer with its detector segments. The figures are taken from [Har12]

$\Delta E \leq 600\text{eV}(\text{FWHM}^1)$ is desired.

High energy resolution at high rates is difficult to realise. To determine the energy of one event, it is useful to increase the shaping length for these events in the read out electronics. But for high rates the shaping length has to be decreased to have a higher detection rate. This is still a problem for the planned electron gun measurements with the detector as these have a high frequency($\approx$ 100kHz) and require a high energy resolution.

An overview of the FPD can be seen in figure 3.4 and the current status of the wafer and its pixels in figure 3.5.

3.2. MAC-E-Filter

In principle it is sufficient to generate an experimental setup with a retarding potential, that isolates the electrons from the tritium beta decay at the endpoint from lower energy electrons. But as the electrons are emitted isotropically, a high activity source would be required and the measurement time would still be long. The solution is the MAC-E-Filter, that enables an acceptance angle of up to 2π.
Furthermore, there is a lot of experience with the MAC-E-Filter as it was already used in Mainz and Troitsk. Both used the beta decay to derive an upper limit for the neutrino mass. These experiments are a solid basis for KATRIN and showed, that the MAC-E-Filter measurement principle works.

The MAC-E-Filter consists of two superconducting solenoids. These create an inhomogenous magnetic field, which has its maxima in the center of the solenoids and a minimum in the analysing plane, between both solenoids. In case of the main spectrometer the solenoids have a magnetic field of 4.5T with a maximum of 6T and in the analysing plane a field of 3G.
The electrons are guided through this magnetic field and perform a cyclotron motion. The proportions of the spectrometer is very huge, hence although the magnetic field drops many magnitudes, the variation of the magnetic field over one cyclotron turn is small.

[1] Full Width Half Maximum

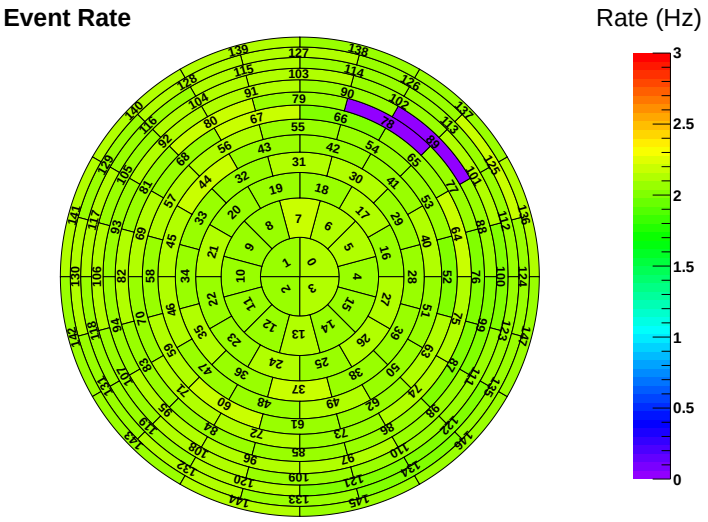

Figure 3.5.: **Measurement of an americium source with the FPD.** This figure shows the rate on each pixel with an americium source, that is very homogeneous. There are also two broken pixels, these are probably shorted on the wafer. [Har13]

Thus the magnetic moment μ, which is given by:

$$\mu = \frac{E_\perp}{B} = const. \tag{3.1}$$

is constant. This leads to a transformation of the perpendicular energy, the cyclotron energy, into longitudinal energy. Hence, in the analysing plane, almost all the energy is within the longitudinal part. If this energy is sufficient to pass the electrostatic potential, these are re-accelerated and collimated onto the detector.

The sharpness ΔE of this integrating high-energy filter can be derived from equation 3.1:

$$\Delta E = \frac{B_A}{B_{max}} \cdot E_0 \tag{3.2}$$

See figure 3.6 for naming convention of the variables. This means, that the sharpness is dependent on the ratio of B_A/B_{max} only and an ideal integrating high-energy filter with maximum sharpness would require $B_A = 0$. This cannot be realised in an experiment. The ideal filter looks like a heaviside function, but in reality it is smeared out by ΔE. According to equation 3.2 and considering the tritium endpoint (18.6keV), the main spectrometer has a resolution of:

$$\Delta E = 0.93eV \tag{3.3}$$

It is also possible to suppress electrons with a large scattering probability (long path) in the source. This is done with a magnetic field B_S (see figure 3.6), that is 3.6T and hence lower than B_{max} with 6T. This magnetic mirror works the same way as the spectrometer from the analysing plane to the second solenoid. The perpendicular momentum increases and if the maximum is reached, the electron is rejected. This leads to a maximal acceptance angle of:

$$\sin\theta_{max} = \sqrt{\frac{B_S}{B_{max}}} = 50.77° \tag{3.4}$$

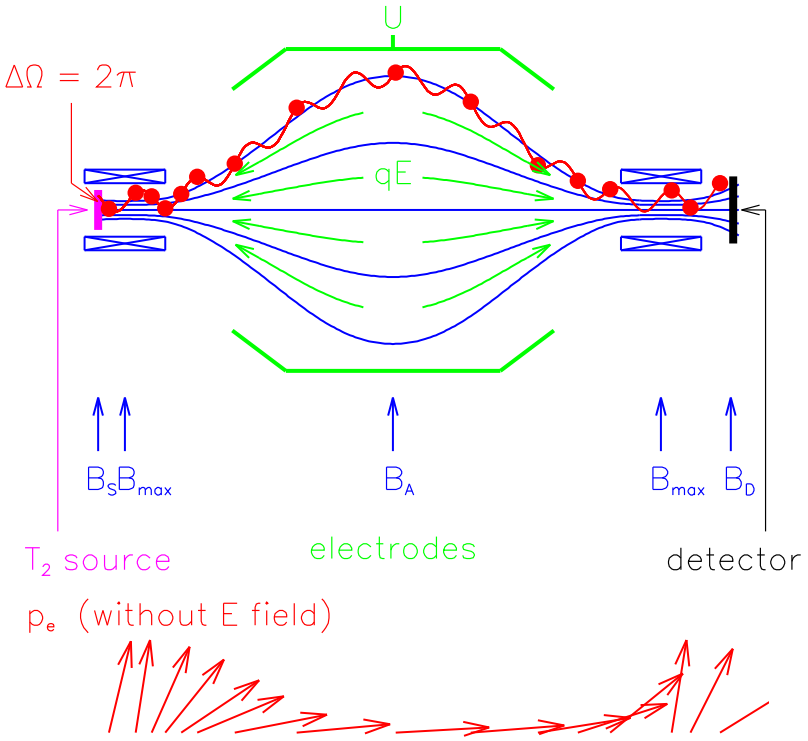

Figure 3.6.: **Working principle MAC-E-Filter.** In the top left an electron entering the MAC-E-Filter can be seen (red). The blue lines show the magnetic field, produced by the two superconducting solenoids in the very left and right. The electron is performing a cyclotron motion caused by the magnetic field. In the center (the analysing plane), the cyclotron motion subsided and the electron may jump over the electrostatical barrier U and can be re-accelerated again. In the bottom of this figure, the behaviour of the perpendicular momentum can be seen. This figure is taken from [Kat05] page 35.

With these information, the analytical transmission function of an isotropical emitting source can be determined:

$$T(E,qU) = \begin{cases} 0 & E - qU < 0 \\ \dfrac{1-\sqrt{1-\frac{E-qU}{E}\cdot\frac{B_S}{B_A}}}{1-\sqrt{1-\frac{\Delta E}{E}\cdot\frac{B_S}{B_A}}} & 0 \leq E - qU \leq \Delta E \\ 1 & E - qU > \Delta E \end{cases} \tag{3.5}$$

with E as the energy of the electrons, q the charge of the electron and U the retarding potential.

3.3. High Voltage Monitoring

The electrons of the tritium beta decay at the endpoint are filtered by the retarding voltage of the spectrometers. Hence, it is necessary to know the voltage very precisely. Already little fluctuations have an influence on the neutrino mass. A smearing of the retarding potential with a Gaussian variance σ^2 results into a systematic shift of:

$$\Delta m_\nu^2 = -2\sigma^2 \tag{3.6}$$

A shift lower than 0.007eV^2 [Zbo11], results into an error of the voltage of $\sigma \leq 0.059\text{eV}$, which is a relative error of 3.17ppm at the tritium endpoint of 18.6keV.

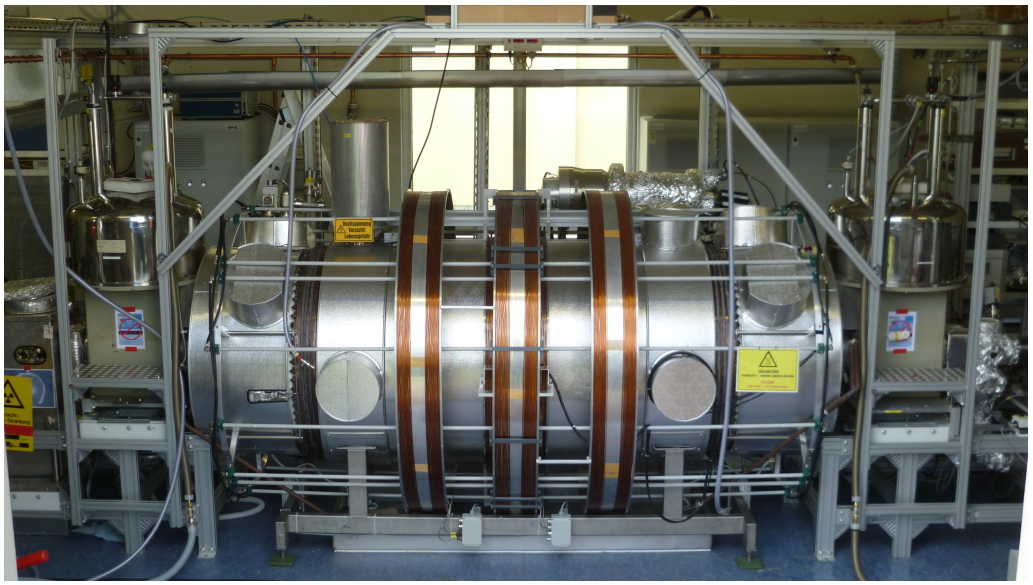

Figure 3.7.: **The monitor spectrometer.** This figure shows the monitor-spectrometer in the building 461 at KIT. On the very left is the source, followed by the spectrometer vessel with the air coils and the detector on the very right. At both ends of the spectrometer vessel, behind the ladders, the shielding of the solenoids can be seen. This figure is taken from [Erh12].

Therefore the KATRIN experiment requires a precise short term stability as well as a method to guarantee the stability over years ($\approx$ 3.17ppm). Besides the precision the accuracy has to be very high as well. A shift of the retarding voltage of 0.05eV leads to systematic error of the fitted neutrino mass of 0.04eV.

There are no voltmeters, that are precise enough to measure 18.6kV directly. Commercially available voltmeters are most precise in the 10V range. Therefore a very precise high voltage divider are required. For KATRIN there will be two high voltage dividers, K-35 and K-65 [Thü07]. Additionally a second spectrometer will be installed. It is based on the MAC-E-Filter principle as well, but this time the requirements on the spectrometer are different. The same voltage, applied on the main spectrometer will be applied on this external spectrometer. It can validate the voltage stability by means of a nuclear standard. That is especially important for long term measurements. It is called the monitor spectrometer. There will be an introduction to the monitor spectrometer in the next section.

3.4. Monitor Spectrometer

As this thesis is mainly based on the work at the monitor spectrometer (see figure 3.7), a short introduction will be given.
The retarding voltage on the main spectrometer vessel will be identical to the retarding voltage on the monitor spectrometer. Therefore K-32 conversion electrons from the ^{83}Rb/^{83m}Kr source with an energy of 17.8keV will be accelerated to leap the retarding voltage of 18.6kV. Therefrom the line position in dependence on the retarding voltage and accelerating voltage can be derived and if the line position does not change, the retarding voltage is stable.

In the following some components of the monitor spectrometer will be explained. If not stated differently, this section is based on [Erh12].

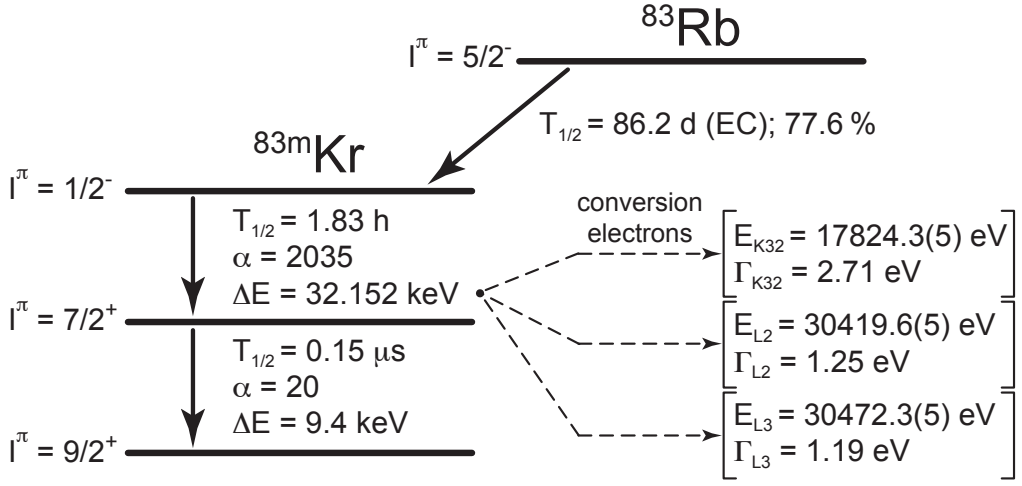

Figure 3.8.: **Rubidium decay.** After about 86 days ^{83}Rb decays to ^{83m}Kr by electron capture. As ^{83m}Kr is not stable it decays also, one conversion line , K-32, will be used at the monitor spectrometer. It has an intensity of 17% [Zbo11]. This figure is taken from [Wie12].

3.4.1. Sources

At the monitor spectrometer ^{83}Rb/^{83m}Kr will be used as source material. For monitoring the retarding voltage of the main spectrometer at about 18.6kV, it is necessary to use a source, that emits electrons close to the tritium endpoint.
Through electron capture ^{83}Rb decays to ^{83m}Kr, that can reach its ground state by internal conversion or gamma emission. One line, that originates from the conversion, will be used at the monitor spectrometer (see figure 3.8). The electrons have an energy of about 17.8keV, which means that they have to be accelerated by 800V to leap the 18.6kV retarding voltage. In comparison to the retarding voltage, the accelerating voltage with about 800V can be measured very precisely with a 8.5 digit voltmeter. If this is not sufficient a high voltage divider can be used.

The rubidium is ion-implanted in a solid (commonly platinum foils). This can be inserted into the source chamber on the source holder. It is possible to insert four source holder into the source chamber at the same time.
The entire source is placed on a cross table, that enables the experimenter to move the source in z-direction, that means in the direction of the beamline to different magnetic fields as well as to move it into the x- and y- direction to position each of the four sources in the center of the flux tube.

Besides, it is possible to apply a voltage to each source separately, so that the energy of the electrons can be matched to the potential on the main spectrometer. During the course of this thesis, the source voltage combined with the retarding voltage was tested and the results can be found in chapter 5.

3.4.2. Spectrometer

The spectrometer tank has a length of three meters and a diameter of one meter. The working principle is identical to the main spectrometer. The difference is, that there is no potential on the outer wall, but there are wire electrodes and solid electrodes (see figure 3.9).

The solid electrodes are in between the outer wall and the wire electrodes. These are

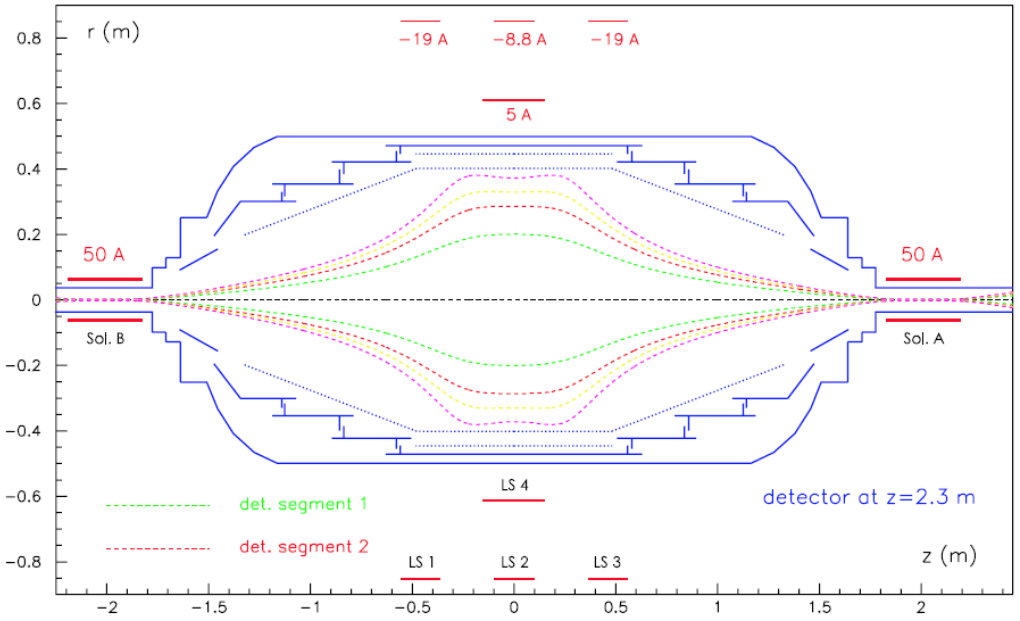

Figure 3.9.: **Magnetic field of the Monitor Spectrometer.** This figure shows the magnetic field of the spectrometer and its components. Towards the outer wall, the wire electrodes and solid electrodes can be seen. On the very left and right are the superconducting solenoids and in the bottom and top the air coils with its currents can be seen. This figure represents the spectrometer, still in the Mainz setup. It is taken from [Thü07].

stepped and arranged cylindrically. That means, that the distance from top to bottom electrode increases towards the analysing plane from both sides. The wire electrodes are arranged as a bilayer in the analysing plane and narrow cylindrically towards the solenoids. The monitor spectrometer was designed to apply different voltages to the solid and wire electrodes. This is very useful to prevent charged particles from the outside for instance cosmic radiation to hit the outer wall and produce secondaries, that can enter the flux tube. The hitrate at the monitor spectrometer from conversion electrons of the source is very high, for this reason both electrodes are set on the same voltage.

3.4.3. Solenoids

At both ends of the spectrometer, in a distance of 2.01m to the analysing plane, solenoids are placed. At a current of 50A, they produce a magnetic field of 6T. Therefore they need to be superconducting and to be operated at 4.2K, which makes liquid helium necessary. To lose as little helium as possible, a liquid nitrogen and vacuum shield is installed.

3.4.4. Low Field Correction System

The task of the Low Field Correction System (LFCS) is to correct of the magnetic field, produced by the two solenoids, so that the magnetic field in the analysing plane of the desired 3G is achieved.
The LFCS consists of four air coils surrounding the spectrometer. These can be seen in the top and bottom of figure 3.9.

3.4.5. Earth Magnetic Field Compensation System

To compensate the magnetic field of the earth, the Earth Magnetic Field Compensation System (EMCS) is installed.

The earth magnetic field in Karlsruhe is 0.5G[2], which is 1/6 of 3G in the analysing plane and has to be corrected.

3.4.6. Detector

The detector consists of five semi-conductor PIN diodes. They are arranged like a cross with one central pixel. The four outer pixels are Hamamatsu S3590-09 PIN diodes, used to align the detector on the spectrometer axis. For spectroscopy only the central pixel, a Canberra PD150-12-500AM, is used. The cross is aligned in vertically(north-south) and horizontal(east-west) direction, hence if the outer pixels show the same hitrate the central pixel is aligned accordingly to the flux tube. To change the position of the detector, it is possible to move it in x-,y- and z-direction.
This setup is very different to the Mainz setup. The Mainz detector had five circular elements, each with a size of $1cm^2$. The new setup eases the replacement of broken detectors [Gou10].

[2] 48270.9 nT total intensity, February 2013 [Hel13]

4. Slow Control of KATRIN

The KATRIN Experiment is going to use ORCA (**O**bject-oriented **R**eal-time **C**ontrol and **A**cquisition) for data acquisition and slow control. The advantage of ORCA is, that it uses a client/server model and separates the hardware controlling computers from the user interface computers. Therefore we have a system that is taking and processing the data while there can be multiple remote clients to control them [Kat05]. Since 2011 data taking has been working fine at the monitor spectrometer using ORCA. But the slow control was still done by a program written in LabVIEW™ by Michael Schupp [Sch11]. It was directly connected to all necessary devices, and so did not fulfill the KATRIN requirements to be an independent, remote controllable system. One main task of this thesis is to switch to an ORCA based slow control and to automatise monitor spectrometer measurements, which is described in this chapter.

4.1. Introduction to ORCA

ORCA evolved from SHaRC(SNO hardware acquisition and real-time control), which was developed by John Wilkerson and Frank McGirt at LANL(Los Alamos National Lab) in the 1980s. Work on ORCA started at CENPA(Center for Nuclear Physics and Astrophysics) at the University of Washington in 2002. It was written almost entirely by Mark Howe, who was also working on SHaRC in the 1990s [How13].

ORCA is running on MacOS® X and is written in Objective-C using the MacOS X Cocoa application framework. Its goal is on the one hand to create a data acquisition and control system general purpose software, that is easy to use, but on the other hand it should be highly modular, object oriented and easy to develop and maintain. To realise that, the design pattern of ORCA is based on MVC(model view controller). In ORCA a "model" is an independent software module, which can be a data analysis module, a data acquisition task or directly a model corresponding to hardware. The "view" is a user interface element, that is displaying model's data while the "controller" passes data from the model to the view and user interface commands from the view to the model. Usually one piece of model, view and controller represent one piece of hardware [HCH+04].

For the ease of use ORCA has a graphical user interface, that can be controlled by a computer mouse. The configuration window is the main window in ORCA, see figure 4.1. Initially it is empty and the user has to add new objects on its own or use pre-configured setups. Objects are selected from the ORCA catalog. The user can drag and

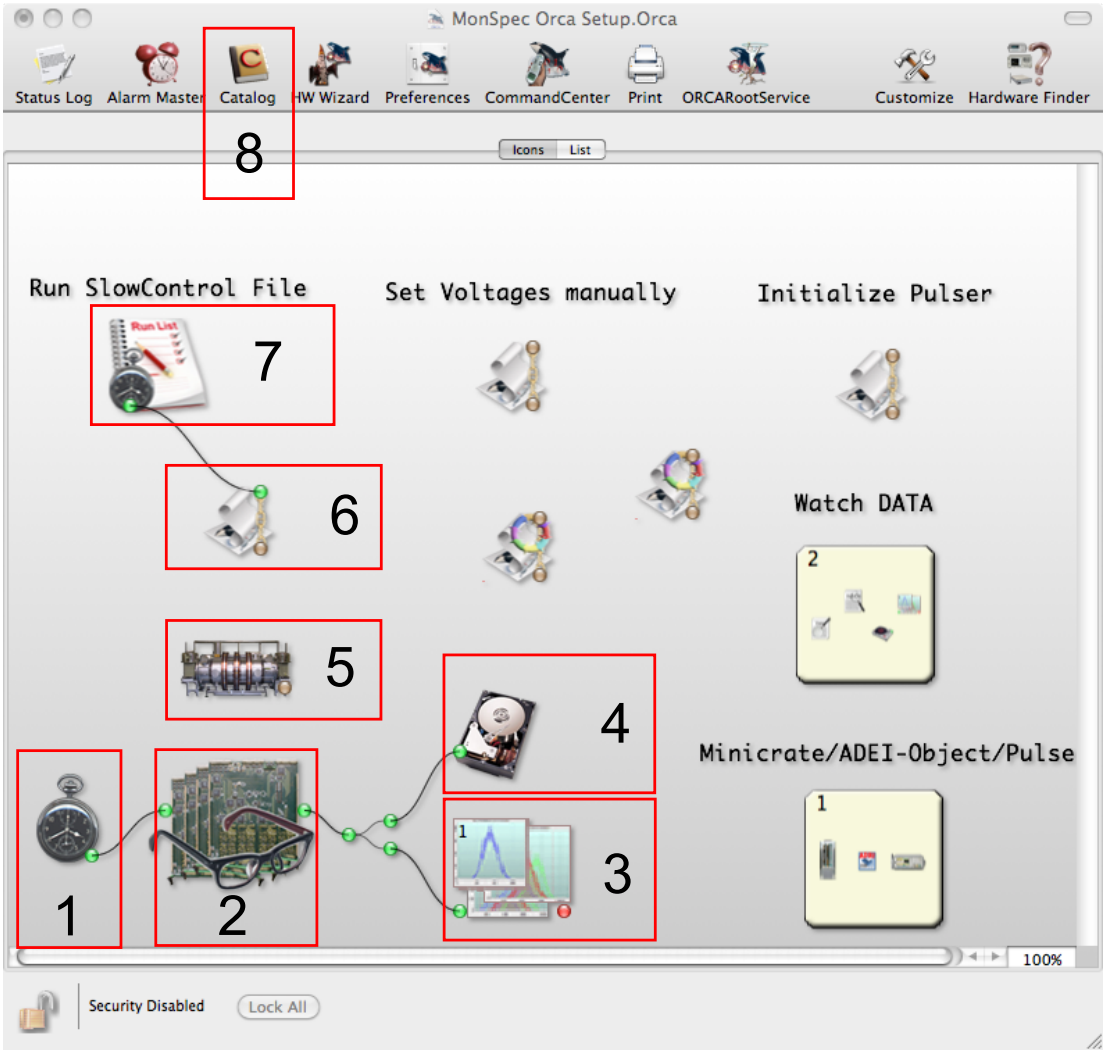

Figure 4.1.: **Overview of the experimental setup at the monitor spectrometer in ORCA (configuration window).** Each icon represents a piece of hardware, a data acquisition task or an analysis module. From this panel the whole measurement can be controlled. The numbered areas are described on page 30

drop new objects from the catalog to the experimental setup in the main window. A detailed description of the most important objects for KATRIN in the example of the monitor spectrometer (see 4.1) follows below.

The description refers partly to [How13]. A picture of of each marked object can be found in the appendix.

ORCA Object Description:

1. **Run Control:** (A.1)
   The main function of Run Control is to start and stop a run, but it is more powerful than just that. The user is able to set Run Numbers, to chose Run Types, for instance the Run Type "Maintenance" enables the user to change values, which are usually fixed while running. These options can be found in the Setup Drawers. Additionally there is Sub Run Control, where the user finds two buttons, one to end sub runs and one to start new sub runs. The last settings are the Run Options. The user can execute ORCA Scripts at run start and run end, set the Run Timer, enable or disable the Repeat run button and checkmark, whether it is a normal or offline

run(offline runs are not saved).

2. **Data Readout:** (A.2)
   This object determines where the data is taken from. It can also output the Readout Rate and display data that is read out but not yet processed in a histogram. For KATRIN the data will be retrieved from a crate, which is one of the IPE-DAQ-V3-, the IPE-DAQ-V4- or the V4-Mini-Crates, the latter one is used at the monitor spectrometer. These crates can be equipped with FLT(First Level Trigger) and SLT(Second Level Trigger) Cards.

3. **Data Monitor:** (A.3)
   The Data Monitor enables the user to take a look at data of all FLT channels (24 per card) online. When the user double clicks on one channel a graph is displayed that plots the counts on the y-axis and the energy on the x-axis. The energy calibration has to be done manually in ORCA. Additionally the Data Monitor has three options:

   - Write (IGOR) Histograms:
     If this option is enabled the Data Monitor will output the data to a file in ascii form. Usually this is deactivated and not necessary for KATRIN.

   - Ship Final Histograms:
     This option accumulates all histograms until the run is finished and ships it then. This option does exist on the FLT card also and was deployed when not using sub runs. This gives small but many output files. Unfortunately it does not work with sub runs yet (see 4.5.1).

   - Accumulate:
     If this option is enabled, the histograms are not cleared at the end of a run.

4. **Data Storage:** (A.4)
   This object determines where the data are saved. There are three different types of data, the run data, the log files and the config files. Each file destination can be set in that object. Additionally the directory structure and a run file prefix can be chosen.

5. **Monitor Spectrometer:** (A.5)
   The monitor spectrometer object consists of a graphical interface, that shows an image of the detector at the monitor spectrometer. If every detector is connected to the correct FLT card channel, this object is capable to show the rates on each channel to the user in real time. There are equivalent ORCA objects for the FPD(Focal Plane Detector). Additionally the user can start and stop a run in that object as well as set the run time and chose between offline and normal runs.

6. **ORCA Script:** (A.6)
   The ORCAScript is a very powerful object. It can access objects and perform the same operations with these objects as a standard user and even more. Scripts are very useful for the automatisation of measurements. These scripts are used at the monitor spectrometer to set and change values, for instance the voltage on the vessel or the offset voltage on the sources.

7. **Run List:** (A.7)
   This object is used for Run Control at the monitor spectrometer. It is able to read ".csv" files, these files contain all necessary information about a run at the monitor spectrometer and the run is totally controlled by that object. An execution count controls how often the Run List is repeated.

8. **Catalog:** (A.9)
   The catolog contains all objects existing in ORCA. These can be dragged and dropped to the configuration window.

There are different connections between objects in ORCA. On the one hand we have objects, that access other objects directly, for instance the monitor spectrometer object and the FLT object or the ORCA Script. On the other hand we have chains, for instance the data chain from Run Control to the Data Readout and from there to the Data Monitor and Storage object. The output of one object is always connected to the input of another object like the Run List to an ORCA Script, this special data chain contains set values for the voltages for instance.

There are two more important objects not discussed so far. These are the IPE Slow Control object (A.8) and the V4-Mini-Crate. In figure 4.1 these are placed in the Minicrate/ADEI-Object/Pulser container, just because it is not necessary to edit them by hand and it improves the clearness of the experimental setup. The crate has already been mentioned at the Data Readout (see page 31) and it is, in case of the monitor spectrometer, responsible to read six channels (five are used for the detector and and one channel is reading a pulser) from one FLT card and transfer the data to ORCA via the SLT card. The IPE Slow Control object enables the user to write data to ADEI-control, which is necessary to perform slow control with ORCA. Within that object the user has to enter the ADEI address and derive the sensor and control channels from it. Now the user is able to select sensors, for just reading values or control channels by setting values. The channels can be dragged and dropped to the IPE Slow Control object. Read only channels are marked in blue, writable control channels in red. There will be a more extensive explanation of slow control in the next section 4.2.

4.2. Overview of the Server System

As the KATRIN experiment requires a lot of sensor and controller data, an elaborate server system is required. An overview, in case of the monitor spectrometer, is given in figure 4.2. All components in this figure are within the KATRIN network.
On the left side of this figure the ORCA slow control data chain is shown. The slow control data is send from ORCA to ADEI(Advanced Data Extraction Interface) control, which is a Linux server. This data is forwarded to ZEUS(ZEntrale datenerfassung Und Steuerung)[1]. At the moment there are four different ZEUS servers at the KATRIN experiment, one for the detector, the high voltage, the air coils and one for the monitor spectrometer. These ZEUS servers are running on Windows® XP and consist of three components. The HMI(Human Machine Interface) proxy, that enables ADEI control to communicate with ZEUS and the HMI, which is able to read and derive set values from a web interface. The connection to the cFP™ (compact Field Point) is established by the third component, the ZEUS engine. It enables to set values to the cFP and read sensor data. The cFP is running on VxWorks®, has a network controller and an eight slot backplane[A+12]. At the monitor spectrometer the cFP is communicating to the high voltage power supplies and the voltmeter. It is planned to integrate the air coil control also. The set values and current values read by the field point are stored into a MSSQL(Microsoft Structured Query Language) database via ZEUS.

4.3. Run Control of the Monitor Spectrometer

Initially a LabVIEW program written by Michael Schupp [Sch11] was used for Run Control. It was running on a Windows machine in the monitor spectrometer building and

[1] Central DAQ and Control System

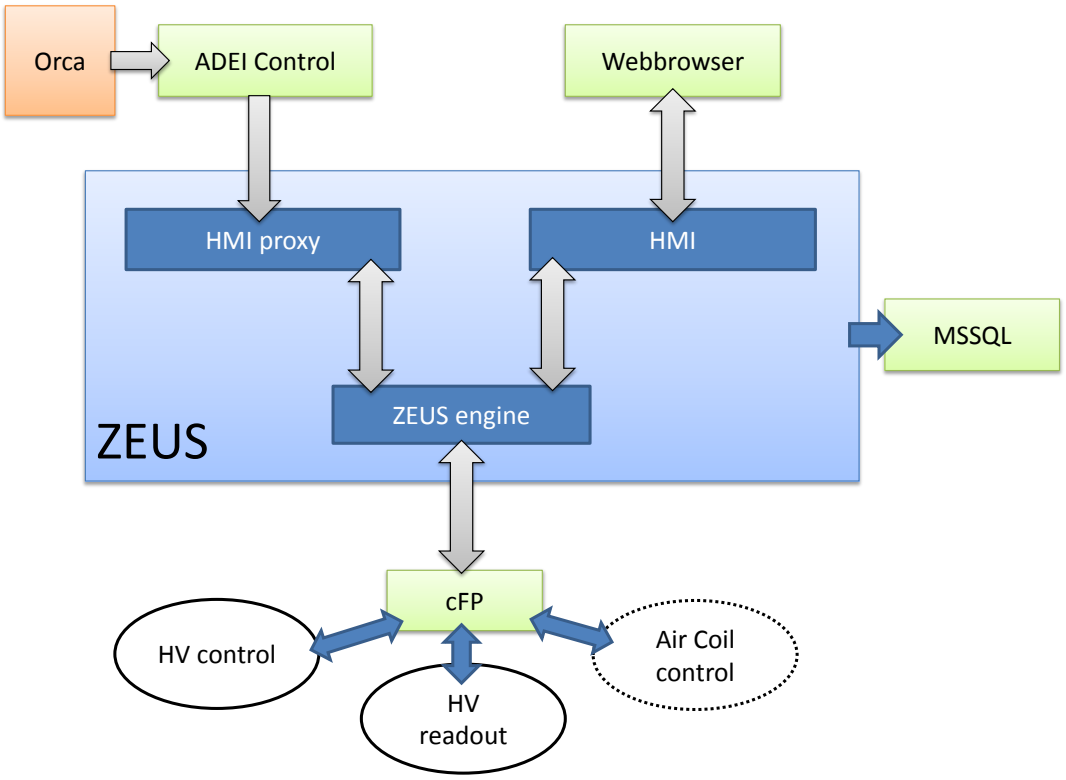

Figure 4.2.: **Overview of the slow control server structure at KATRIN.** On the left hand side this figure shows the data flow of slow control values from ORCA to the compact Field Point. The right side shows the data flow from the Webbrowser to the compact Field Point. The current and set values are saved in a MSSQL database.[Chi13]

able to communicate with all necessary hardware devices, ORCA and the IPE(Institut für Prozessdatenverarbeitung und Elektronik)[2] Database. The program was able to read Excel® files, which were used to set all parameters. These parameters are the set values of the voltage, the waiting time between runs while the voltage is set and the measurement time. As data from the crate is recorded by ORCA, the LabVIEW program had to be able to control ORCA and set ORCA parameters remotely. The connection to the hardware was realised through direct connections to the devices, for instance a serial line to the high voltage power supply from the Windows machine to the device or via Ethernet to the GPIB converters connected to the voltmeters and to the MAC Mini running ORCA.

Because there were constantly measurements at the monitor spectrometer the implementation of Run Control with ORCA had to be smooth and user friendly as well as instantly during measurement pauses. The only problem was the high voltage power supply, which is absolutely necessary for measurements at the monitor spectrometer and had to be integrated into the Field Point still. The final integration caused some days of no measurements. The overall idea was to keep the measurement control simple and alike the measurement control with LabVIEW, which was proven to be convenient.
A so called scan is controlled by an appropriate run list which contains all required parameters. The run list is read from a "*.csv" file, which can be produced with most spread sheet programs. Spread sheet functionality is very helpful to create run lists. For each set of measurement parameters (e.g. for each voltage step) a line in the run list is required.

[2]Institute for Data Processing and Electronics

The parameters are explained below in more detail. They are all stored in the database.

1. **Line Number:**
   The Line Number is useful for the analysis only, it counts up and down for one line scan up/down or down/up.

2. **Voltage:**
   This is the set voltage for the high voltage power supply, that puts voltage on the vessel.

3. **Waiting Time:**
   Defines the time between runs/sub runs. Within this time, a new HV-value is set and stabilized when properly chosen. (see 4.5.1).

4. **Run Time:**
   This sets the length of a run in ORCA and is therefore the measurement time.

Two additional columns had to be added:

5. **Voltage on the Source:**
   The slow control has to be able to set offset voltages on an additional Power Supply. This is necessary during KATRIN measurements.

6. **Sub Run:**
   This option enables the user to control whether a new run should start or if the following set points do still belong to the previous run as a sub run. If the user wants to start a new run a "0" has to be entered into that column and line and for the following sub runs a "1" .

For OpenOffice™ a macro and a template is provided, which outputs the active sheet in the correct ".csv" format. The data is saved in "∼/Measurement" and the file name is the name of the active sheet. Now it can be read by the Run List. If the user has done everything correctly it should look like in figure A.7. By clicking the start button all script parameters are sent to a script. This script sends the set values for the voltages to ADEI control as well as the current line and run number. Afterwards it waits until the set waiting time has passed. This marks also a little difference to the old program. The waiting time has to be increased a little bit, because it includes the time the current value needs to reach the set value.
When the script is finished, the Run List starts a run with its given parameters. Usually for the first run the sub run box is not check marked although it does not make any difference for the first run, because a new run is started anyways. All settings from the crate object are written to the crate, at the monitor spectrometer, as we are measuring in histogram mode, it is very important to check the histogram length on the FLT card. The longer they are, the smaller the output data becomes, which is good in the first place. But this has one huge side effect, the histogram length influences the measurement time at one point and also the time between runs/sub runs. The reason for this is, that the crate sends a histogram always in the same interval, thus ORCA Run Control waits after the set measurement time for the next histogram to finish that run, because one does not want one histogram at different set values. Hence the histogram length has to be synchronized with the Run Length. Additionally the histogram length influences the time between runs/sub runs, because ORCA waits for a histogram to be received before starting the next run/sub run. Thus it has to be synchronized with the time between runs/sub runs also, this is even the more important part as the experimenter wants to lose as less time as possible between runs/sub runs. At the moment the waiting time is set to 13 seconds, because it takes one second for the set value to reach the power supply, then it has to change the value and the experimenter has to wait for the voltmeters to retrieve the correct values as these have an

integration time of about 3-4s. For the histogram length four seconds turned out to be a good number.
After the last histogram of the first run is retrieved the Run List jumps into the next line executes the Script again with the parameters given there. After the script finished the Run List waits for the next histogram and starts a new sub run afterwards, if the sub run box is check marked or a new run. At the monitor spectrometer one run equals one line scan with as many sub runs as the user wants data points.

4.4. ORCA Scripting

At the monitor spectrometer the ORCA Script needs to be able to access the IPE Slow Control Object and the Run Control. The Script that was used until December 2012 can be found in figure 4.3. The operating principle is described in the following enumeration, which refers to the ORCA Script figure.

1. **function main(arg):**
   In ORCA Scripting it is possible to define functions. These functions may have arguments as in the case of the monitor spectrometer the function main(arg) has the argument "runList". As described in section 4.3 the input of this Script object is connected to the output of the Run List and the Script parameters are sent to the Script in an array, which is called "runList". In ORCA Scripting it is absolutely necessary to define at least one function, that is called "main()", because ORCA Scripts do not work without this function.

2. **find(arg):**
   The "find()" function is necessary to add objects, that are in the experimental setup in ORCA. The access to this object is shifted into a variable, it is called "ADEI" in this case. This variable links to the IPE Slow Control object. It is not necessary to look for the name of one object as they can be dragged and dropped into a script, which immediately displays its name. The name consists of the object name and the counter of objects of this kind, this is necessary because an experimental setup may use many objects of the same kind for instance several scripts or pulser objects.
   This script also accesses the Run Control to check whether the Run State is set to "Normal Run" to prevent unrecorded measurements.

3. **findChanOfControl:(arg1) path:(arg2):**
   This function shows how to access any Object defined by "find()". The variable, in this case "ADEI", has to be put in brackets and the function after one space character [ADEI findChanOfControl:()]. The possible functions for each object can either be found in the source code or by clicking the "ORCAScript Quick Guide" button, this opens another windows showing general scripting hints. In the bottom of this window a classname can be entered, the classname is just the name of the object. This lists all available functions, which is usually the fastest possibility to find desired functions. Unfortunately there are no deeper descriptions available, which makes it necessary to take a look into the source code sometimes.
   Especially when using findChanOfControl() function the script wants to find a channel in the IPE Slow Control object. For this script the channel has to be dragged and dropped previously to that object or it cannot be accessed.
   The function requires two arguments, the first one is the ADEI control address and the second one is the path on that machine to the desired control channel. It is very important to take care that only MACs have rights to write to ADEI control, where it is necessary and desired. Reading sensors with ORCA is possible from anywhere around the world using the standard external ADEI address [3]. The external ADEI

[3] http://katrin.kit.edu/adei/

has the advantage, that it can access all sensors not just the sensors read by ZEUS. This address is saved into a variable, that works the same way as the variable derived by the the "find()" function. The highlighted variable called "VoltageChanVessel" enables access to the set value for the High Voltage Power Supply on the vessel at the monitor spectrometer.

4. **queueControlSetpointForChan:(arg1) value:(arg2):**
   This is another IPE Slow Control function, that uses the "VoltageChanVessel" variable to access the control channel and queue values to that channel. It uses two variables, the first is the channel "VotageChanVessel" and the second one is the set value, that is derived from the runList array.
   It is also possible to write values directly to a channel of control with the function "postControlSetpointForChan:()", that requires identical arguments.

5. **sendSetpointRequestQueue():**
   This function does not require any arguments and sends all set values into the ADEI queue. At the monitor spectrometer this queue has six entries. Four for the high voltage power supplies, consisting of the two set values and the set commands, and the current line number as well as run number. The run number is just saved as an integer value, hence just the run numbers and not the sub runs numbers are saved.

This kind of ORCA Scripting is confusing and hard to use for future experimenters. Additionally the DAQ machine at the detector will probably not use the Run List, but control the measurements with ORCA Scripts only. Hence, every experimenter has to write his own scripts, which is made easier by an ORCA Script library package. It can be found on the Git[4] Repository [5] and all necessary functions will be included there. For the monitor spectrometer all required functions are already included and working fine. The addresses of sensors and control channels are already included, if one channel does not exist in the IPE Slow Control object it will be created automatically.
These libraries can be included via the "#import" function at the top of an ORCA Script. A list of functions can be found in the included documentation of these libraries. A description of functions (A.2) for the monitor spectrometer and the script (A.3) used right now can be found in the Appendix.

4.5. Problems and Solutions

Accompanied by the switch to ORCA run control sub runs became available. Therefore first test measurements with sub runs were done to write raw data analysis software, that is capable to handle sub runs (see 5.2.1). When a first look into the data was taken, it turned out, that the error on the voltage was large and there was one measurement point within the run files, that could not be explained. An explanation is given in this section. The monitor spectrometer has also been testing the server structure of the KATRIN experiment and its reliability. It turned out, that a lot of improvement considering slow control is still necessary. In this section problems and solutions for Run Control are discussed.

4.5.1. Sub Runs

In the beginning of measurements at the monitor spectrometer no sub runs had been used due to a missing integration of sub runs in Run Control with LabVIEW. As Run Control with ORCA had been realised, it became possible to use sub runs with the Run List. Immediately after the switch of slow control to ORCA sub runs were not used, because the Analysis Software had not been ready for it. As soon as it became possible to analyse

[4] Git is a version control system to handle projects
[5] https://nuserv.uni-muenster.de/cgit/cgit.cgi/ORCARunControl.git/

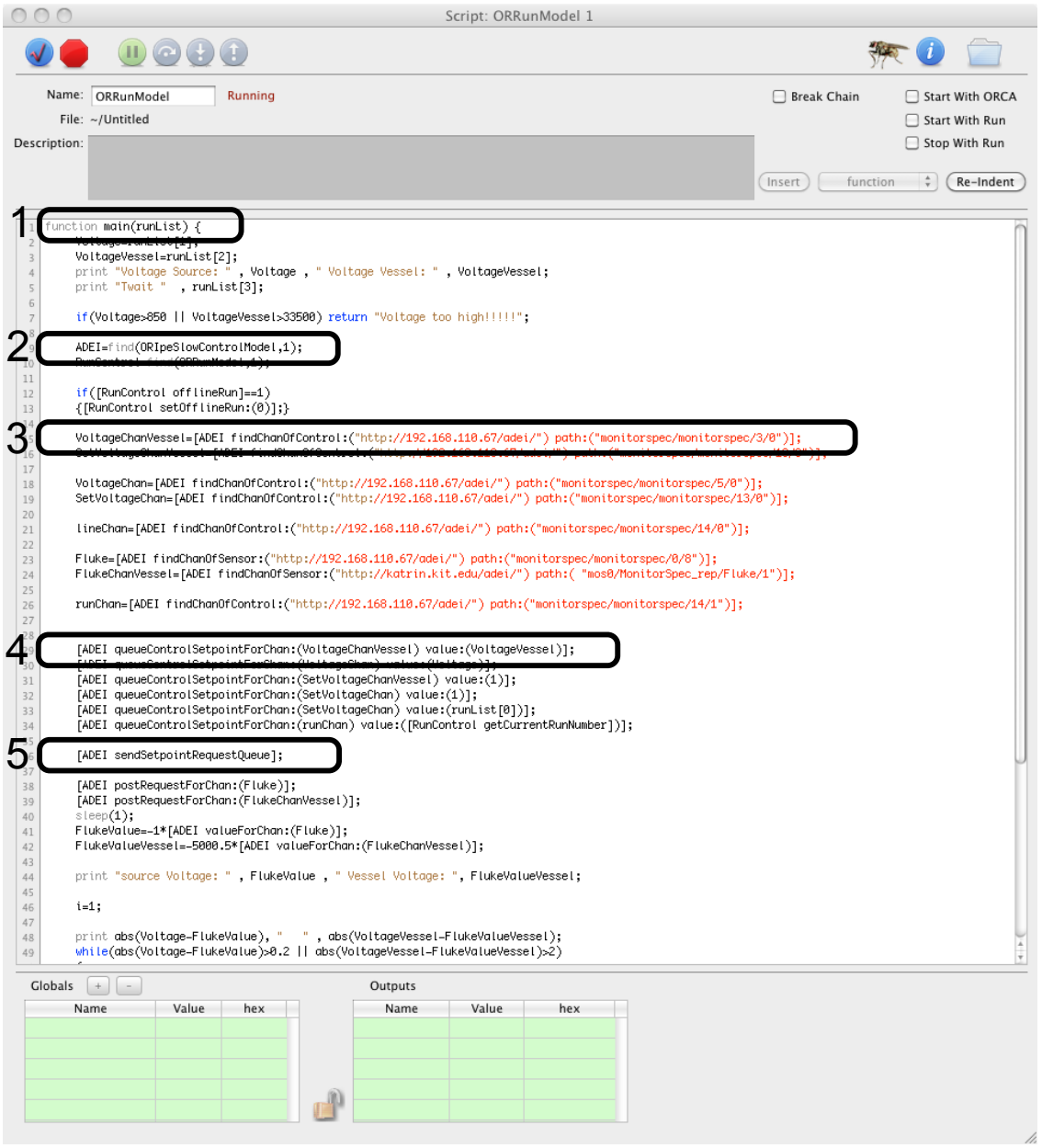

Figure 4.3.: **The ORCA Slow Control Script at the Monitor Spectrometer.** This Script is able to access the Run Control object and the IPE Slow Control object. The Script gets its parameters from the Run List. In the highlighted lines the following is written down: 1. function main(runList) 2. ADEI=find(ORIpeSlowControlModel,1); 3. VoltageChanVessel=[ADEI findChanOfControl:("http://192.168.110.67/adei/") path:("monitorspec/monitorspec/3/0")]; 4. [ADEI queueControlSetpointForChan:(VoltageChanVessel) value:(VoltageVessel)]; 5. [ADEI sendSetpointRequestQueue]; For a detailed description see page 35.

sub runs, first runs with sub runs were recorded. To make analysis easy, the idea has been that one run equals one line scan and each measurement point one sub run. The first runs have been filled with just one histogram, the reason has been a Filterscript written by Mark Howe, that has prevented histograms to be written to the output files except the last one. This makes sense for normal runs without sub runs, because all histograms are just summed up to one histogram and just this histogram is saved. This has the huge advantage, that the output files are really small and the analysis is really fast. Thus this script had to be removed from the experimental setup and additionally the option "Ship Sum"on the FLT card had to be deactivated as the last summed histogram is not necessary and consists of no useful information for analysis[6]. The histogram length has been set to two seconds and the size of such a histogram as a Raw ORCA file is about 65kB average. This means that saving all histograms requires about 114MB of hard disk space per hour. In comparison to runs without sub runs and a run time of 30s for one measurement point and the using of the Filterscript requires about 8MB only. Hence the output file is about 14 times larger than without sub runs. As a consequence the output file size has been decreased by about a factor of 2 by doubling the histogram length. Increasing the histogram length further might cause problems (see 4.3).
There is no final solution to that problem yet. It has not been possible to realise a Filtescript, that is capable to handle sub runs. The only solution might be a hard-coded solution, that would have to be realised by Mark Howe and Till Bergmann. At the moment the monitor spectrometer is using sub runs and except the size of the output files it works fine.

In the very beginning of using sub runs there has also been a problem that the Run List in ORCA has executed the trailed script immediately as the Run Length timer reached zero. This must not happen until the last histogram is received and it has been fixed by Mark Howe.

4.5.2. Timestamps

After the switch to Run Control with ORCA large errors on the voltage occurred during analysis. This has been caused by a time offset between ORCA timestamps and voltage timestamps. It turned out, that ZEUS had a time offset of ten seconds. This is caused by Windows XP, that is very inaccurate considering the local PC time. An external program called "About Time" [7], that synchronizes the ZEUS local time every sixty minutes with the local time server[8], fixed that problem.

4.5.3. Slow Control

The setting of Slow Control values via ORCA has been very problematic. About 30% of set values have been lost on the way to the Field Point with the "postControlSetpointForChan()" (see section 4.4) function. For every single control channel the values have been set one after another. One solution for this has been to write loops in ORCA Script that should wait until each current value equals its set value. This was on the one hand very slow as the current value needs some additional time to be written to ADEI. On the other hand it is not reliable as the current value read differs from the set value and the offset is not constant (see figure 4.4). The final solution is to use queues. These are much more reliable and seemed to be the final solution. During a test measurement from 22nd of December 2012 till 2nd of January 2013 about 14% of values have not been set. Within

[6] The summed histogram contains histograms between sub runs and histograms at different voltages, hence no conclusion can be derived from this histogram.
[7] http://www.arachnoid.com/abouttime/index.html
[8] IP: 141.52.8.18

this measurement the high voltage power supply has been ramped up and down from 0-32000V in 10V steps every 10s. To change the values a queue with the set value and the set command is required. The set value (from ZEUS) and the current value (K35-divider) are read back. About 13.39% of set values have reached ZEUS, but these have not been set (these are the points at ±10 and ±20 V). To check whether this problem has been caused at ZEUS and the Field Point or whether the set command as the second entry in the queue a second measurement was done. This has been done from the 4th of January till the 10th of January and just two values in a queue have been written to ZEUS. The outcome is that either both values do reach ZEUS or both are lost. The loss rate from the slow control MAC to ZEUS is 0.08% and during the christmas measurement 0.26%. On the one hand this outcome shows that using queues does not guarantee a success in changing Slow Control values and on the other hand that there is a problem between ZEUS, the Field Point and the High Voltage Power Supply. Both do require further investigation.
The same measurement has been done for the source power supply. But this time no queues have been used, the values are written directly to ADEI control with a 2s offset between them. The outcome can be seen in figure 4.5. The slow control worked fine for two days, but on one day slow control did not work reliable (red triangles).
If the loss of data between the MAC and ZEUS cannot be solved it might be useful to introduce a Field Point object to ORCA, that ORCA is able to talk to the Field Point directly, which is possible as these are within the same intranet.

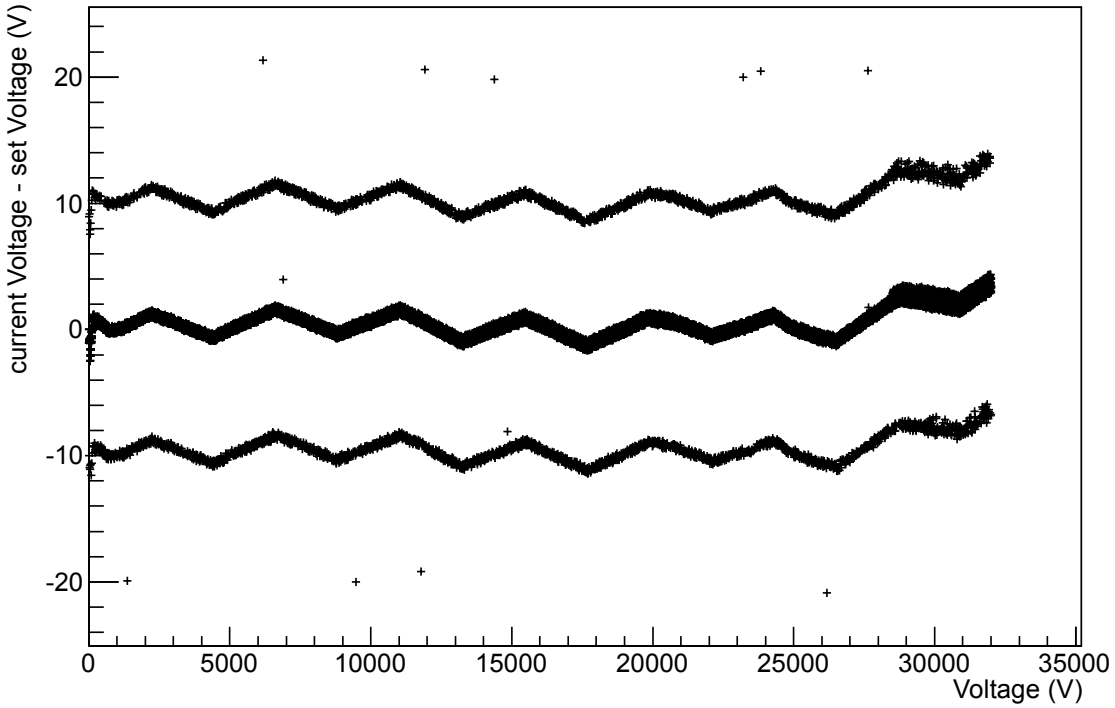

Figure 4.4.: **The behaviour of the High Voltage Power Supply** is shown in this picture. From the 22nd of December 2012 to the 2nd of January 2013 the Voltage was ramped from 0-32000V in 10V steps. On the x-axis the set voltage is drawn and on the y-axis the current voltage, read by the K35-divider, minus the set voltage is drawn. The trend is on the one hand not linear and the measurement points at ±10 and ±20 volts are set values not set by the system(about 14%). Overall the graph contains 30898 measurement points.

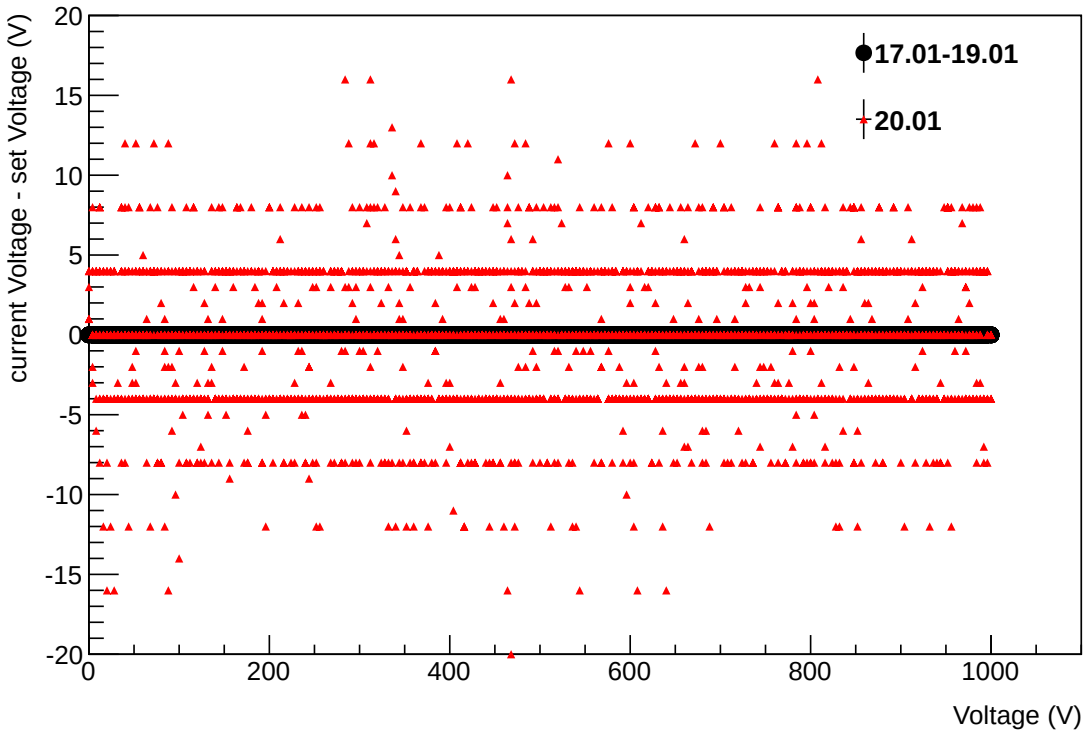

Figure 4.5.: **The behaviour of the Source Power Supply.** On the y-axis the set voltage-current voltage can be seen and on the x-axis the set voltage. The black circles show a measurement from January, 17th till January, 19th and the red triangles the measurement on January, 20th.

5. Data Analyis Software

The Analysis Software at the monitor spectrometer is splitted into two parts. On the one hand the raw data analysis, this is done by a program called "createfilterspec". It is able to connect to the KDBServer (KATRIN Database Server) through KaLi (KATRIN library) and derive the slow control data and run files from it. On the other hand a fit program called "MoS_fitter", based on a fit program from Mainz, that was rewritten by Martin Slezak and is able to handle the output files created by the createfilterspec program and to fit the output data.

As the measurement process at the monitor spectrometer is automatised with ORCA Scripts, the same is wanted for its analysis. A large amount of this thesis has been to rewrite the createfilterspec program and make it as user independent as possible. The idea is, that the raw data analysis of the monitor spectrometer is done on the server side in future and not on the local user machine. This makes analysis faster and more fail safe. In this chapter an introduction to the server structure and KaLi is given and the data analysis is described in details.

5.1. Introduction to the Server Structure

To enable the user to analyse data, the access to slow control and run data is required. The data flow is shown in figure 5.1. This figure is a direct continuation of the server structure of slow control in figure 4.2.
The slow control data from ZEUS stored in the MSSQL database (see 4.2) are replicated from the KATRIN network to a MSSQL database on a server located at the IPE. With these data also the PCS7 (Process Control System) data is stored in that MSSQL database. The database is read by ADEI and enables access to the slow control including PCS7 data. A direct link to ADEI is possible via web browser and the KATRIN DataProcessor. The data transfer between ADEI and the KDBServer, that is an integral part of the KATRIN DataProcessor, is realised with XML files.
The access to the run files is granted from the same IPE server. The MAC, on which ORCA is installed, is using the RSync[1] protocol to synchronize run data between the MAC and the harddrives within the IPE server. At the monitor spectrometer a RSync protocol is checking for new run files every minute. When new run files are uploaded to the

[1] http://rsync.samba.org/

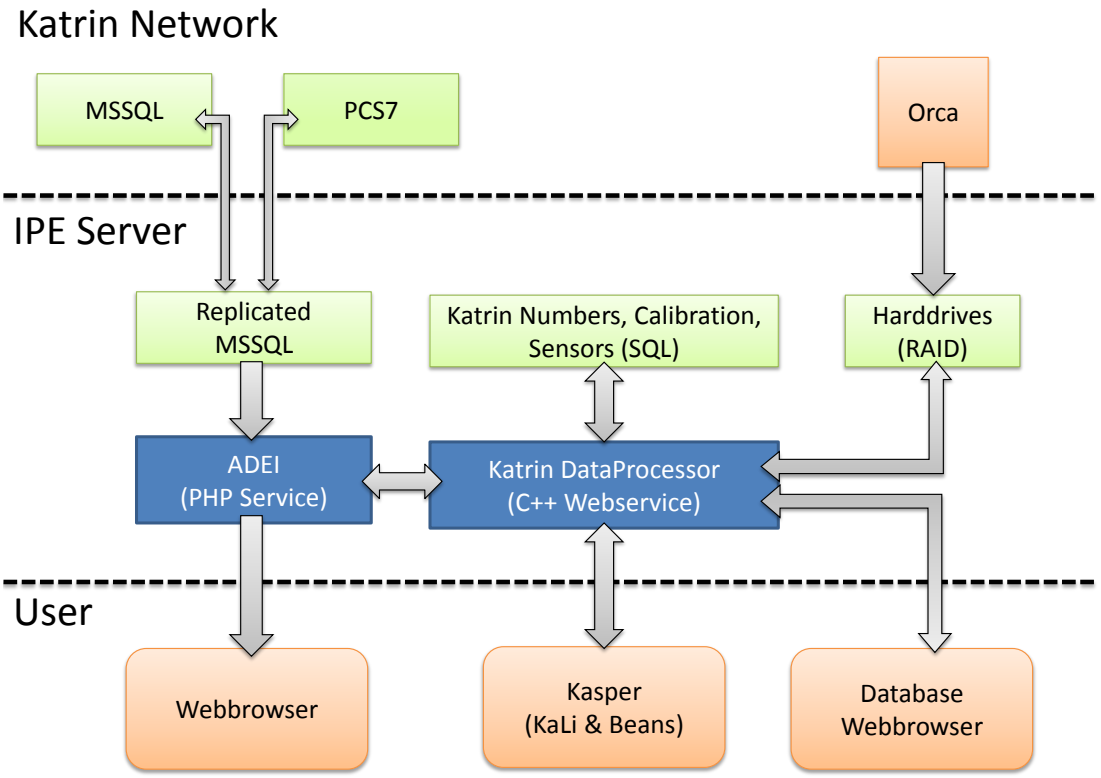

Figure 5.1.: **Overview of the server structure for data analysis of KATRIN.** The data chain can be splitted into three parts. The first is the data recording in the KATRIN network, then it is derived by the IPE server and made accessible for the user via web browser or Kasper.(The figure is adopted from [Haa12])

IPE server, a script is started, that executes ORCARoot[2], which transforms the ORCA run files to ROOT[3] files. The KATRINDataprocessor is able to access the run data via KDBORCA.
The IPE server does have an additional SQL database, this database contains the different KATRIN numbers, their calibrations and sensor addresses on ADEI. It serves also as a slow control cache. The slow control data, that was downloaded from ADEI once is stored there and enables a faster access to this data. The database can be edited and new sensors can be added with the database webbrowser.
Besides the access to the KATRIN Dataprocessor with the web browser, it is possible to access it via Kasper, which contains KaLi. KaLi is able to download run and slow control data available on the IPE server and it is able to write to the calibration database also.

5.2. The Monitor Spectrometer Analysis Software

In the course of this work the analysis of monitor spectrometer data was improved. A new program for raw data analysis incorporating new features had to be written and the Doniach-Sunjic function was introduced alongside with a new fit program. In the following a detailed description of raw data analysis and an introduction to the fit program is given.

[2]http://orca.physics.unc.edu/~markhowe/Subsystems/ORCARoot.html
[3]http://root.cern.ch/

5.2.1. Raw Data Analysis

Responsible for the raw data analysis of the Monitor Spectromter data is a program called "createfilterspec", originally written by Stefan Groh and Moritz Erhard. It was able to download runs and access slow control with KaLi data to generate the filterspectra from that data. In the following section a rewritten version of this program is presented. This version is capable to perform the same as the old program, but also supports runs including sub runs, it can output all derived data into a ROOT file, can handle offset source voltage, detects line positions automatically, finds peaks in the histograms automatically and is able to derive the source position as well as the source, that is used. The latest version can be found on the Git repository[4]. After the program is downloaded, it does need Kasper[5], which includes KaLi, and the boost[6] libraries as well as ROOT to compile.

To run createfilterspec at least one argument is required. This argument is the run number of the desired run. Specifying one argument makes sense if the run consists of sub runs, else two arguments should be used, the first one is the start run number and the second one the end run number. Two arguments do make sense for analysing old runs, that were not recorded with sub runs or if the user wants to analyse more than one run with sub runs. But the user has to be careful as start and end run number need to be exact for runs without sub runs and in case of analysing more than one run with sub runs, there may not be a run without sub runs in between. As the third argument the location of a parameterfile can be stated. The default is "parameter.txt" in the home directory of the program.

The Parameter File

The Parameter File contains the most important settings for the createfilterspec program. The current version can be found in the appendix section A.4. At the monitor spectrometer a pulser is connected to the zeroth channel of the FLT card and also to the central detector segment (channel 4). This enables dead time correction, but also the possibility to calculate the run time with it. In the parameter file the user can specify, whether a pulser is connected and its frequency and also whether the run time should be derived from the pulser. If the user wants to analyse many runs at the same time it is possible to deactivate the time consuming plotting of the data as well as the read out of source data. For some analysis it might also be interesting to take a look at data of a different detector segment as well as to save the output data into a ".txt" file and not just a ROOT output file. These settings are available in the parameter file.
Additionally it is possible to influence the integration with a specified standard deviation (sigma) and a ratio of peaks, these will be described in the next section.

Deriving peak counts from the Energy Histogram

The input of KaLi are ROOT files containing the run data. KaLi downloads these files and access their data. As the monitor spectrometer is measuring in histogram mode, the ROOT file consists of histograms. For each run/sub run these histograms need to be summed and put into one histogram. Histograms between sub runs need to be neglected. The summed histogram is the so called energy histogram. It shows the counts of one run/sub run on the y-axis and the ADC-channel on the x-axis. Usually this histogram has two distinct peaks at detector 4, the first one shows the counts on the detector by electrons at lower ADC-values and the second one, at higher ADC-values, is caused by

[4] https://nuserv.uni-muenster.de/cgit/cgit.cgi/createfilterspec.git/
[5] https://nuserv.uni-muenster.de/cgit/cgit.cgi/Kasper.git/
[6] http://www.boost.org/

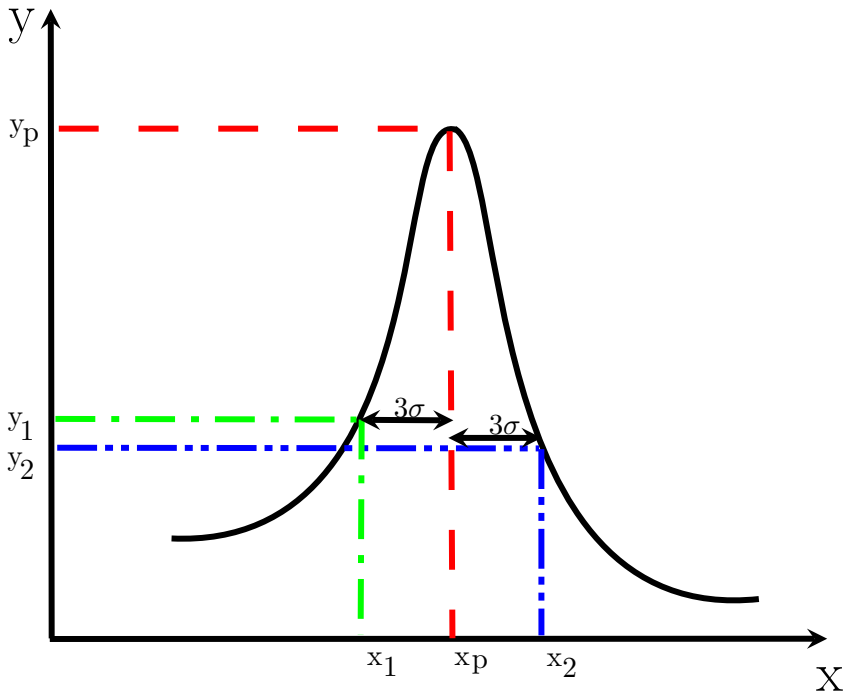

Figure 5.2.: **The peak search of TSpectrum.** This picture shows how TSpectrum evaluates a peak. If a peak is found with x-coordinate x_p, the sigma, entered in the constructor of TSpectrum, is used to derive new x coordinates $x_{1/2} = x_p \pm 3 \cdot \sigma$. The y-values of x_1 and x_2 are averaged to gain the peak height $h = y_p - ((y_1 + y_2)/2)$. This sigma is hard-coded in createfilterspec, it is set to 20.

the pulser. To integrate these two peaks a special class of ROOT called TSpectrum() is used. This class is able to perform a peak search in a one dimensional histogram. It does require a default standard deviation for the searched peaks, a sigma of "20" is reasonable for the monitor spectrometer. If one peak is found, the y-values of three times sigma in positive and negative x-direction are taken and averaged. This value is subtracted from the y-value of the peak, what defines the peak height (see figure 5.2) [Mor03]. Although the real standard deviation for the peaks in our histograms is lower, a higher standard deviation leads to less found peaks in the background. Additionally a threshold called "Peak Ratio" in the parameter file is necessary. This threshold defines the ratio of the y-value of the low peak divided by the high peak. If this ratio is below the threshold the small peak is neglected. This value is set to 0.01 by default, as it is reasonable for most line scans, sometimes it is necessary to be lowered, which is done by the program automatically.
If the program found the correct amount of peaks, a check of their positions and sigma is done. The sigma is calculated with a gaussian fit of these peaks. Their boundaries are derived from the x-value, the peak search found previously, and three times a standard sigma, that has to entered in the parameter file. It turned out, that "8" is a reasonable number for the standard sigma. These boundaries are used for gaussian fit, that returns the real fitted sigma. Createfilterspec checks whether the fitted sigma and the positions of the peaks are correct and starts the integration. If the check fails it either stops, because it cannot find the correct peaks or it lowers the peak ratio automatically and restarts the peak search.
The integration is done in a three sigma range, therefore the fitted sigma is added three times towards lower ADC values and towards higher ADC values from the maximum. All counts within this range are summed and represent the peak counts.

If the createfilterspec is not able to find the correct peaks within one histogram, these are skipped to the end. After all histograms are available, these are summed and the peak search is started within the summed histogram. The found peaks and its emanating boundaries are used for the integration of the missing histograms.
If createfilterspec cannot find any peaks, the current histogram is plotted and the program exits. Usually this histogram is empty.

Additionally it is possible to set integration boundaries manually and deactivate the peak search. This can be very useful for some measurements, but the user has to be careful to set these boundaries very exact as no fitting is done. The option for that can be found in the parameter file and the boundaries are set in "integrationbound.txt".

The Run Time

To calculate rates it is necessary to know the Run Time of one (sub) run. There are several possibilities to derive the Run Time. The previous createfilterspec did not use the time stamps, that ORCA recorded. The problem was, that the option Sync with Run Control was not enabled on the FLT card. This resulted in wrong time stamps for ORCA run files. The solution was to count the histograms of one run and multiply this number with the histogram Length. To enable the latest version of createfilterspec to analyse old data the same way of Run Time calculation is used. Additionally a cross check with the pulser time is included. The counts of the pulser on the channel "0" are summed and the counts divided by the frequency result in the run time. If these two run time values differ too much an error is put to console and the program uses the run time derived from the histograms.
It is also possible to use the pulser run time, this option can be found in the settings of the parameter file. As the settings on the FLT are fixed the Run Time may be derived by the ORCA time stamps, too.

The Slow Control Data

The Slow Control Data is obtained through KaLi. Therefore the KATRIN Number as well as its time stamps for the desired channel are necessary. The KATRIN Numbers for the voltages are not hard coded and can be edited in the parameter file. The time stamps are derived from the header files of the runs or sub runs. Then it is possible to download the mean values as well as the standard deviation of each channel via KaLi functions. After the voltages for the vessel and the source are derived, the program automatically subtracts the source voltage from the vessel voltage to get the filtervoltage. If the voltage applied to the source is below 5V, it is expected that the source is not connected to the source power supply, and the source voltage is neglected.
Createfilterspec is also able to download the source position as it is necessary for the fit program. This works the same way as in the case of the voltage data, but the KATRIN Numbers are hard coded. Additionally the download has to be done just one time for a complete run with sub runs. As the mean voltage and their standard deviation for three sensors(x,y,z) need to be calculated it can take some time. That is the reason for the ability to deactivate this read out in the parameter file. As nothing should be changed at the sources during one run the program outputs an error if the standard deviation is higher than "0.1". For each line scan it is also very important to know which source has been used. To automatise this readout the calibration database is used. As it is possible to put four sources into the source holder at one time an efficient method is required to read the sources out. After each re-inserting of sources a calibration has to be done. In four channels the x- and y-coordinates of each source as well as an error on these have to

be written. In another four channels each source holder position needs to be identified to its source. Overall this has the advantage that this has to be done once until the source chamber is opened again and something has been changed on the source holder. The error on the coordinates is necessary, because the positions are only reproducible within a certain tolerance.
For old data it has not been possible to use this method. Thus each source was included manually with a validation time stamp. Now all sources are included in the database since September 2011 and can be read out automatically for older runs also.

Visualisation of Data

After all data for one line scan are derived and calculated, createfilterspec is able to plot the data. One example can be seen in figure 5.3. This output enables the user to detect possible problems during the analysis or the line scan. On the left side is the filterspectrum, on the top right the pulserspectrum and in the bottom right all energy histograms with the peaks found(red triangles) and the used integration boundaries(green lines). To take a closer look at data it is also possible to zoom into these graphs. The header of the filterspectrum shows the run number, the line position and the used source.
If the user does analyse more than one scan at a time, createfilterspec is able to plot the output data for all of them as long as these are runs with sub runs. But it is recommended to deactivate the drawing function in the parameter file, because it does require a lot of calculation time.

Storing of Data

The output data is stored into a ROOT file. The home folder of createfilterspec includes a "filterspecdata" sub folder. After a run is analysed another folder within this sub folder named according to the conversion line is created. If the folder already exist the data is just saved within that existing folder. The file is named after its run numbers. The advantage of ROOT files is, that they are small, easy to access and with the TBrowser() command a look into the data can be taken immediately. As the pulserspectrum and filterspectrum are saved as TGraphErrors() into the root file directly it is not even necessary to plot them again as the TBrowser() is able to draw them immediately. The fit program for the monitor spectrometer has been changed in a way, that it can easily access these output files.
Within those output files all necessary data for one line scan can be found. These are the filterspectrum, the pulserspectrum, all histograms for each measurement point, their integration boundaries as well as the source name, the source position and its errors. Additionally the line position, line name and the time stamps for all runs/sub runs.
It is also possible to output the data into a ".txt" file. This enables easier access to the data for the user, but just the filterspecdata, the time stamps and the source position as well as the used source is saved. This is not recommended to be used with the fit program.
In future this ROOT file should be saved on the IPE server, containing the usual run files, and enable an easy access to analysed data via KaLi and the ADEI webinterface. The webinterface is also able to draw the filterspectrum plots of each run.

5.2.2. The Fit-Program

In the following section an introduction to the fit program is given. A lot of information is derived from the manual of the fit program [Sle12]. The program can be found on the GIT repository [7].
After the program is downloaded successfully it should compile without any errors as it

[7] https://nuserv.uni-muenster.de/cgit/cgit.cgi/MoS_fitter.git/

does require the same packages as Kasper and createfilterspec. When everything worked fine, the program is able to fit a K-32 spectrum using the Doniach-Sunjic model by default. A fit can be started by running the "fit.sh" script with the path to a createfilterspec output file as an argument. It does not matter, whether the output file is a ".txt" file or a ROOT file.
The general settings for the fit program can be found in the "setup.txt". To change fit parameters, the user may edit the "param.dat". Within this file the user can edit the fit boundaries, set the source position, which is usually derived from the ROOT file and set all the fit parameters and step sizes. A detailed description of the fit parameters can be found in the manual [Sle12]. Another important setup file is the "setup_root.txt". The user can specify whether data should be taken from the ROOT file recorded by the createfilterspec or the data from the fit program settings.

The fitting is based on the minimisation of the chi square function:

$$\chi^2(\vec{\alpha}) = \sum_{i=1}^{N} \frac{[y_i - f(x_i, \vec{\alpha})]}{\sigma_i^2} \tag{5.1}$$

where x_i are the voltages, y_i the count rates and σ_i the error of these data points. The function $f(x_i, \vec{\alpha})$ is a model function depending on the voltages and a parameter vector $\vec{\alpha}$. In the fit program there are two main fitting functions.

- **Doniach-Sunjic**
  This function is preset in the fit program. This function looks like a normal bell-shape, but has an asymmetrical part in the lower energy region. This asymmetry is described by the α parameter, that is not the same parameter as in the χ^2 function.
- **Voigt**
  This function is a convolution of a Lorentzian and a Gaussian function. For the spectra of implanted sources a single Voigt function is not sufficient and a doublet of Voigt function has to be used.

To switch between those functions the "fit.cpp" needs to be edited and the program needs to be recompiled.

5.2.3. Outlook

As createfilterspec is able to run autonomous it should be possible to integrate it into the KATRIN DataProcessor. This makes it possible to download the ROOT files directly from the server, which is faster for the user as the raw data is already analysed, but also the ROOT files are much smaller as they consist of much less histograms. But the user has still to be able to analyse the data on its own, thus the createfilterspec on the end user machine needs to be able to perform the same work, but with an extended program to offer an option to download the analysed data immediately.
There are also thoughts to combine the createfilterspec and the MoS_fitter into one program package, once a standard model for the line shape is established.

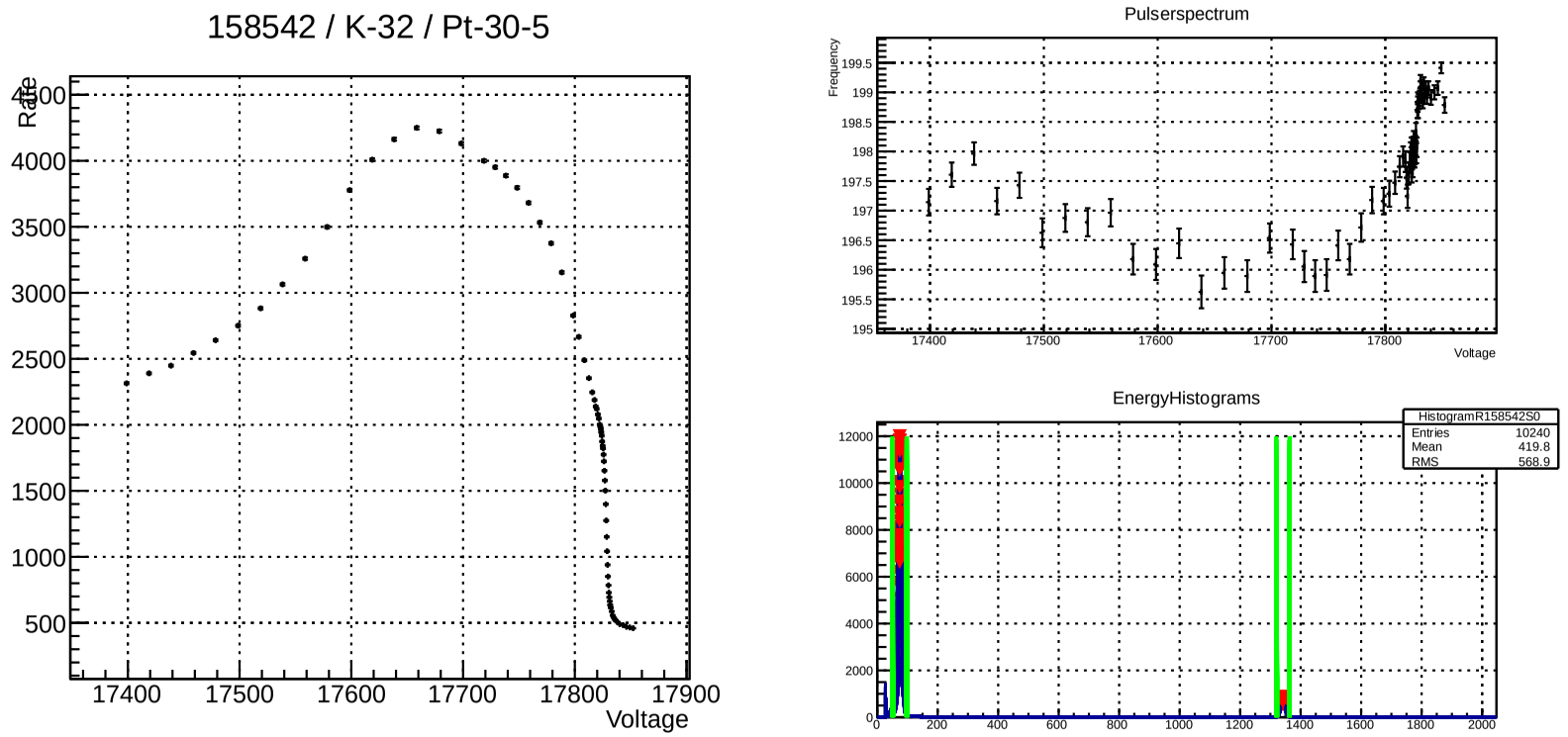

Figure 5.3.: **Raw Data analysis of run 158542 with createfilterspec.** On the left side the filterspectrum is plotted with the count rate (Hz) on the y-axis and the voltage(V) on the x-axis. The header shows the run number, the scanned line and the used source. On the top right is the pulser spectrum. Towards higher voltages(x-axis) on can see that the less electrons reach the detector in the filterspectrum and in the pulserspectrum the frequency (y-axis) converges towards the set value of 200Hz. Also the highest rate in the filterspectrum corresponds to the lowest rate in the pulserspectrum. In the bottom right all energy histograms are plotted. On the y-axis are the counts and on the x-axis the ADC-value. The red triangles are caused by TSpectrum() and show the found peaks, the green lines are the integration boundaries. The peak on the right is the pulser and the peak on the left is the ROI(Region of Interest). This histogram is plotted to cross check the data.

48

6. Line Position Stability during KATRIN-Measurements

The main task of the monitor spectrometer in KATRIN is to enable a voltage monitoring of the retarding potential on the Main Spectrometer on a nuclear standard. Therefore the monitor spectrometer needs to be able to guarantee a constant line position within a $\pm 59mV$ range per two months [Erh12].

During KATRIN measurements the same voltage applied on the main spectromter will be applied to the monitor spectrometer. As Tritium endpoint measurements do require a voltage of 18.6kV, the K-32 conversion electrons need to be accelerated from 17.8kV to 18.6kV. This is realised with an accelerating voltage applied directly on the sources. Within the switch to ORCA slow control, a new power supply was integrated to the Field Point, that can be connected to each source individually. One part of this thesis is to check, whether the source potential does influence the line position. Additionally oscillations on the power supplies were observed and the influence on the line positions will be discussed here.

Using sub runs requires to save every single histogram within the run files. But this makes it possible to take a closer look at every single histogram. In this chapter a closer look at one run and its single histograms is taken to determine the least required measurement time in dependency of the activity of the source.

6.1. Measurements with varying Source Potential

In the course of this thesis stability measurements with a varying source potential have been done. For the K-32 conversion line the retarding potential was set to 18000V and the source potential was scanned from -150V to -200V. Afterwards the voltages were increased in 150V steps and the scan was done again until a retarding potential of 18600V was reached. These scans can be seen in figure 6.1. Additionally a scan of the L-32 conversion line was done. These scans were carried out with identical source voltages and the retarding potential was set from 30650V to 31250V. These scans can be seen in figure 6.2. For both scans the Pt30-5 source was used as it was the source with the highest activity during these measurements.

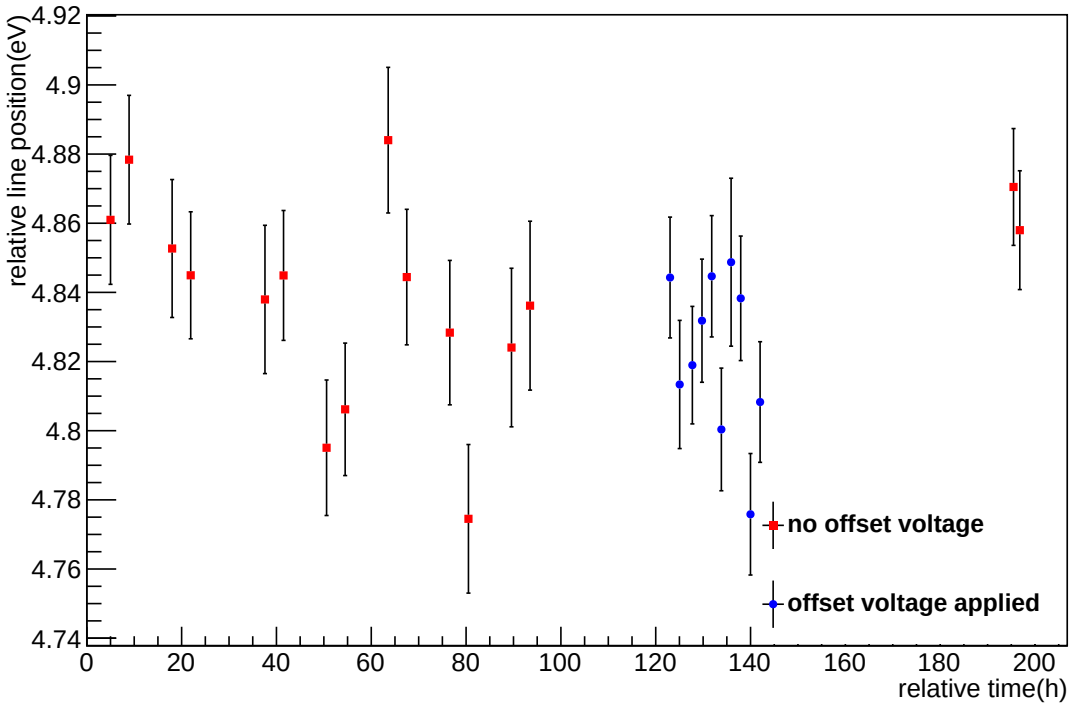

Figure 6.1.: **The position of K-32 conversion line of source Pt30-5.** On the y-axis the relative line position in electron volts can be seen and on the x-axis the relative time in hours. The blue circles are measurements with varying source potential and the red squares measurements without.

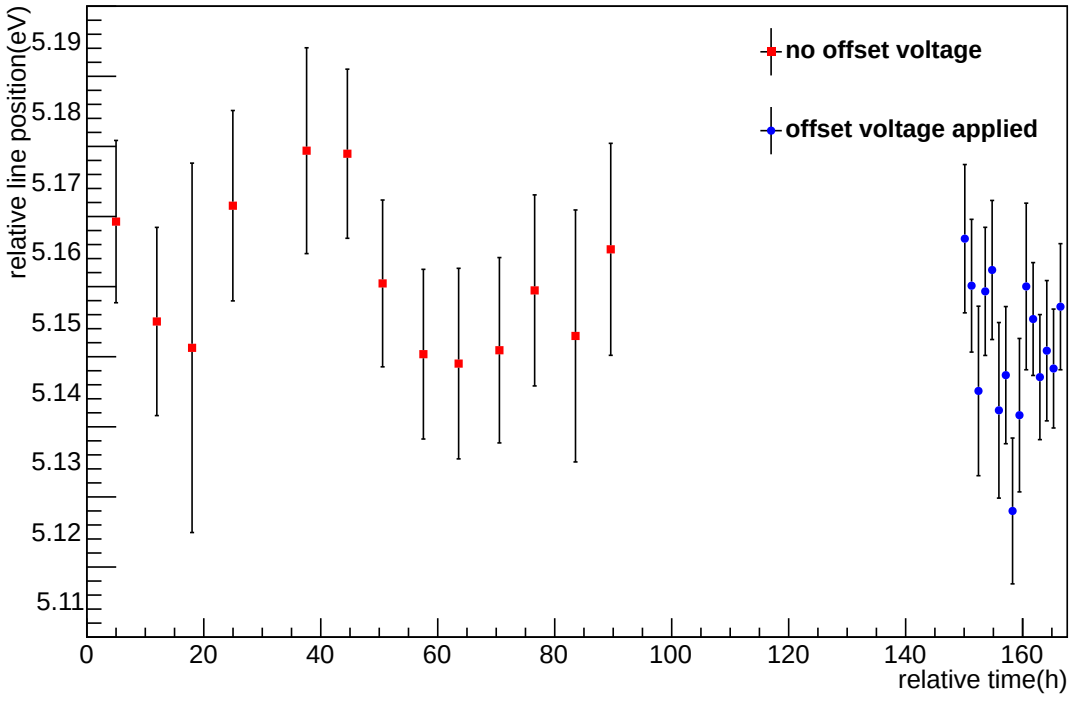

Figure 6.2.: **The position of L-32 conversion line of source Pt30-5.** On the y-axis the relative line position in electron volts can be seen and on the x-axis the relative time in hours. The blue circles are measurements with varying source potential and the red squares measurements without.

The outcome of these measurements show, that measurements with varying source potential do work. The weighed mean values are:

$$P_{K32} = 17829.140\ \text{V} \pm 0.005\ \text{V} \tag{6.1}$$
$$P_{K32_{off}} = 17829.123\ \text{V} \pm 0.006\ \text{V} \tag{6.2}$$
$$P_{L32} = 30477.460\ \text{V} \pm 0.004\ \text{V} \tag{6.3}$$
$$P_{L32_{off}} = 30477.452\ \text{V} \pm 0.002\ \text{V} \tag{6.4}$$

The difference in line position is less than 20mV for both line positions. On the one hand this result is still better than KATRIN requirements, but on the other hand further measurements with varying source potential are required. By taking measurements with source potential two additional uncertainty factors do occur. These are the power supply and the voltmeter. The voltmeter used for these measurements is a 6.5 digit voltmeter with a resolution of 1mV within the required 1000V range. Additionally this voltmeter is not calibrated. In future measurements a 8.5 digit voltmeter, that is calibrated on a regular basis, will be used to measure the source voltage.
It is also necessary to perform more line scans to reduce the influence of statistical fluctuations. These can be seen in figure 6.1 and 6.2 also. These measurements have proven, that the KATRIN measurement principle for the monitor spectrometer does work.

6.2. Least Required Measurement Time

To optimise the measurement mode of the monitor spectrometer, it is important to make line scans as effective as possible. A line scan is done by shifting the set value of the source- or vessel-power supply. This shifting can be done from up/down or just random values close to the actual line position. The advantage of up- and down-scans is a more stable voltage as the shifts are usually small. There are two possibilities to decrease the time of one line scan. First, the count of measurement points can be decreased. This was already done in the diploma thesis of Michael Schupp [Sch11] and Moritz Erhard [Erh12]. Both diploma thesis also treated the dependence of the measurement time on the line position, but with the switch to sub runs it became possible to look at on single run and split it into its single histograms and check the dependence of the measurement time.

Therefore a closer look at run 150662 is taken. This run consists of 44 sub runs with a run time of 62 or 64 seconds each. The histogram length is set to two seconds. In figure 6.3 the K-32 line position is plotted at different run lengths. On the x-axis the run length can be seen, the run time needs to be a multiple of the histogram length(2s). On the y-axis the relative line position of the K-32 conversion line can be seen. Within this figure are three different strands. The blue triangle shows the behaviour of the line position in standard analysis, the first histogram of one run is taken and the following are processed sequentially. The black circles show the line position beginning with the last histogram of one sub runs and processing them sequentially but downwards. The red squares show the trend of the line position by using the central histogram of each sub run. The following run times are calculated by using the histogram before and after the central histograms until all histograms are used at 62 seconds.

The first measurement points show a large error on the line positions. The run length of 2s causes an error above 100meV for all three measurement points, additionally the line position between the central histogram and the first histogram are over 100meV apart. This shows, that one histogram of a length of two seconds is not enough, but it is an acceptable appraisal as the line position with its errors contain the correct line position. After a measurement time of eight seconds, the error on the line position drops below

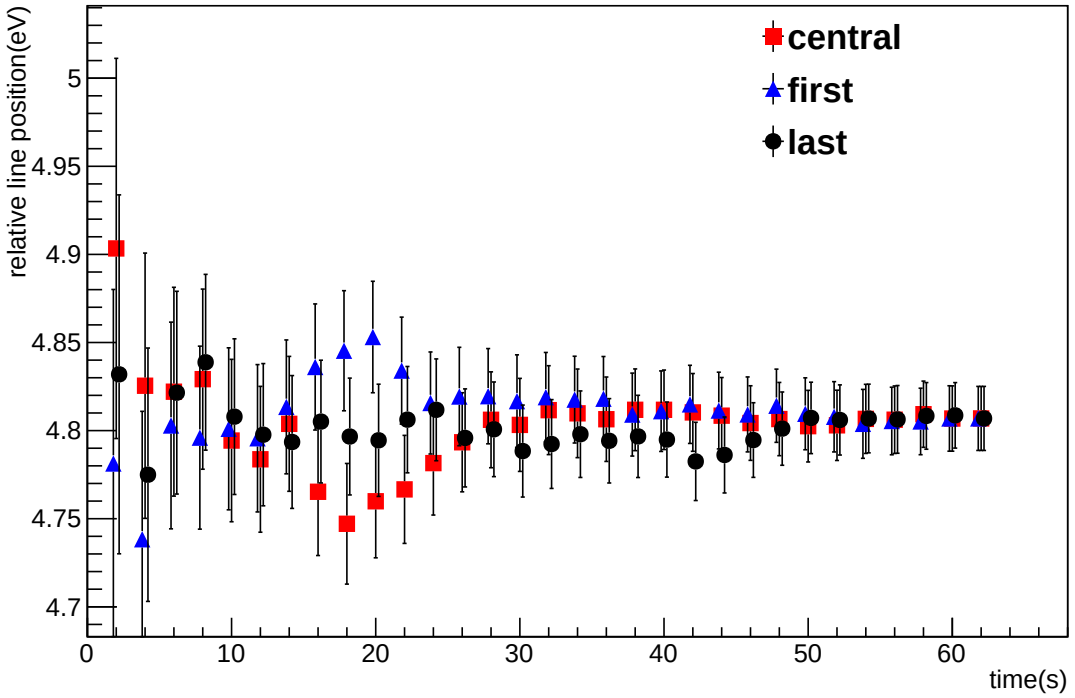

Figure 6.3.: **The dependency of the measurement time on the line position.** On the y-axis the relative line position in electron volts can be seen. On the x-axis the measurement time in seconds is shown. The blue triangles show the progression of the line position beginning with the first histogram, the red squares the progression beginning with the central histogram of one sub run and the black circles beginning with the last histogram. The histogram length for this run is two seconds. For a better overview an offset of 0.2s on the x-axis for the first and last histogram plot is used.

59meV. But this measurement time is not enough as a huge fluctuation of the line position can be seen for the central and the first histograms at about 18s. Hence, for low measurement times the single histogram does have a huge influence on the line position. After 30s the line position becomes stable and the fluctuations have averaged out.
Very interesting is, that starting at the central histogram still causes huge fluctuations of the line position and starting with the last histogram gives a rather stable line position. These fluctuations might be caused by the high voltage power supply for the vessel. Although the voltage for that run has been constant relatively huge fluctuations occurred and the standard deviation for the first half of one sub run was partially a factor of two different to the second half and the mean voltage up to 5mV different. Within the scope of voltmeter accuracy these differences were not caused by the source power supply.
When taking a look at this data the statistical dependence of the measurement points have to be considered. At low measurement times, the influence of single histograms is large, which can cause large fluctuations. These average out at higher measurement times and the influence of single histograms becomes lower.

To give a statement to the required measurement time it is necessary to derive a relation to the activity of the used source. For this measurement Pt10-1 was used. It is possible to derive the activity of the source from it, in case no electrons are lost and all of them are detected. Assuming a point source. the ratio between the isotropic emitted

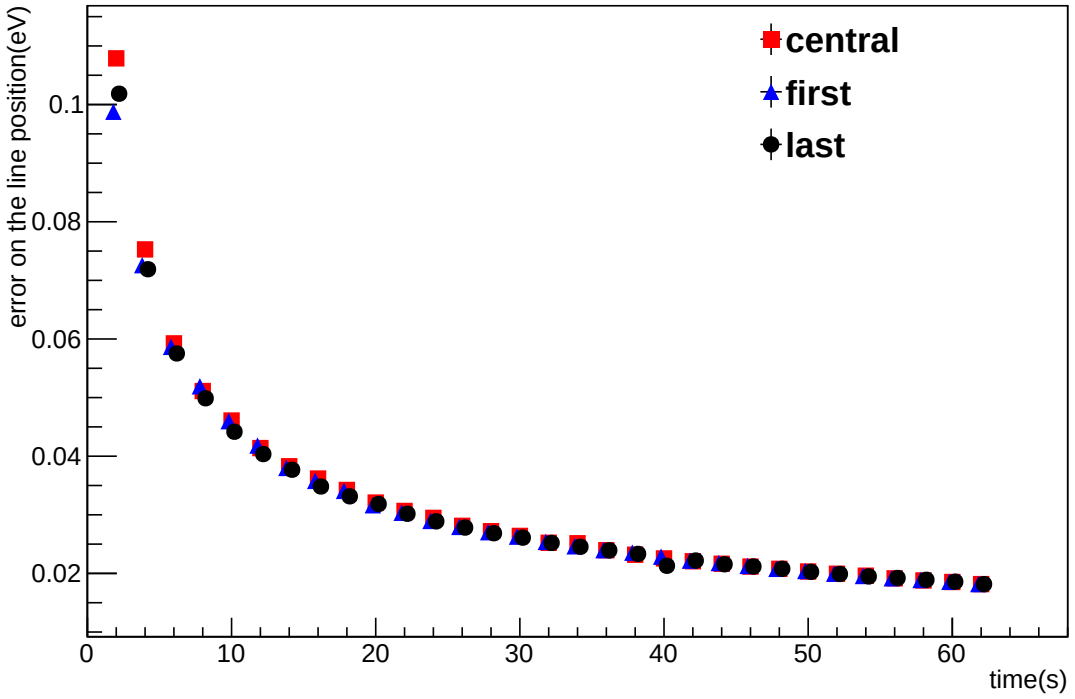

Figure 6.4.: **The dependency of measurement time on the line position error.** On the y-axis the error on the line position in electron volts can be seen. On the x-axis the measurement time is plotted.

electrons and the electrons within the acceptance angle can be calculated as follows:

$$R = \frac{2\pi\,(1-\cos\theta)}{4\pi} = \frac{1}{2}\,(1-\cos\theta) \tag{6.5}$$

The angle θ is the maximum acceptance angle, electrons below this angle are accepted and above neglected. It can be calculated as follows:

$$\sin\theta = \sqrt{\frac{B_p}{B_{max}}} \tag{6.6}$$

The ratio between the magnetic field can be derived from field cards by Oxford Instruments[1]. For a source position of 220.17cm from the analysing plane (z-axis) this results in:

$$\frac{B_p}{B_{max}} = 0.42 \Rightarrow \theta = 40.4^\circ \tag{6.7}$$

With an acceptance angle of 40.4°, the ratio of accepted electrons is:

$$R = 11.9\ \% \tag{6.8}$$

The electrons, that hit the detector per second can be derived from the amplitude. Therefore also the loss electrons (see figure 5.3) are considered and the highest rate reduced by the background gives the amplitude. For the date of the considered run, the amplitude is $y = 3315.19\frac{\text{counts}}{\text{s}}$. This amplitude is an indicator for the K-32 conversion electrons. But

[1] http://www.oxford-instruments.com/

the intensity of K-32 conversion electrons is just 17% [Zbo11]. This leads to the following equation:

$$A_{calc} = \frac{y}{0.17R} = \frac{3315.19\frac{1}{s}}{0.17 \cdot 0.119} = 163874.94 \text{ Bq} = 163.87 \text{ kBq} \tag{6.9}$$

From activity measurements in Rez, the back-calculated activity is:

$$A_{meas} = 309.43 \text{ kBq} \tag{6.10}$$

This results in a ratio of:

$$\frac{A_{calc}}{A_{meas}} = \frac{163.87 \text{ kBq}}{309.43 \text{ kBq}} = 52.95 \text{ \%} \tag{6.11}$$

This means, that the monitor spectrometer has a transmission of about 53% , and the activity has to be about two times higher than the calculated.

For voltage monitoring it is feasible to use a 30s measurement time per sub run at this activity. All huge fluctuations are averaged out and the line position has an offset of maximal 10mV to the position after 62s. This enables a fast analysis of the line position, but the same statistics if the scan is done twice. The problem is the necessary time for slow control between sub runs. It does still take too long to use shorter measurement times effectively. If there are new sources with activities in the MBq order, the required measurement time can be very short and the slow control becomes the handicap.

As a conclusion it can be said, that the measurement time multiplied with the activity should not be lower than $30 \text{ s} \cdot 309.43 \text{ kBq} \approx 9300 \text{ kBqs}$ for an error on the line position ≤ 25 mV. For an error ≤ 20 mV this value may not be lower than ≈ 16100 kBqs. A plot of the error on the line position over time can be seen in figure 6.4.

6.3. Temperature Dependencies

During measurements with varying source potentials, the voltage on the vessel is constant and it becomes possible to take a look at the behaviour of the power supply at constant voltages. For that power supply oscillations became visible (see 6.5). After further investigation it turned out, that further meters show the same behaviour and it is caused by temperature fluctuations. In this section a look at these fluctuations is taken and their consequences for the measurement.

6.3.1. Influence on the High Voltage System

In figure 6.5 oscillations of the high voltage at the monitor spectrometer can be seen. The voltage is set to constant 18000V within the power supply. This voltage is applied to the vessel. These oscillations have a period of about 1h for the K-35 and JR divider voltmeter and show the same behaviour. Both are in separate buildings. The JR divider and voltmeter is in the monitor spectrometer building and the K-35 in the main spectrometer building. Hence, the power supply has to be responsible for the voltage oscillation.
It turned out, that the oscillations are caused by the temperature. In figure 6.7 the same behaviour as for the voltage can be seen on the temperature. The used time interval for this plot is exactly the same as for the voltage.
The difference in voltage from tale to peak is 100mV. The question is the influence on the line position. A plot of 100s intervals for the same time range can be seen in 6.6. The voltage within these intervals is relatively constant and the maximum error on the flank is 12mV. Usually even shorter measurement times than 100s per measurement point are taken, which results into shorter time intervals with smaller errors on the voltage.

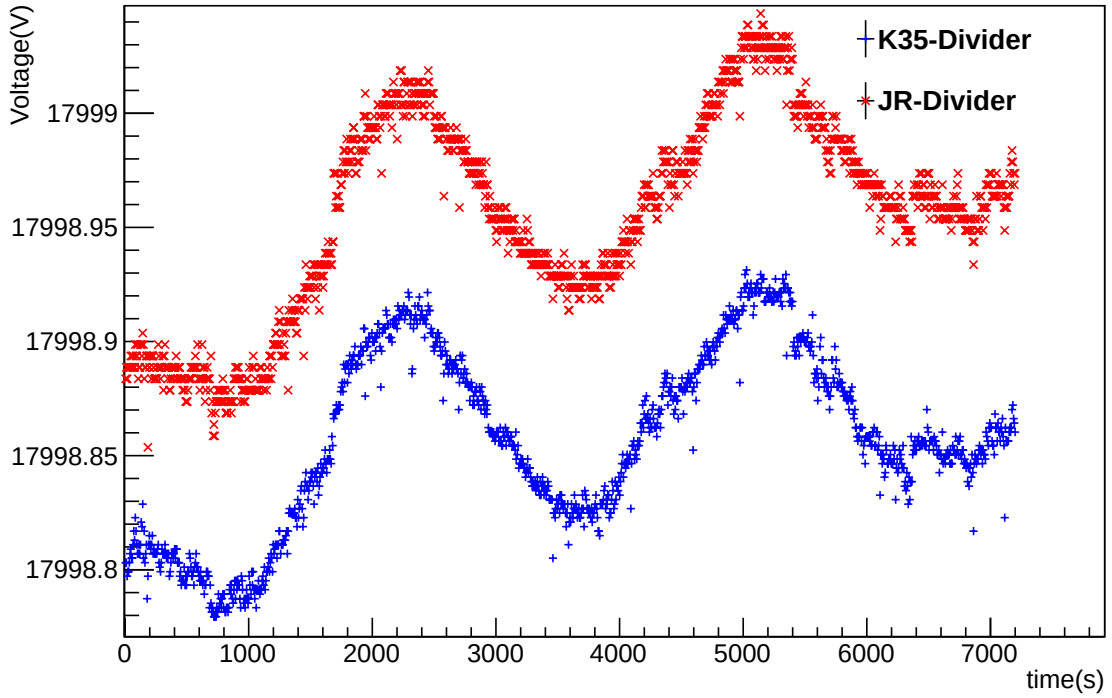

Figure 6.5.: **Voltage oscillation of the high voltage power supplies at constant set value.** On the y-axis the voltage can be seen. During this measurement the voltage was set to 18000V at the power supply. On the x-axis is the time in seconds. The blue crosses are the measurement points of the K-35 divider and the red, rotated crosses show the voltage at the JR divider. Usually the offset between the JR and K-35 divider is greater, the y-values of the JR divider were reduced by 1V manually to show, that both voltmeter have the same behaviour.

For KATRIN measurements the voltage on the vessel at the monitor spectrometer should be more stable as the voltage is identical to the main spectrometer voltages and the power supplies in the main spectrometer hall are placed in much more stable temperature conditions. These measurements were done during noon, but identical curves during night measurements can be seen. Probably these fluctuations are caused by the air conditioning/heating system at the monitor spectrometer building. Unfortunately these cannot be read out directly.
As the power supplies as well as the voltmeters are sensitive to temperature changes, the gate to the east should not be used, but the small door to the west especially during winter and summer season. In future run control should be done from the control room.

6.3.2. General influence on the Monitor Spectrometer

The temperature does not just have an influence on the high voltage system, fluctuations can also be seen on different sensors. For instance the pressure sensors show the same behaviour (see 6.8).
Of course, these temperature fluctuations do not influence the pressure directly, but they do influence the sensors. Again, the conclusion has to be to keep the temperature as constant as possible by influencing the temperature as little as possible from outside.

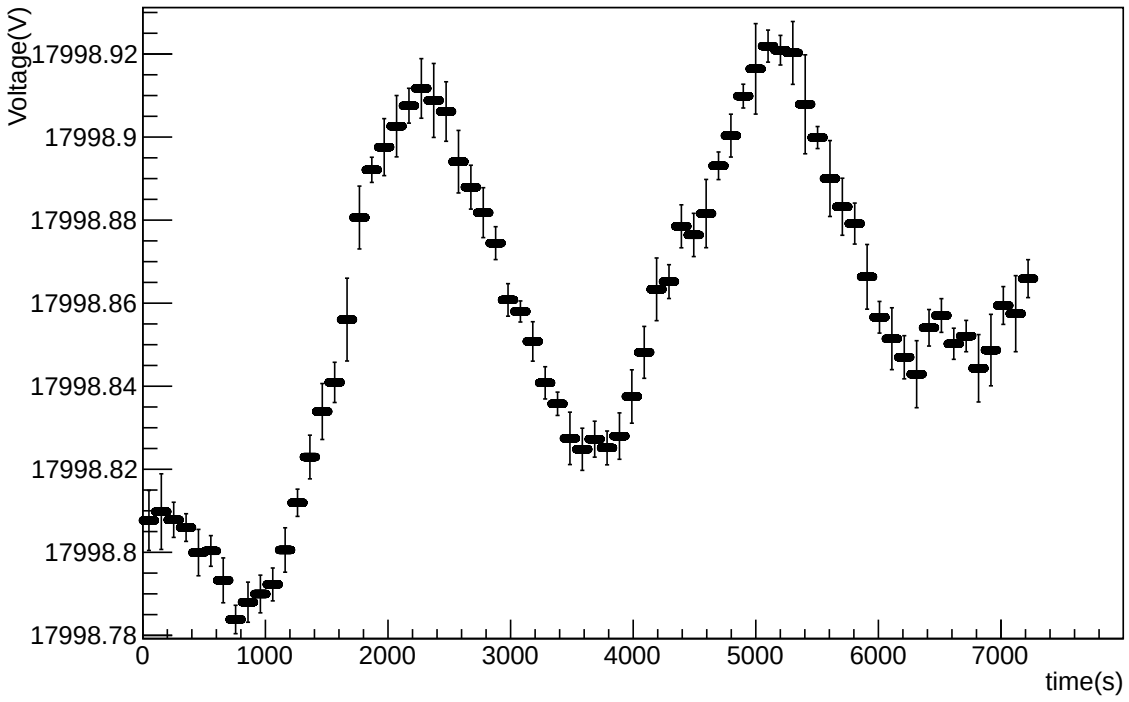

Figure 6.6.: **Voltage oscillation of the high voltage power supplies at constant voltage, split into 100s intervals.** This figure is equivalent to figure 6.5 and the K-35 divider, but the meanvalues of 100s intervals are plotted. Additionally the standard deviations of these 100s intervals are shown.

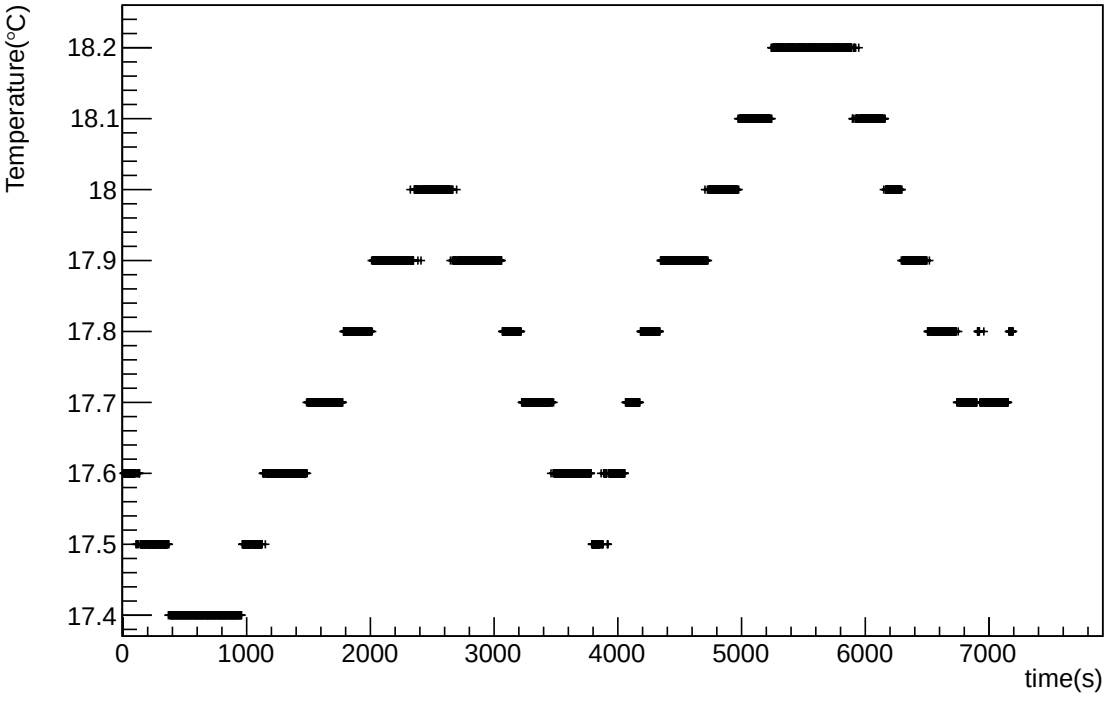

Figure 6.7.: **Temperature oscillation in the Monitor Spectrometer building.** On the y-axis the temperature in degrees celsius can be seen. On the x-axis is the time in seconds. This plot shows the read out of a temperate sensor, which measures the room temperature.

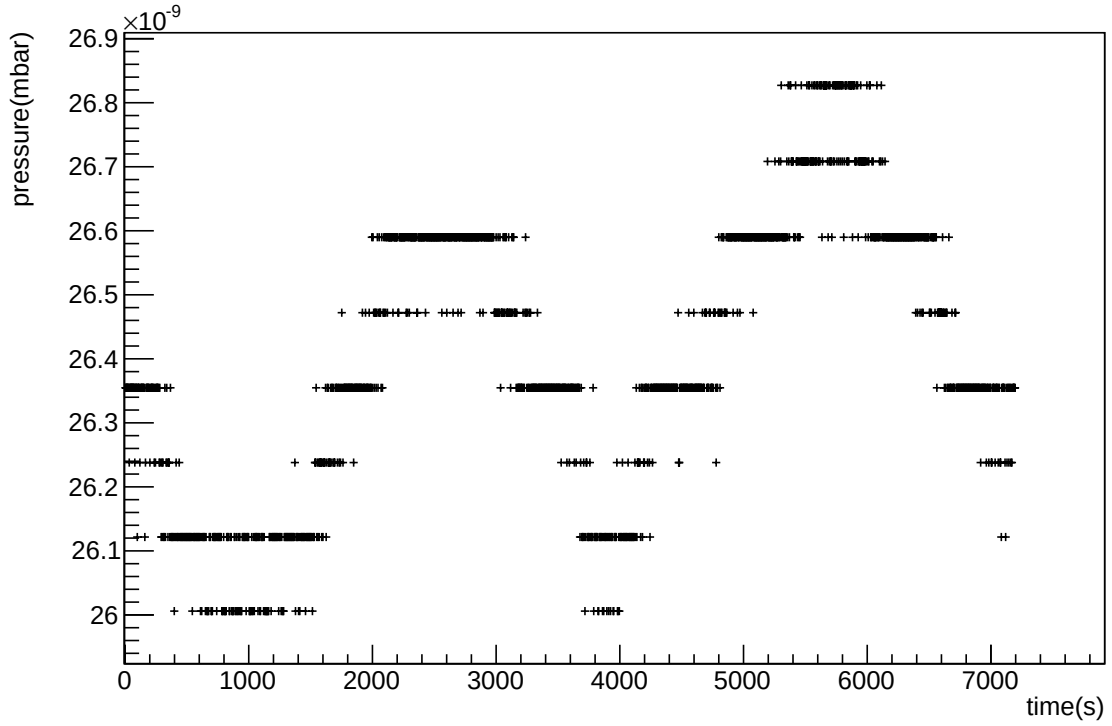

Figure 6.8.: **Apparent pressure oscillation at the detector.** On the y-axis the pressure in millibar can be seen. On the x-axis is the time in seconds. The time interval is identical to the previous figures.

6.4. Problems and Solutions

As the monitor spectrometer is responsible for monitoring the voltage on the main spectrometer, it is important to guarantee a stable line position. There are two different measuring principles, on the one hand usual line scans by changing the source voltage or on the other hand by choosing a voltage, that is very close to the line position and directly on the flank. The first possibility enables reliable long term measurements and stability of the voltage within the KATRIN requirements. The second one enables the experimenter to spot changes of the voltage almost immediately. In this section some problems and solutions are discussed.

6.4.1. Accuracy and Precision of Set Values

Hand in hand with the investigation of the reliability of slow control, measurements for the accuracy and precision of the set values have been done. For the vessel voltage these can be seen in figure 4.4 on page 39 and for the source voltage in figure 4.5 on page 40.
For the vessel voltage the accuracy of data points only at about zero are considered, as the other values are caused by slow control problems. The trend of the plot does look like a triangular voltage with a period of about 5000V. Hence, the power supply does have different calibrations for different voltage regions. The maximum offset between the measured and the set values below 28000V is 1V. At higher voltages the offset can even be up to 5V. Thus the accuracy of that power supply can be increased by a software calibration. The width of the plot shows the precision of the power supply. The precision is about 0.5V. This can partly be explained by temperature fluctuations, but the overall precision of the power supply is not very high. This cannot be fixed by software.
For the source power supply only the black circles are considered. This measurement was

done just in the 0V to 1000V range and the outcome is very exact. The accuracy and precision is very high. The size of the circles is chosen larger than the size of the triangles to give a better overview on that figure.
Overall this measurement shows, that the power supply is not usable for measurements of a distinct point on the flank. In future this might become possible for KATRIN measurements. But the power supply works fine for line scans as it is shown in this chapter, that the voltage is constant for short time intervals. The source power supply is ready for both modes, as it has a good accuracy and precision. In future better measurements of the source power supply become available, when the 6.5 digit voltmeter is replaced by a 8.5 digit voltmeter.

6.4.2. Time Discrepancy

The monitor spectrometer has proven to generate a stable line position within the KATRIN requirements (see [Erh12]). But it is rather difficult to determine a stable line position in a short time. The consequences of a reduction of measurement points can be found in [Erh12] also.
The monitor spectrometer will enable a long term observation of the K-35 divider with respect to a nuclear standard and the possible drift over time. Therefore run files need to be created to change voltages of the source power supply. The measurement time per sub runs has to be dependent on the activity of the source (see page:51). These run files need to be adapted after a while to the weaker activities. Within this chapter it is shown, that the measurement principle does work and gives expected results. In future further measurements have to be done by varying the source potential and by using a more precise voltmeter. Additionally for KATRIN measurements slow control has to become more reliable and faster to make short measurement times and high activity sources much more efficient.

7. Conclusion

Since the first idea of neutrinos in 1930 over 80 years have passed. In these years the neutrino research progressed and occasionally performed giant leaps, the discovery of three neutrino generations and neutrino oscillations, which comes along with massive neutrinos. Neutrino oscillation experiments cannot measure the absolute mass, which makes different experiments necessary. Until now, it was possible to measure an upper limit of neutrinos $m(\nu_e) < 2.05$eV (95% C.L.). The KATRIN-Experiment(KArlsruhe TRItium Neutrino) is the successor experiment to Mainz and Troitsk. From the electron beta decay spectrum, the mass of the electron anti neutrino can be determined. KATRIN will improve the sensitivity by a factor of ten and set an upper limit of the electron anti neutrino mass of 0.2eV(90% C.L.), if the absolute mass cannot be determined.

KATRIN is planned to have a measurement cycle of five years, therefore it is necessary to have an effective Run Control program. This task is done by ORCA, which is capable to perform the data acquisition and real time control. In the course of this thesis, ORCA was used at the monitor spectrometer, performing Run Control for the first time.
It was possible to obliterate many problems that occurred. But slow control still needs improvement. Some set values do not result in their appropriate current value. At present the loss of data between ORCA and ZEUS is investigated, till now it turned out, that there are timeouts from time to time. This might be caused by an overload of the server structure and hence the timeout was increased from 200ms to 500ms, additionally the connection from the KATRIN- to the IPE-network will be switched to 1Gbit/s as it used to be just 100Mbit/s.
The connection ZEUS, cFP and the devices is currently being improved. The cFP and its end devices will be put into a separate network to obviate network problems. The system will be tested, when the monitor spectrometer starts measurements again.
Overall it needs to be pointed out, that Run Control works fine with ORCA and the developed ORCA Script libraries will ease ORCA Scripting in future.

The monitor spectrometer is using sub runs for line scans, this decreases the amount of runs, but on the other side a filterscript cannot be used, which prevented all histograms from being saved in the output file but the last one. This makes the output files large in comparison to old runs. For the sub run mode a new raw data analysis program was written, that fulfills all requirements for the monitor spectrometer and can easily be combined with the fit program. In future this program can work autonomous on an IPE server and the user can download the output ROOT files, containing all necessary data.

Sub runs, due to saving of all histograms, enable a detailed look into single runs. This was done to check the dependence of the run length and the error on the line position. In combination with the source activity, it can be stated, that the measurement time multiplied with the source activity may not be lower than 16100kBqs for an error below 20mV. This means, that a source of 1MBq requires about 16s of measurement time per measurement point to derive an error below 20mV on the line position. It should be noted, that the transmission of the monitor spectrometer is just 53%, which is already included in that calculation. This leads to a netto measurement time of 160s for 10 measurement points.
Furthermore temperature fluctuations influence the high voltage system. A change of 1°C at 18000V leads to a shift of 100mV on the high voltage system. Hence, the air conditioning and heating system influences the high voltage, but it has been shown, that the time intervals per measurement point are too short to directly influence the line position.

Glossary

- **ADEI** Advanced Data Extraction Interface
- **cFP** compact Field Point
- **CPS** Cryogenic Pumping Section
- **DPS** Differential Pumping Section
- **EMCS** Earth Magnetic Field Compensation System
- **FLT** First Level Trigger
- **FPD** Focal Plane Detector
- **HMI** Human Machine Interface
- **IPE** Institut für Prozessdatenverarbeitung und Elektronik
- **KaLi** KATRIN Library
- **KATRIN** KArlsruhe TRItium Neutrino
- **KDBServer** KATRIN Database Server
- **LFCS** Low Field Correction System
- **MAC-E-Filter** Magnetic-Adiabatic Collimation with an Electrostat. Filter
- **MVC** Model View Controller
- **ORCA** Object-oriented Real-time Control and Acquisition
- **PCS** Process Controll System
- **ROI** Region Of Interest
- **SLT** Second Level Trigger
- **WGTS** Windowless Gaseous Tritium Source
- **ZEUS** ZEntrale datenerfassung Und Steuerung

Bibliography

[A+12] J. F. Amsbaugh *et al.*, *Prototype focal-plane detector system for the KATRIN experiment*, 2012. [Online]. Available: https://fuzzy.fzk.de/bscw/bscw.cgi/706270/FPD_System_Prototype_Jan2012.pdf

[AA+13] Abe, Aberle *et al.*, *First Measurement of θ_{13} From Delayed Neutron Capture on Hydrogen in the DoubleChooz Experiment*, 2013. [Online]. Available: http://arxiv.org/abs/1301.2948

[AAA+11] Aharmim, Ahmed, Anthony *et al.*, *Combined Analysis of all Three Phases of Solar Neutrino Data from the Sudbury Neutrino Observatory*, 2011. [Online]. Available: http://arxiv.org/abs/1109.0763v1

[ACC+12] Ahn, Chebotaryov, Choi *et al.*, *Observation of Reactor Electron Antineutrinos Disappearance in the RENO Experiment*, 2012. [Online]. Available: http://dx.doi.org/10.1103/PhysRevLett.108.191802

[Bil12] S. M. Bilenky, *Neutrino. History of a unique particle*, 2012. [Online]. Available: http://arxiv.org/abs/1210.3065

[BPG04] J. N. Bahcall and C. Peña-Garay, "Solar models and solar neutrino oscillations," *New Journal of Physics*, vol. 6, no. 1, p. 63, 2004. [Online]. Available: http://dx.doi.org/10.1088/1367-2630/6/1/063

[CDD+98] Cleveland, Daily, Davis, Distel, Lande, Lee, and Wildenhain, *MEASUREMENT OF THE SOLAR ELECTRON NEUTRINO FLUX WITH THE HOMESTAKE CHLORINE DETECTOR*, 1998. [Online]. Available: http://dx.doi.org/10.1086/305343

[Cha32] J. Chadwick, "Possible Existence of a Neutron," *Nature*, p. 312, 1932. [Online]. Available: http://dx.doi.org/10.1038/129312a0

[CHH+99] M. Cribier, W. Hampel, G. Heusser *et al.*, *Results of the whole GALLEX experiment*, 1999. [Online]. Available: http://dx.doi.org/10.1016/S0920-5632(98)00438-1

[Chi13] S. Chilingaryan, "Private communication," 2013.

[CRH+56] Cowan, Reines, Harrison, Kruse, and McGuire, "Detection of the Free Neutrino: a Confirmation," *Science*, 1956. [Online]. Available: http://dx.doi.org/10.1126/science.124.3212.103

[Day07] Daya Bay Collaboration, *A Precision Measurement of the Neutrino Mixing Angle θ_{13} using Reactor Antineutrinos at Daya Bay*, 2007. [Online]. Available: http://arxiv.org/abs/hep-ex/0701029

[DGG+62] G. Danby, Gaillard, Goulianos, Lederman, Mistry, Schwartz, and Steinberger, "Observation of High-Energy Neutrino Reactions and the Existence of Two Kinds of Neutrinos," *American Physical Society*, 1962. [Online]. Available: http://prl.aps.org/abstract/PRL/v9/i1/p36_1

[DHH68] Davis, Harmer, and Hoffmann, *SEARCH FOR NEUTRINOS FROM THE SUN*, 1968. [Online]. Available: http://dx.doi.org/10.1103/PhysRevLett.20.1205

[Dou13] Double Chooz collaboration, "Homepage," February 2013. [Online]. Available: http://doublechooz.in2p3.fr/Public/German/welcome.php

[Dre10] G. Drexlin, *Physik 6,Kerne und Teilchen Vorlesung*, 2010. [Online]. Available: http://www-ik.fzk.de/~drexlin/

[Ell01] S. Elliott, *A Brief Description of SAGE*, 2001. [Online]. Available: http://ewi.npl.washington.edu/sage/

[Erh12] M. G. Erhard, "Untersuchung der Langzeitstabilität des nuklearen Standards für die Energieskala des KATRIN-Experiments," 2012, Diploma Thesis Karlsruhe Institute of Technology.

[Fer34] E. Fermi, "Versuch einer Theorie der β-Strahlen," *Zeitschrift für Physik*, pp. 161–177, 1934. [Online]. Available: http://dx.doi.org/10.1007/BF01351864

[For13] Forschungsgruppe Neutrinophysik, "Homepage Forschungsgruppe Neutrinophysik," February 2013. [Online]. Available: http://neutrino.desy.de/projekte/lena/

[FY03] M. Fukugita and T. Yanagida, *Physics of neutrinos : and application to astrophysics; with 64 tabl.*, ser. Texts and monographs in physicsPhysics and astronomy online library. Berlin: Springer, 2003, includes bibliographical references and index. [Online]. Available: http://swbplus.bsz-bw.de/bsz101226632inh.htm

[GGP+06] Gatti, Gallinaro, Pergolesi *et al.*, *MARE Microcalorimeter Arrays for a Rhenium Experiment*, 2006. [Online]. Available: http://crio.mib.infn.it/wig/silicini/proposal/proposal_MARE_v2.6.pdf

[GGS58] Goldhaber, Grodzins, and Sunyar, "Helicity of Neutrinos," *American Physical Society*, 1958. [Online]. Available: http://dx.doi.org/10.1103/PhysRev.109.1015

[Gil12] W. Gil, *Collaboration Meeting XXIII, Fall 2012, Session 02 Main Components, Status of Cryogenic Pumping Section, unpublished*, 2012.

[Gou10] J. D. Goullon, "Installation and commissioning of the monitor spectrometer of KATRIN," 2010, Diploma Thesis Karlsruhe Institute of Technology.

[GTC12] A. Ghosh, T. Thakore, and S. Choubey, *Determining the Neutrino Mass Hierarchy with INO, T2K, NOvA and Reactor Experiments*, 2012. [Online]. Available: http://arxiv.org/abs/1212.1305

[Haa12] M. Haag, *Collaboration Meeting XXIII, Fall 2012, Session 09 Offline Analysis, unpublished*, 2012. [Online]. Available: https://fuzzy.fzk.de/bscw/bscw.cgi/d752519/Offline%20Analysis%20(KaLi).pdf

[Har12] F. Harms, "Assembly and First Results of the KATRIN Focal-Plane Detector System at KIT," 2012, Diploma Thesis Karlsruhe Institute of Technology.

[Har13] ——, *Private Communication*, 2013.

[HCH+04] M. A. Howe, G. A. Cox, P. J. Harvey, F. McGirt, K. Rielage, J. F. Wilkerson, and J. M. Wouters, *Sudbury Neutrino Observatory Neutral Current Detector Acquisition Software Overview*, 2004. [Online]. Available: http://ieeexplore.ieee.org/xpl/articleDetails.jsp?arnumber=1311985

[Hel13] Helmholtz-Zentrum Potsdam Deutsches GeoForschungsZentrum, *Website*, 2013. [Online]. Available: http://www-app3.gfz-potsdam.de/Declinationcalc/declinationcalc.html

[Höt12] M. Hötzel, "Simulation and analysis of source-related effects for KATRIN," Ph.D. dissertation, Karlsruhe Institute of Technology, 2012.

[How13] M. Howe, *About Orca*, 2013. [Online]. Available: http://orca.physics.unc.edu/~markhowe/Orca_Help/About_Orca.html

[HRR03] A. Haungs, H. Rebel, and M. Roth, "Energy spectrum and mass composition of high-energy cosmic rays," *Reports on Progress in Physics*, vol. 66, no. 7, p. 1145, 2003. [Online]. Available: http://dx.doi.org/10.1088/0034-4885/66/7/202

[Kat05] Katrin Collaboration, *Katrin Design Report 2004*, 2005.

[KKZ97] H. V. Klapdor-Kleingrothaus and K. Zuber, *Teilchenastrophysik : mit zahlreichen Tabellen*, ser. Teubner Studienbücher : Physik. Stuttgart: Teubner, 1997. [Online]. Available: http://www.gbv.de/dms/goettingen/22727833X.pdf

[KUA+01] Kodamaa, Ushidaa, Andreopoulosb, Saoulidoub, Tzanakosb *et al.*, "Observation of tau neutrino interactions," *sciencedirect*, 2001. [Online]. Available: http://dx.doi.org/10.1016/S0370-2693(01)00307-0

[Mel12] M. Meloni, "Private communication," 2012.

[Mor03] M. Morhac, *Processing and Visualization Functions*, 2003. [Online]. Available: ftp://root.cern.ch/root/Spectrum.doc

[PRSZ09] B. Povh, K. Rith, C. Scholz, and F. Zetsche, "Teilchen und Kerne : Eine Einführung in die physikalischen Konzepte," Berlin, Heidelberg, 2009. [Online]. Available: http://dx.doi.org/10.1007/978-3-540-68080-2

[Sch97] N. Schmitz, *Neutrinophysik : mit 23 Tabellen*, ser. Teubner-Studienbücher : Physik. Stuttgart: Teubner, 1997. [Online]. Available: http://www.gbv.de/dms/goettingen/227563085.pdf

[Sch11] M. Schupp, *Inbetriebnahme des Monitorspektrometers und erste Messungen*, 2011, Diploma Thesis Karlsruhe Institute of Technology.

[Sle12] M. Slezak, *Fit program of the KATRIN Monitor spectrometer User's manual*, 2012. [Online]. Available: https://nuserv.uni-muenster.de/cgit/cgit.cgi/MoS_fitter.git/

[Stu12] M. Sturm, *Collaboration Meeting XXIII, Fall 2012, Session 02 Main Components, New concept for the differential pumping section, unpublished*, 2012.

[Thü07] T. Thümmler, "Präzisionsüberwachung und Kalibrationder Hochspannung für das KATRIN-Experiment," Ph.D. dissertation, Universität Münster, 2007.

[Web12] D. M. Webber, *An Improved Measurement of Electron Antineutrino Disappearance at Daya Bay*, 2012. [Online]. Available: http://arxiv.org/abs/1211.1609

[Wie12] V. Wiedmann, "Systematische Untersuchungen zur Hochspannungsstabilisierung am KATRIN-Monitorspektrometer," 2012, Diploma Thesis Karlsruhe Institute of Technology.

[Zbo11] M. Zboril, "Solid electron sources for the energy scale monitoring in the KATRIN experiment," Ph.D. dissertation, Universität Münster, 2011.

[Zub04] K. Zuber, *Neutrino physics*, ser. Series in high energy physics, cosmology and gravitation. Bristol [u.a.]: Inst. of Physics Publ., 2004, includes bibliographical references and index.

List of Figures

2.1. Overview neutrino sources . . . 6
2.2. Air shower caused by cosmic radiation . . . 7
2.3. Solar Neutrinos . . . 8
2.4. Neutrino Oscillation . . . 12
2.5. Neutrino Mass Eigenstates . . . 13
2.6. Energy Density . . . 13
2.7. Mass parabola . . . 14
2.8. Tritium electron spectrum . . . 16

3.1. Katrin Beamline . . . 17
3.2. Scheme of WGTS . . . 19
3.3. Transportsection with the DPS and CPS . . . 20
3.4. The Focal Plane Detector . . . 21
3.5. Americium measurement FPD . . . 22
3.6. Working principle MAC-E-Filter . . . 23
3.7. The monitor spectrometer . . . 24
3.8. Rubidium decay . . . 25
3.9. Magnetic Field Configuration Monitor Spectrometer . . . 26

4.1. Overview of the experimental setup at the monitor spectrometer in ORCA 30
4.2. Overview of the server structure for slow control . . . 33
4.3. The ORCA Slow Control Script at the monitor spectrometer . . . 37
4.4. Behaviour of the High Voltage Power Supply . . . 39
4.5. Behaviour of the High Voltage Power Supply . . . 40

5.1. Overview of the server structure for data analysis . . . 42
5.2. Overview of TSpectrum peak search . . . 44
5.3. Filterspectrum of run 158542 . . . 48

6.1. Line stability K-32 Pt30-5 . . . 50
6.2. Line stability L-32 Pt30-5 . . . 50
6.3. The dependency of the measurement time on the line position . . . 52
6.4. The dependency of the error over time . . . 53
6.5. Voltage oscillation due to temperature oscillation . . . 55
6.6. Voltage oscillation due to temperature oscillation in 100s parts . . . 56
6.7. Temperature oscillation in the Monitor Spectrometer building . . . 56
6.8. Pressure oscillation of the detector sensor . . . 57

A.1. Run Control . . . 69
A.2. Data Readout . . . 70
A.3. Data Monitor . . . 70
A.4. Data File . . . 71
A.5. Monitor Spectrometer object . . . 72

A.6. Orca Script 73
A.7. Run List 73
A.8. IPE Slow Control object 74
A.9. The Orca catalog 74

Appendix

A. Orca

A.1. Additional Orca graphics

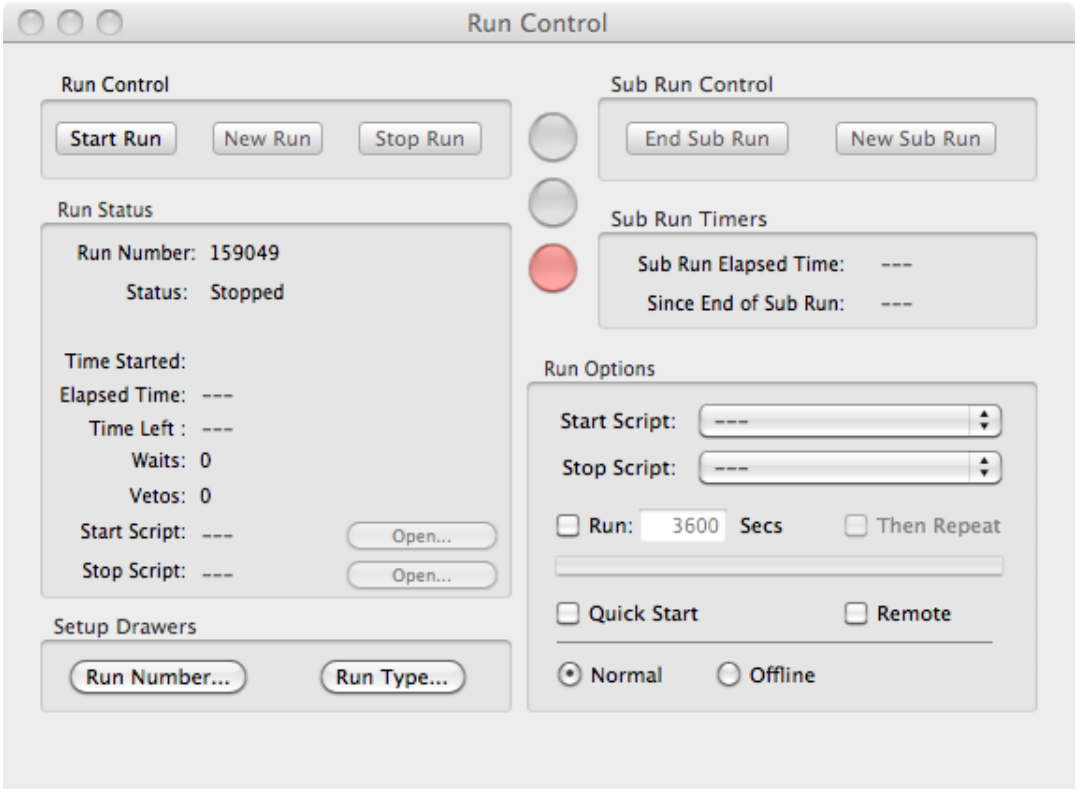

Figure A.1.: **Run Control within Orca.**In the top left runs can be started and stopped as well as a new run can be started. Below is the Run Status and the Setup Drawers. In the Setup Drawers the Run Number and Run Type can be specified. In the top right is the Sub Run Control where the user can start and stop new sub runs manually. Below are the Run Options, the user can add start and stop scripts and chose offline or normal runs.

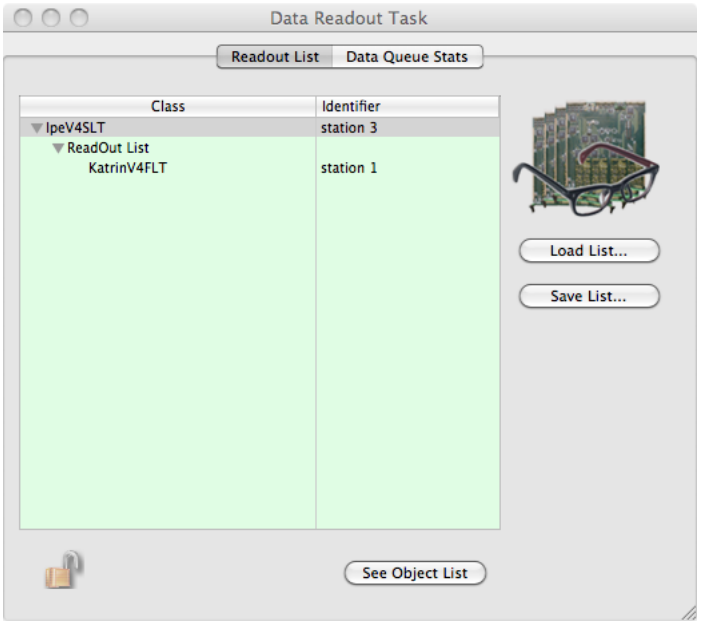

Figure A.2.: **Data Readout Task.** The FLT card has to be included here to enable Orca to read data.

Figure A.3.: **Data Monitor.** The user can take a look at the data, that is read out immediately with this object.

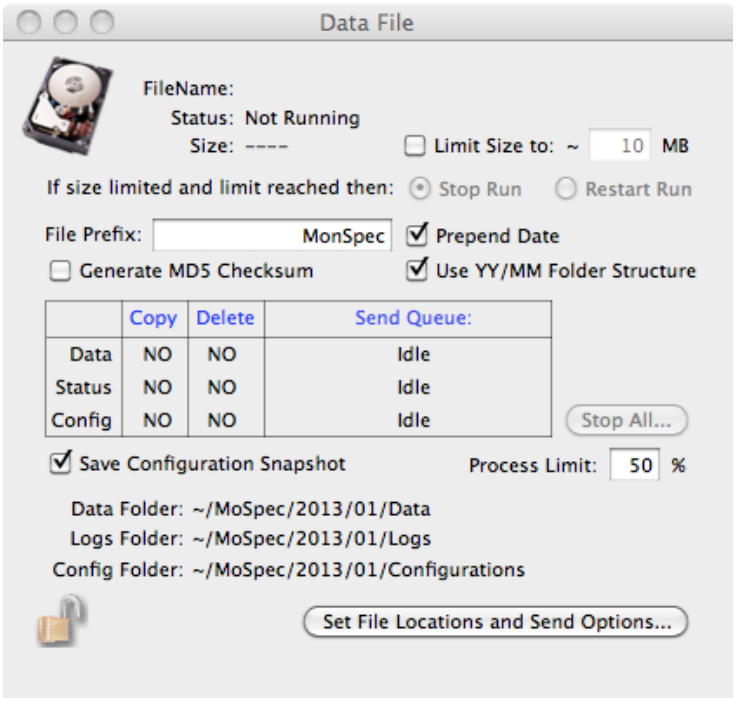

Figure A.4.: **Data File.** The user can chose where to save all the output data. The structure of the output files can be edited within this object as well.

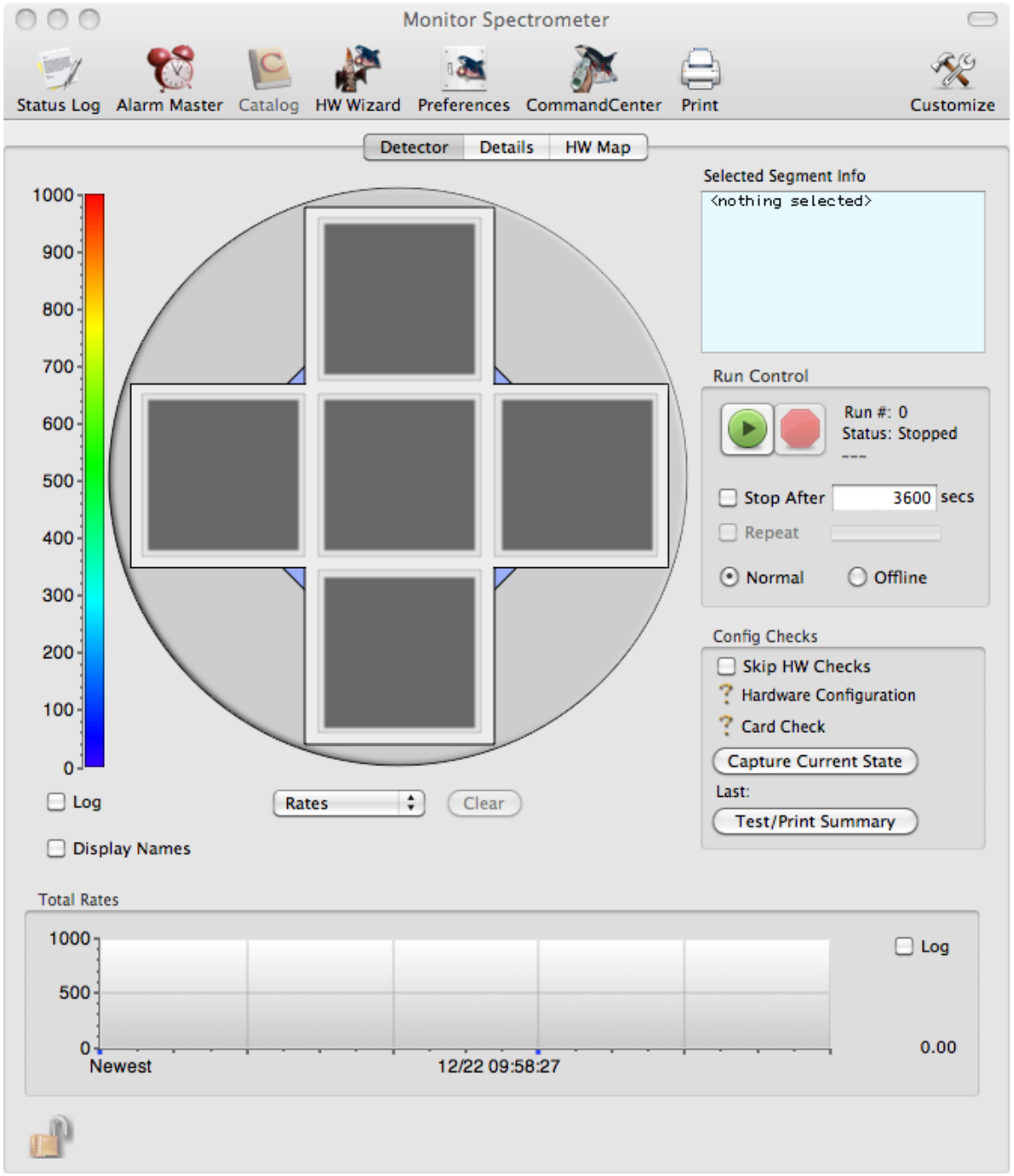

Figure A.5.: **The Monitor Spectromter object.** This object shows an image of the detector and if connected to the FLT card also the hit rates on each detector channel. in the bottom the total rates over time are plotted and the user can access features of Run Control from within this object.

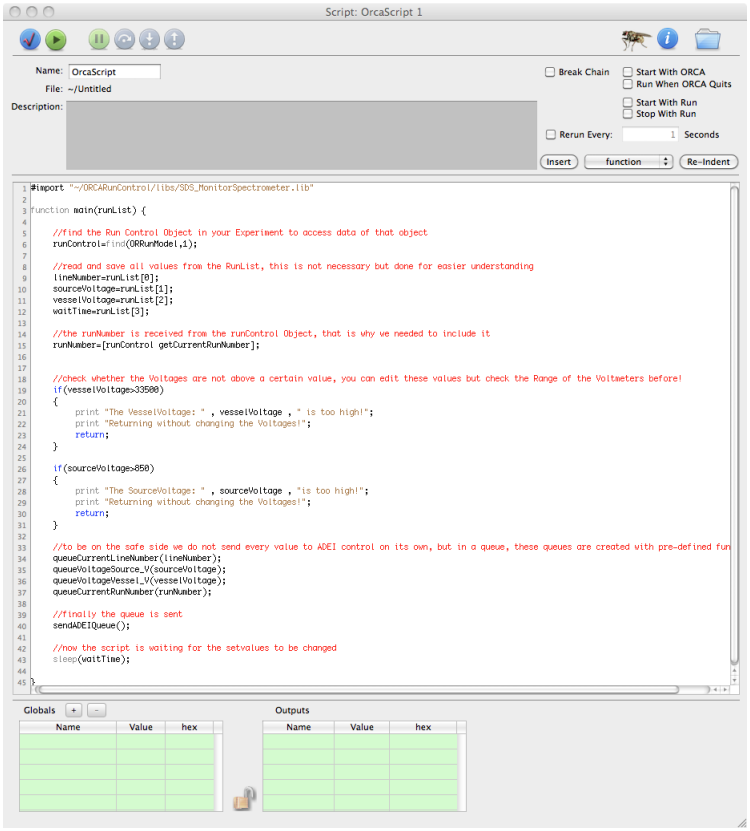

Figure A.6.: **The Orca Slow Control script.** This script was used till December 2012 at the Monitor Spectrometer. The latest version can be found in A.3.

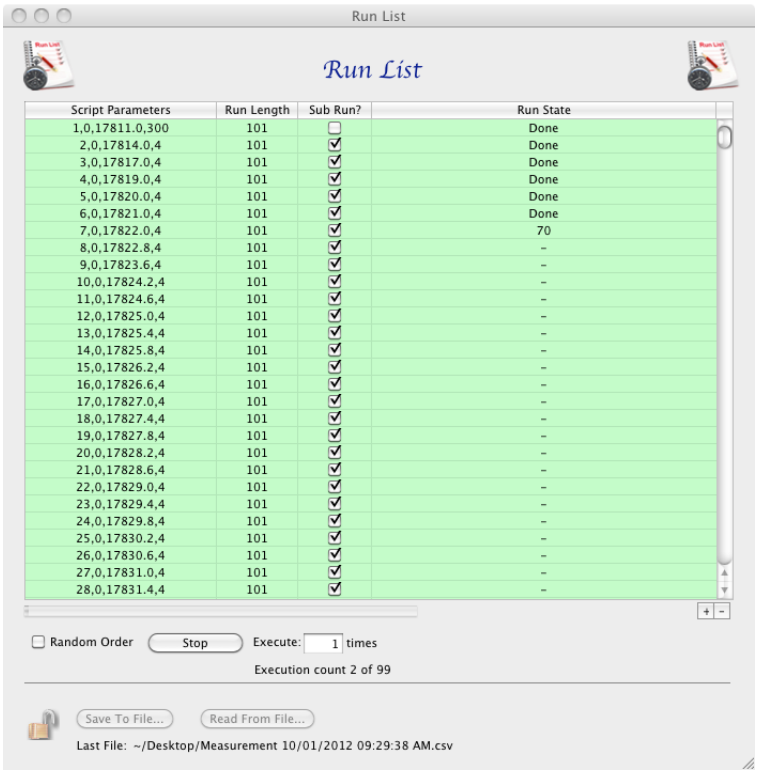

Figure A.7.: **The Run List.** The Run List reads Run Control files made by the user. It sends the Slow Control data to a script and is able to access Run Control.

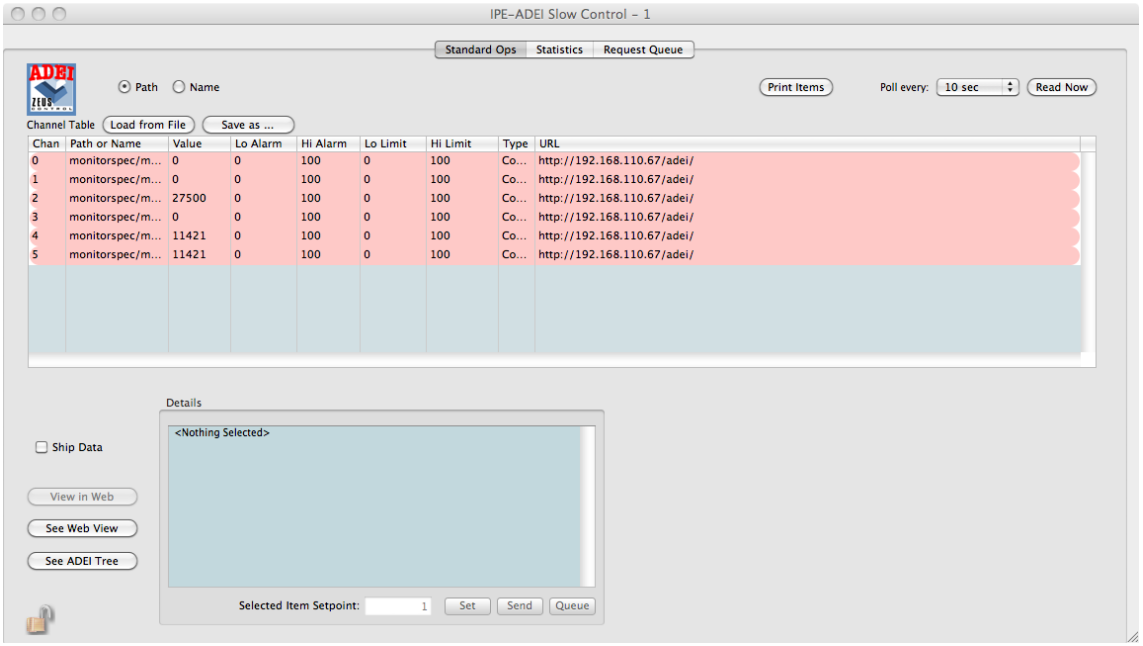

Figure A.8.: **The IPE Slow Control object.** This object grants access to ADEI and enables the user to read sensor data and write to control channels. In this figure all control channels necessary for the Monitor Spectrometer are show. These are highlighted in red.

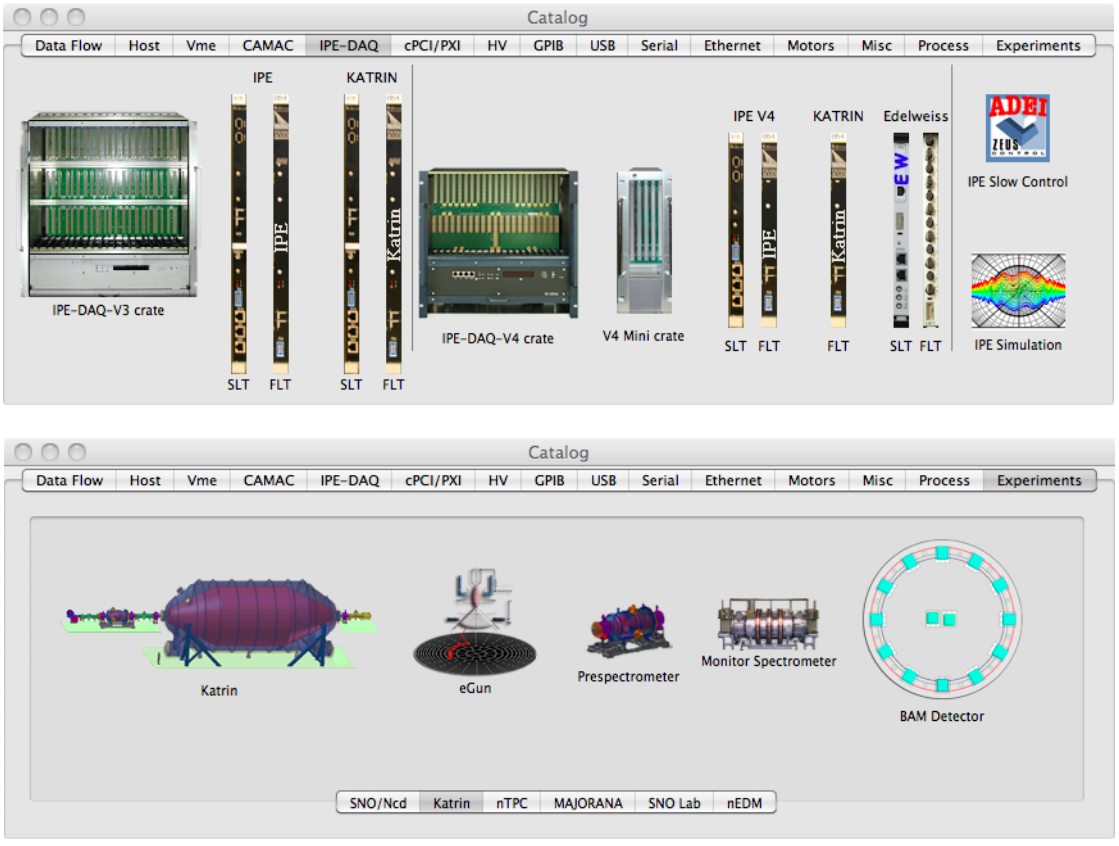

Figure A.9.: **The Orca catalog.** In this figure two tabs of tha catalog are show. In the top an overview of IPE objects and in the bottom an overview of the Katrin experiment objects. These objects can be dragged and dropped to the experimental setup.

A.2. Orca Script library package functions at the Monitor Spectromter

- **setVoltageVessel_V(val):**
  This function needs an argument and puts the desired voltage on the High Voltage Power Supply for the vessel immediately.
- **queueVoltageVessel_V(val):**
  This function puts the set values into a queue, that still needs to be send.
- **setVoltageVessel_kV(val):**
  This function does the same as "setVoltageVesselV_V()", except the argument has to be in kilovolts.
- **queueVoltageVessel_kV(val):**
  Puts the set value into a queue, but the argument has to be in kilovolts.
- **setVoltageSource_V(val):**
  The argument defines the set voltage on the source.
- **queueVoltageSource_V(val):**
  This function puts the set value into a queue.
- **queueCurrentLineNumber(val):**
  Puts the line number into a queue. This is retreived from the Run List at the Monitor Spectrometer.
- **queueCurrentRunNumber(val):**
  Puts the run number into a queue. The run number is the argument.
- **getVoltageVessel_V():**
  This function returns the voltage read by the High Voltage Power Supply in volts.
- **getVoltageVesselHVDivider_V():**
  This function returns the Voltage on the vessel read by the Julie-Research-Divider.
- **getSourceVoltMeter_V():**
  This function returns the voltage on the source read by a voltmeter.
- **getSourcePosition_mm():**
  This function returns the position of the source in millimeters as an array and in x/y/z order.
- **getDetectorPosition_mm():**
  This function return the position of the detector in millimeters as an array and in x/y/z order.
- **getDetectorTemperatur():**
  Returns the temperature of the detector in °C.
- **getPressureVessel():**
  Returns the pressure on the vessel in millibar.
- **getPressurePreVacuum():**
  Returns the pre vacuum pressure in millibar.
- **getPressureDetector():**
  Returns the pressure at the detector in millibar.
- **getPressureSource():**
  Returns the pressure at the source in millibar.

- **getLHeLevel():**
  Returns the liquid helium level as an array, in the order of source/detector.
- **getLN2Level():**
  Returns the liquid nitrogen level as an array, in the order of source/detector.
- **getAirCoilCurrent():**
  Has no function yet as it is not integrated into ZEUS.

A.3. Orca Slow Control Script at the Monitor Spectrometer

```
#import "~/ORCARunControl/libs/SDS_MonitorSpectrometer.lib"

function main(runList) {

//find the Run Control Object in your Experiment to access data of that object
runControl=find(ORRunModel,1);

//read and save all values from the RunList,
//this is not necessary but done for easier understanding
lineNumber=runList[0];
sourceVoltage=runList[1];
vesselVoltage=runList[2];
waitTime=runList[3];

//the runNumber is received from the runControl Object,
//that is why we needed to include it
runNumber=[runControl getCurrentRunNumber];


//check whether the Voltages are not above a certain value,
//you can edit these values but check the Range of the Voltmeters before!
if(vesselVoltage>33500)
{
print "The VesselVoltage: " , vesselVoltage , " is too high!";
print "Returning without changing the Voltages!";
return;
}

if(sourceVoltage>850)
{
print "The SourceVoltage: " , sourceVoltage , "is too high!";
print "Returning without changing the Voltages!";
return;
}

//to be on the safe side we do not send every value to ADEI control on its own,
//but in a queue, these queues are created with pre-defined functions
queueCurrentLineNumber(lineNumber);
queueVoltageSource_V(sourceVoltage);
queueVoltageVessel_V(vesselVoltage);
queueCurrentRunNumber(runNumber);

//finally the queue is sent
sendADEIQueue();

//now the script is waiting for the setvalues to be changed
sleep(waitTime);

}
```

A.4. Parameter file of createfilterspec

#This is the parameterfile for the createfilterspecv2 version	
Pulser on/off	1
Pulser Frequency	200
Sigma for Integration	8
Source Voltmeter	446-REU-0-0101
Vessel Voltmeter	446-REU-0-0003
Read Source Position/Name	1
Detector Pixel Number	4
Draw Histograms	1
Get Runtime from Pulser	0
Set Peak Ratio	0.01
Save filterspec in .txt	0
Use manual boundaries	0

Table A.1.: **The parameter file of the createfilterspec.** This tabular shows all entries and default values of the "parameter.txt" in the createfilterspec home folder. The settings for the manual boundaries can be found in "integrationbound.txt", that is in the createfilterspec home folder also.

Danksagung

Mein Dank gilt allen, die zu dieser Arbeit beigetragen haben, insbesondere:

- Prof. Dr. Guido Drexlin für die spannenden Astroteilchenphysikvorlesungen, die mich motiviert haben meine Diplomarbeit bei KATRIN zu schreiben
- Prof. Dr. Wim de Boer für die Übernahme der Zweitkorrektur und die Kosmologievorlesungen, die mich motiviert haben freitags zeitig aufzustehen
- Dr. Klaus Schlösser für eine super Betreuung, einem freundschaftlichen, humorvollem Umgang und für die qualvollen Stunden des Korrekturlesens meiner geistigen Ergüsse
- Dr. Joachim Wolf für die Ünterstützung, speziell zu Beginn dieser Diplomarbeit
- Philipp Rovedo und Moritz Erhard für viele humorvolle Stunden im Büro, den lockeren Umgang miteinander und viele Diskussionen über Themen jeglicher Art
- Martin Slezák für den vielen Spaß mit LabVIEW, aber vor allem für den freundschaftlichen, humorvollen Umgang miteinander
- Dr. Till Bergmann für eine tolle Einführung in ORCA und die sehr große Hilfe bei allen Fragen sowie dem "KATRIX" Projekt
- Suren Chilingaryan und Armen Beglarian für die super Hilfe rundum Slow Control
- Marco Haag für viele gelöste C++ Probleme und eine super KaLi Unterstützung
- Mark Howe für einen super Support für ORCA Probleme jeglicher Art

Und dem ganzen KATRIN Team für eine super Atmosphäre auf und abseits der Arbeit. Meinen Freunden und meiner Familie gilt natürlich auch besonderer Dank.